



**Molecular Modelling Approaches in Parkinson's Disease:  
Enhancing Domperidone Oral Availability through  
Nanopolymers**

**Mr Stalielson T. Ndlovu**

**2019**

A thesis submitted to the School of Health Sciences, University of KwaZulu

Natal, Westville, in fulfilment for the degree of Masters in Pharmacy

(Pharmaceutical Chemistry)

*Supervisor*

**Prof. Mahmoud Soliman**

**Molecular Modelling Approaches in Parkinson's Disease: Enhancing  
Domperidone Oral Availability through Nano-polymers**

**Mr Stalielson T. Ndlovu**

**211531796**

**2019**

A thesis submitted to the School of Pharmacy and Pharmacology, Faculty of Health Sciences, University of KwaZulu-Natal, Westville, for the degree of Master of Philosophy.

This is the thesis in which the chapters are written as a set of discrete research publications, with an overall introduction and final summary. Typically these chapters will have been published in internationally recognized, peer-reviewed journals.

This is to certify that the contents of this thesis are the original research work of Mr Stalielson Tatenda Ndlovu.

As the candidate's supervisor, I have approved this thesis for submission.

Supervisor:

Signed: *Mahmoud E. Soliman*

Name:

Prof Mahmoud Soliman

Date: 01 November 2019

PREFACE

This thesis is divided into six chapters, including this one:

### **Chapter 1:**

This is an introductory chapter that addresses the background, rationale and relevance of the study as well as the proposed aim and objectives. The general outline and structure of the thesis concludes this chapter.

### **Chapter 2:**

This chapter provides a comprehensive literature review on discovery and patenting of Domperidone drug, and the urgent research, taking place toward the development of FDA approved oral DOMPolymeric nanoparticle formulations. Included in this chapter is the historical background, mechanism of action (MOA) of domperidone, choice polymers, the use of computational chemistry and molecular modelling oral route of administration.

### **Chapter 3:**

This chapter conceptualizes computer-aided drug design by discussing various molecular modeling and molecular dynamic tools and applications. The computational strategies needed to investigate comparative polymeric structural/conformational properties as well as methods used to analyze binding affinity are explicated upon.

### **Chapter 4: (Published work- this chapter is presented in the required format of the journal and is the final version of the accepted manuscript)**

This chapter employs molecular modelling studies to provide underpinning insight at the molecular level of the DOMP-polymer nanocrystal interactions to substantiate the experimental studies. This included an understanding of the impact of polymers on the size of nanocrystals and their associated stability characteristics.

### **Chapter 5: (Published work- this chapter is presented in the required format of the journal and is the final version of the accepted manuscript)**

This chapter identifies shortcomings that linked with PD pharmacological treatment and substantiates the emergence of the role played by *In Silico* investigation in formulating and validating new compounds and the use of nanopolymers to achieve more effective therapy.

### **Chapter 6:**

III This is the final chapter that proposes future work and concluding remarks.

## DECLARATION I -PLAGIARISM

I, Stalielson T. Ndlovu, declare that

1. The research reported in this thesis, except where otherwise indicated, is my original research.
2. This thesis has not been submitted for any degree or examination at any other university.
3. This thesis does not contain other persons' data, pictures, graphs or other information, unless specifically acknowledged as being sourced from other persons.
4. This thesis does not contain other persons' writing, unless specifically acknowledged as being sourced from other researchers. Where other written sources have been quoted, then:
  - a. Their words have been re-written but the general information attributed to them has been referenced.
  - b. Where their exact words have been used, then their writing has been placed in italics and inside quotation marks, and referenced.
5. This thesis does not contain text, graphics or tables copied and pasted from the internet, unless specifically acknowledged, and the source being detailed in the thesis and in the References sections.

A detailed contribution to publications that form part and/or include research presented in this thesis is stated (include publications submitted, accepted, in press and published).

Signed: **S.T. Ndlovu**  
DECLARATION II- LIST OF PUBLICATIONS

Date: 01 November 2019

1. Stalielson Tatenda Ndlovu, Naseem Ullah, Shahzeb Khan, Pritika Ramharack, Mahmoud Soliman, Marcel de Matas, Muhammad Shahid, Muhammad Sohail, Muhammad Imran, Syed Wadood Ali Shah, Zahid Hussain (2018). Domperidone nanocrystals with boosted oral bioavailability: fabrication, evaluation and molecular insight into the polymer-domperidone nanocrystal interaction. *Drug Delivery and Translational Research (DOI: 10.1007/s13346018-00596-w)*

Contribution:

**Stalielson T. Ndlovu**: contributed to the project by performing all the experimental work and Manuscript preparation and writing.

Dr. Pritika Ramharack: contributed to manuscript editing and providing technical support.

Prof. Mahmoud E.S. Soliman: Supervisor

2. Stalielson Ndlovu, Ransford Oduro Kumi, Pritika Ramharack, Manimbulu Nlooto, Mahmoud E. S. Soliman (2019). Review: Permeating The Blood Brain Barrier; Computational Exploration Of Chemotherapeutic Paradigms Towards Effective Treatment Of Parkinson's Disease. *Frontiers In Computational Neuroscience (Manuscript ID: 509302)*

Contribution:

**Stalielson T. Ndlovu**: Author-contributed to the project by performing all the research work and manuscript preparation and writing.

Ransford O. Kumi: contributed to manuscript editing and providing technical support.

Dr. Pritika Ramharack: contributed to manuscript editing and providing technical support.

Dr. Manimbulu Nlooto: Co-Supervisor

Prof. Mahmoud E.S. Soliman: Supervisor

## ***A- LIST OF PUBLICATIONS***

1. Stalielson Tatenda Ndlovu, Naseem Ullah, Shahzeb Khan, Pritika Ramharack, Mahmoud Soliman, Marcel de Matas, Muhammad Shahid, Muhammad Sohail, Muhammad Imran, Syed Wadood Ali Shah, Zahid Hussain (2018). Domperidone nanocrystals with boosted oral bioavailability: fabrication, evaluation and molecular insight into the polymer-domperidone nanocrystal interaction. *Drug Delivery and Translational Research* (DOI: 10.1007/s13346018-00596-w)
2. Stalielson Ndlovu, Ransford Oduro Kumi, Pritika Ramharack, Manimbulu Nlooto, Mahmoud E. S. Soliman (2019). Review: Permeating The Blood Brain Barrier; Computational Exploration Of Chemotherapeutic Paradigms Towards Effective Treatment Of Parkinson's Disease. *Frontiers In Computational Neuroscience* (Manuscript ID: 509302)

## **ACKNOWLEDGEMENTS**

*My Creator:* Thank you for being the great Father that you are to me.

*Professor M.E.S Soliman:* I would like to thank you for accepting me into your prestigious department and for your untiring leadership, support and wisdom throughout this degree.

*Dr Manimbulu Nlooto:* I am everly grateful for your contributions to my work and person.

*Dr Pritika Ramaharack:* Thank you for your patience and dedication in assisting me with my work and helping me face up to the demands of the degree. You have been an amazing mentor and I am grateful for all your support; may the Lord bless you.

*The Molecular Modeling and Drug Design Group:* Thank you to the molecular modelling family for bringing insight, support, inspiration, comfort and friendship through thick and thin from the first day I stepped foot into the computational lab to this day.

*My Loved ones and Friends:* Thank you to my father and mother for letting me explore my dreams and being my greatest supporters. My siblings, for the constant care and support. And to my bigger family the Mpolis and Machekas for your love, what a family.

I am grateful to friends who have supported me through tough times and brought joy and laughter to my life. Special mention, to my friends and all my brothers and sisters in Christ who have inspired me to excel and be a better person.

## VII

### TABLE OF CONTENTS

<b>DECLARATION I- PLAGIARISM</b>	IV
<b>DECLARATION II- LIST OF PUBLICATIONS</b>	V
<b>RESEARCH OUTPUT</b>	VI
<b>ACKNOWLEDGEMENTS</b>	VII
<b>LIST OF ABBREVIATIONS</b>	XI
<b>LIST OF FIGURES</b>	XIV
<b>LIST OF TABLES</b>	
<b>ABSTRACT</b>	XVI
<b>CHAPTER 1</b>	
1. Introduction	
<i>1.1 Background and Rational</i>	1
<i>1.2 Aim and Objectives</i>	2
<i>1.3 Novelty and Significance of Study</i>	3
<i>1.4 Overview of Thesis</i>	4
<i>1.5 References</i>	5

## CHAPTER 2

### 2. Background on Domperidone - VIII –

2.1	<i>Introduction</i>	8
2.2	<i>Discovery and structure of Domperidone</i>	9
2.3	<i>Domperidone's unique mechanism of action</i>	10
2.4	<i>Domperidone is a drug with multiple uses in the field of medicine</i>	11
2.5	<i>Physicochemical properties of DOMP and its effect on various routes of administration</i>	13
2.6	<i>Transition of DOMP-nanopolymers from transdermal to oral route of administration</i>	15
2.7	<i>Adverse effects and low solubility of Domperidone</i>	16
2.8	<i>The emergence of polymers salvaging the drug crisis in Parkinson's Disease</i>	17
2.9	<i>The inevitable merge of nano polymers with computational chemistry References</i>	18
		21

## CHAPTER 3

### 3. Molecular Modeling and Computational Approaches to Biomolecular Structure and Drug Design

3.1	<i>Introduction</i>	38
3.2	<i>Principle of Quantum Mechanics</i>	40
	<i>The Schrödinger equation</i>	40
	<i>The Born-Oppenheimer Approximation Theory</i>	42
3.2.1	<i>Potential Energy Surface</i>	43
3.3	<b>The Molecular docking</b>	45
3.4	<b>Molecular Mechanics</b>	45
3.4.1	<i>Force Field</i>	48
3.5	<b>The Principle of Molecular Dynamics</b>	49
3.5.1	<i>Molecular Dynamics Post Analysis</i>	50
3.5.1.1	<i>System Stability</i>	51
3.5.1.2	<i>Thermodynamic Energy Calculations</i>	53
3.5.1.3	<i>Conformational Features of the System</i>	55
3.5.2	<i>Molecular Docking</i>	55
		56
3.6	<b>Summary of Methods</b>	57
3.7	<b>References</b>	58
		59

## CHAPTER 4

<b>4. Domperidone Nanocrystals with Boosted Oral Bioavailability: Fabrication, Evaluation and Molecular Insight into the Polymer-Domperidone Interaction</b>	65
<b>4.1 Introduction</b>	67
<b>4.2 Materials and Methods</b>	69
4.2.1 <i>Materials</i>	70
4.2.2 <i>Preparation of DOMP nanosuspension</i>	73
4.2.3 <i>Physicochemical characterization</i>	74
4.2.4 <i>Stability studies</i>	75
<b>4.3 Computational methods</b>	79
4.3.1 <i>Molecular Docking of polymers and DOMP</i>	80
4.3.2 <i>Molecular Dynamic Simulations</i>	81
4.3.3 <i>Binding free energy calculation</i>	85
<b>4.4 Conclusion</b>	87
<b>4.5 References</b>	88

## CHAPTER 5

<b>5. Permeating The Blood Brain Barrier; Computational Exploration Of Chemotherapeutic Paradigms Towards Effective Treatment Of Parkinson's Disease (Review)</b>	81
5.1 <i>Introduction</i>	
5.2 <i>Computational Methods</i>	96
5.3 <i>Results and Discussion</i>	98
5.4 <i>Conclusion</i>	97
5.5 <i>References</i>	98

## IX

<b>APPENDIX</b>	106
-----------------	-----

### LIST OF ABBREVIATIONS

ADME	Absorption, distribution, metabolism, excretion
AMBER	Assisted Model Building with Energy Refinement
API	Active Pharmaceutical Ingredient
BCS	Biopharmaceutics Classification System
CHARMM	Chemistry at Harvard Macromolecular Mechanics
CLOGP	Calculated log P values
CNS	Central Nervous System
COMT	Catechol-O-Methyl-Transferase
CTZ	Chemoreceptor Trigger Zone

DA	Dopamine Agonist
DBS	Deep brain stimulation
DMF	Dimethylformamide
DOMP	Domperidone
DSC	Differential Scanning Calorimetry
EC	Ethyl Cellulose
EUD	Eudragit
f	Hydrophobic fragmental constant
FDA	Food and Drug Administration
GAFF	General AMBER Force Field
GERD	Gastroesophageal Reflux Disease
GIT	Gastrointestinal Tract
GPU	Graphics Processing Unit
HPMC	Hydroxypropyl Methylcellulose
IM	Intramuscular
Levocarb	Levodopa Carbidopa
Log kw	Capacity factor values from RPHPLC
L-dopa	Levodopa
MAO	Monoamine Oxidase
MD	Molecular Dynamics
MLP	Molecular lipophilic potential
MMGBSA	Molecular Mechanics/Generalized Born Surface Area
MM	Molecular Mechanics
MMPB-SA	Molecular Mechanics/Poisson-Boltzmann Surface Area
MOA	Mechanism of Action
MPPP	Desmethylprodine
MPTP	1-methyl-4-phenyl-1,2,3,6-tetrahydropyridine

NAMD	Nanoscale Molecular Dynamics
ND	Neurodegenerative Diseases
NP	Nanoparticles
OL	Odorranalectin
p	Hansch
PD	Parkinson's Disease
PEG	Polyethylene glycol
PES	Potential Surface Energy
PI	Polydispersity Index
PLGA	Poly-Lactic-Co-Glycolic Acid
PMEMD	Particle Mesh Ewald Molecular Dynamics XI
PVA	Polyvinyl Alcohol
PVP	Polyvinyl Pyrrolidone
QSAR	Quantitative Structure Activity Relationship
QM	Quantum Mechanics
RESP	Restrained Electrostatic Potential
RMSD	Root Mean Square Fluctuation
RSPM-	Respirable Suspended Particle Matter
SEM-	Scanning Electron Microscopy
SEM	Standard Mean Error
STN	Subthalamic nucleus
TEM	Transmission Electron Microscopy

## LIST OF FIGURES

<b>Figure 1.1:</b> Pie chart showing the foreseen increase in global prevalence of PD	3
<b>Figure 2.1:</b> A diagram of risk factors that are associated with Parkinson's disease	8
<b>Figure 2.2:</b> The key drugs in the treatment of PD symptoms	9
<b>Figure 2.3:</b> Complete diagram of the distribution and metabolism of Levodopa and Levodopa/Carbidopa	10
<b>Figure 2.4:</b> The 2D structure of domperidone	11
Figure 2.5:	11
<b>Figure 2.6:</b> Known mainstream uses of Domperidone	13
<b>Figure 2.7:</b> Summary of considerations to be made upon transition to oral administration of drugs.	15
<b>Figure 2.8:</b> Adverse effects of Domperidone (Prepared by Author).	44
<b>Figure 2.9:</b> Essential qualities of polymeric nanoparticle in formulations (Prepared by Author)	47
<b>Figure 3.1:</b> Graphical representation of a 2-D potential energy surface (PES).	53
<b>Figure 3.2:</b> Cycle of molecular dynamics steps (prepared by author).	58
<b>Figure 4.1:</b> Chemical structure of domperidone	40
<b>Figure 4.2:</b> Diagrammatic representation of thermodynamic calculation (MM/GBSA) used in the study (Prepared by Author)	46
<b>Figure 4.3:</b> Particle size distribution of DOMP nanoparticles.	50
<b>Figure 4.4:</b> SEM image of raw DOMP (A) and TEM micrographs of processed DOMP particles (B)	52
<b>Figure 4.5:</b> PXRD patterns of Unprocessed (A) and DOMP nanoparticles (B).	54
<b>Figure 4.6:</b> DCS Thermograms of Unprocessed DOMP and DOMP nanocrystals.	55
<b>Figure 4.7:</b> Binding affinity results from molecular docking of domperidonenanopolymer complexes.	56
<b>Figure 4.8:</b> Binding affinity results from molecular docking of domperidone copolymer complexes.	56
<b>Figure 4.9:</b> The lowest energy conformation of HPMC-PVA-DOMP complex (-25.25 kcal/mol); (A) depicts the molecular surface of HPMC-PVA encapsulating DOMP, (B) displays the hydrogen bond interaction between DOMP and HPMC.	57
<b>Figure 4.10:</b> The PVA-DOMP complex (-18.88kcal/mol) (A) Molecular surface	

interaction between PVA and DOMP, (B) graphical representation of the lack of hydrogen bonds between PVA and DOMP. 61

**Figure 4.11:** The lowest energy conformation of Ethocel-DOMP complex (-27.26kcal/mol) after molecular dynamic simulations; (A) molecular surface interaction between Ethocel and DOMP, (B) presents three stabilizing hydrogen bonds of Ethocel-DOMP complex. 62

**Figure 4.12:** Comparative in-vivo Pharmacokinetic profile of (Domperidone) (n=6, ±SD) \*\*P< 0.001. 63

**Figure 4.13:** Stability studies of DOMP nanoparticles stored at 2.8 °C (A), 25°C (B) and 40 °C. 69

**Figure 4.14:** Comparative dissolution profile of unprocessed and DOMP nanoparticles at acidic pH: 0.1MHCL (A) and phosphate buffer pH: 6.8 (B). 71

**Figure 5.1:** Pathologic degeneration of the dopamine pathway during Parkinson's disease. Decreased dopamine levels lead to staggered or minimal excitement through peripheral neurons, thus resulting in movement disorders (created by Authors). 82

**Figure 5.2:** Anti-Parkinson's drugs that can pass the blood-brain-barrier, versus drugs that cannot. 89

**Figure 5.3:** Graphical representation of interventions to unstitch the obstacle in the treatment of PD. 90

**Figure 5.4:** depiction of the major characteristics of nanocrystals (Prepared by author)

## LIST OF TABLES

Table 2.1: Table showing choice polymers and their properties

Table 4.1: Impact of polymers on particle sizes and PDI values of DOMP nanosuspension.

Table 4.3: Summary of pharmacokinetic parameters for domperidone.

Table 4.4: Stability study of DOMP optimized nanocrystals as a function of time.

Table 5.1: Drug target and pharmacokinetics of approved PD drugs and those in clinical stages.

Table 5.2: Properties exhibited by potential Parkinson's drug carriers

## ABSTRACT

Parkinson's disease is symbolized by resting tremor, rigidity, and bradykinesia caused by the loss of dopaminergic neurons in the substantia nigra, the presence of Lewy bodies, and a decent response to levodopa. However, a domperidone (DOMP) supplement is often necessary to remedy the nausea and vomiting caused by this prodrug and its therapeutic counterparts, namely metoclopramide must be supplemented with domperidone therapy to treat nausea and vomiting. Even though it is potentially the best antiemetic by reason of its unique mechanism of action, this drug presents with low solubility. In addition to a plethora of adverse effects; these shortcomings necessitate the use of polymeric nanoparticles (nano-polymers) to boost the dissolution rates by improving the solubility of DOMP. The resultant enhancement in bioavailability of the active ingredient is envisaged to address the challenge of increase adherence and reduce frequency dosing through controlled release. Therefore, the aim of this study was to employ molecular modelling approaches to rationalize the selection of suitable polymers for use in the production of stable domperidone nanopolymers with enhanced bioavailability. Polymers-combinations were designed and synthesized by collaborators and structures were made available for this study. Docking and binding free energy calculations were carried out for on 12 polymers-DOMP complexes. Results showed stability for all complexes, converging at 20ns over a 50ns simulation. Of the polymer-complexes, the HPMC-PVA-DOMP (25.22 kcal/mol) system showed the most optimal binding free energy based on the intermolecular interactions. This demonstrates favorable affinity of DOMP to the polymer, thus justifying its use in Parkin's disease therapy. The Molecular modelling tools provided in this study underpin knowledge at a molecular level of DOMP-polymer nanocrystal interactions. This was further substantiated by collaborative experimental studies. This study has contributing immensely to the understanding of nano-polymers toward enhanced therapy against Parkinson's disease.

## Isiqephu

Isifo i- Parkinson sibonakala ngokuqhahazela, ukuqina komzimba ngokungajwayelekile kanye ne bradykinesia okudalwa ukungasebenzi ngendlela kwama-dopaminergic neurons kwi-substantia nigra, ukuba khona kwama-Lewy bodies kanye nokusebenza ngendlela kwe-levodopa. Kodwa idomperidone (DOMP) eyisilekeleli iyadingeka ukwelapha inhliziyu encane kanye nokuphalaza okudalwa i-prodrug kanye nendlela elilapha ngayo, esibala i-metoclopramide kumele ilekelelwe ngedomperidone therapy ukuze ilaphe inhliziyu encane kanye nokuphalaza. Noma le-prodrug ibe iintiemetic engungqa phambili kodwa ngenxa yesizathu sendlela esebenza ngalo incibilika ngokungagculisi. Ngaphezu kwalokho

esikubala kwizingqinamba ze-plethora kuba nesidingo sokusetshenziswa kwama- polymeric nanoparticles (nano-polymers) ukukhuphula izinga lokuncibilika ngokudlondlobalisa i-solubility ye-DOMP. Lo mthelela ukhulisa i-bioavailability yesithako esisebenzayo ibukwa njengendlela yokumelana nengqinamba yokunyusa ukunamathela futhi iphinde inciphise izinga lokudedela i-dosing. Ngakho-ke lolucwaningo luqonde ekusebenziseni izindlela ze-molecular modelling ukuqonda indlela yokukhetha ama-polymers afanele ekusetshenzisweni ekwakhweni kwe-domperidone nanopolymers azoba-stable futhi ane-bioavailability ethe xaxa. Izingxubevange zama-polymers akhiwe futhi enziwa ama-collaborators nezakhiwo ebezikhona kulolu cwaningo. Izibalo ze-docking kanye ne-binding free energy zenziwe kuma polymers-DOMP complexes ayishumi nambili. Imiphumela ikhombise istability kuwona wonke ama-complexes, abehlangana ku 20ns esikhathini esibalelwa kwizilinganiso eziwu 50 ns. Kulama polymer-complexes, i-HPMC-PVA-DOMP (-25.22 kcal/mol) iwuhlelo olukhombise i-binding free energy enkulu ehlaluka kuma-intermolecular interactions. Lokhu kukhombisa ukunamathela okuhle kwe-DOMP kwi-polymer, okuyimbangela yokusetshenziswa ekulashweni kwesifo se-Parkin. Amathuluzi e-molecular modelling kulolu cwaningo asinike ulwazi ezingeni lama-molecules lokusebenzisana kuma DOMP-polymer nanocrystals. Lokhu kuphinde kwagcizelelwa ngokuhlolwa okunobambiswano. Lolu cwaningo selusize kakhulu ekuqondeni kahle hle kwama nano-polymers ekukhulisweni kolapho oluqondene nesifo se-Parkinson.



## CHAPTER 1

### 1. Introduction

#### *1.1. Background and Rationale of the study*

Neurodegenerative diseases (ND) transpire when neurons in the brain and spinal cord and begin to deteriorate (Maiti et al., 2017). As neurons continue to deteriorate symptoms progressively worsen and in certain cases patients lose ability move normally, think clearly, or generally function on a daily basis (French & Muthusamy 2016). Finally, the majority of these diseases are injurious.

Parkinson's disease (PD) is an extremely incapacitating neurodegenerative disorder that develop in motor circuit disturbance and eventually, causes deterioration of movement (Beall et al., 2013; Mariani et al., 2005). This condition is due to the selective degradation of the dopaminergic neurons in the substantia nigra pars compacta in the midbrain, which consequently results in the pathological symptoms namely bradykinesia, resting tremor, postural instability and rigidity (Bhatia 2012). It was originally suggested that patients who develop PD were exposed to an environmental trigger(s) e.g. pesticides that caused the onset of the disease, but more recently, a significant genetic component, paired with environmental factors have been incriminated in disease pathogenesis (Hatcher et al., 2008; Freire & Koifman 2012). Currently, there are eight genes (Parkin, PINK1, LRRK2, SNCA, DJ-1, ATP13A2, EIF4G1 and VPS35) that have been candidly associated with PD (Klein & Westenberger 2012).

A wide range of treatment has been availed to reduce symptoms related with Parkinson's disease since it cannot be cured using pharmacological treatment. The disease continues to progress and no medication has been discovered to slow down or stop PD disease progression in patients (Oertel 2017).

Even though a lot of ground has been covered since the introduction of Levodopa made resulted in breakthrough in the treatment of motor symptoms, there still remains more

therapeutic avenues to be explored in the arena of Parkinson's symptoms (Brück 2002). This void in symptomatic relief regimens for PD has sparked greater interest in research to come up with better drug delivery strategies and drug re-inventions to bridge the gap of therapeutic inadequacy and multiple side effects caused by the current treatment regimens to be filled since symptoms differ from person to person (Rodriguez-Aller et al., 2015).

Nano-drug delivery are now the critical approach to scale up PD treatment solubility, drug discharge profiles, and to lower dosing recurrence and side effects (Parhi et al., 2012). The utilization of Nano-drug delivery transport has proved a critical method of to revamp managing patients with neurodegenerative diseases. Nanoparticles-based drug transport mechanisms have given rise to controlled and efficacious release of drugs at the affected neurons, improved solubility, bioavailability and strength (Ravichandran 2009).

Computational methods are becoming indispensable in drug delivery and development ventures, they are rapidly intensifying in terms of growth, application and popularity (Hopkins 2008). Molecular docking and molecular dynamics in particular are regarded very essential in interpretation of the binding systems, conformational investigation and computing the binding affinities between drugs and sundry systems as protein, polymers and other bioorganic molecules (Okimoto et al., 2009). Sundry molecular modelling apparatus have been hugely harnessed in to grasp the progression of drug delivery systems and pharmaceuticals in general (Ullah et al., 2018).

## ***1.2 Aims and objectives***

1. The aims of this study were therefore: (1) to provide insights of the structural and conformational features in the designed polymeric nanoparticles. In order to achieve aim 1 the objectives of this study were therefore:
  - 1.1 To explore the structural and conformational dynamics of the designed nanopolymers via molecular dynamics simulations
  - 1.2 To explore the binding mechanism of the designed polymers and their interactions modes with DOMP and

- 1.3 To provide a technical guidance on how to set up a simulation protocol for investigating drug interactions with polymeric targets.
2. To provide comprehensive molecular insight into the interaction and the conformational landscape of a series of polymeric nanoparticles structures, In order to achieve aim 2, the objectives of this study were therefore:
  - 2.1 To understand the structural and conformational landscape as well as the binding mechanisms of DOMP-nanopolymer by applying a wide range of molecular modelling tools, such as molecular docking, molecular dynamics and conformational analysis protocols.
3. To apply experimental and molecular modelling tool to design the first account of stable DOMP-nanopolymeric particles with enhanced dissolution rate for increased bioavailability:

In order to achieve aim 3, the objectives of this study were therefore:

- 3.1 To design and prepared different DOMP nanopolymeric particles with HPMC, PVP, PVA, ethyl cellulose (EC) Eudragit and Pluronics,
  - 3.2 Characterize the DOMP nano-polymeric particles in terms of particle size, zeta potential, surface morphology, in vitro drug release,
- 4 To employ in silico molecular modelling strategies such as molecular docking and dynamics in order to provide in-depth knowledge into the molecular nature of the designed nanoparticles, binding mechanism and polymer choice in relation to the overall physicochemical properties and anti-Parkinson's activities of the processed Domperidone particles. (Ullah et al., 2018)

### 1.3 Novelty and Significance of study

The average global life expectancy of many populations throughout the world now extends late into the eighth decade, and the prevalence of most neurodegenerative disorders increases dramatically with advancing age (Abegunde et al., 2007). Parkinson's disease is a gradual deterioration of the central nervous system that essentially affects the aged. An Investigation on 588 newly diagnosed patients showed there are over 91% more men who are plagued by PD than there is among women and only 4% of the patients were less than 50 years of age yet the frequency increased for the more aged, above 60 years. PD incidences are expressed at all ages, nonetheless are still rare in people youthful patients, under 40 and usually induced by an inherited or impromptu genetic effects deformities (Fahn & Sulzer 2004). Thus, if efficient remedies or preventive interventions for Parkinson's disease and other neurodegenerative disorders are not discovered in the near future, the financial, societal and emotional costs of these aging-related brain disorders will be overwhelming (Maresova et al., 2016).

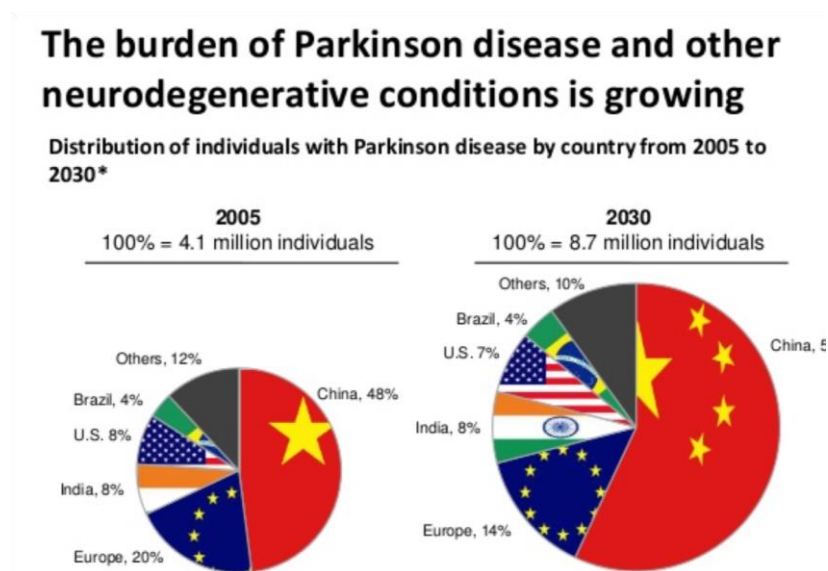


**Figure 1.1:** Pie chart showing the foreseen increase in global prevalence of PD

Notable progress has already been made finding the treatment for nano-polymeric delivery of DOPM. Despite these attainments using polymers in transdermal administration these and other nanopolymers still need to be explored for oral delivery (Shah et al., 2011). It cannot vaguely be assumed that the same polymers are able to deliver this *Dopamine<sub>2</sub>* Receptor antagonist transdermally, will also deliver against the peculiar odds of first-pass effect in the oral route of

transport (Kaestli et al., 2008). Therefore, it is of necessity for polymers that not only have favorable properties for boosting the dissolution of DOMP, but also possesses protective qualities to traverse the drug across the gastrointestinal-tract without exposing it to metabolism and finally reducing the frequency of repeated daily dosing through controlled release.

Various means of exploring the interactions between the polymer and DOMP became needful. The investigations were to be done using computational simulation of structure and binding selected polymers with the antiemetic as a way of buttressing the experimental trials on the dissolution of the drug with different combinations of polymeric nanoparticles (Rodriguez-Aller et al., 2015). There is therefore a need for growing advancement in drug design. This has provoked us to scrutinize potential polymers, based on the interactive features of DOMP, and suggest potential efficient formulations stemming from pronged research. Beyond the desired oral DOMP polymeric nanoparticle (DOMP-nanoparticle) formulation, this research will indeed usher several step closer finding a sure pattern for boosting low solubility drugs the class of BSC II and BSC IV for exceptional drug delivery (Rodriguez-Aller et al., 2015; Ullah et al., 2018). These findings therefore showcase the potential of these systems in enhancing patient therapy and treatment of ND, thereby ultimately improving the quality of life and saving lives.

#### ***1.4 References***

- Abegunde, D.O. et al., 2007. The burden and costs of chronic diseases in low-income and middle-income countries. *Lancet*.
- Beall, E.B. et al., 2013. The Effect of Forced-Exercise Therapy for Parkinson's Disease on Motor Cortex Functional Connectivity. *Brain Connectivity*, 3(2), pp.190–198.
- Bhatia, K.P., 2012. Clinical Approach to Parkinson ' s Disease : , pp.1–16.
- Brück, C., 2002. Drug interactions in the treatment of Parkinson ' s disease. , pp.24–29.
- Fahn, S. & Sulzer, D., 2004. art%3A10.1602%2Fneurorx.1.1.139.pdf. , 1(January), pp.139–154.
- Freire, C. & Koifman, S., 2012. Pesticide exposure and Parkinson's disease: Epidemiological evidence of association. *NeuroToxicology*, 33(5), pp.947–971.

- French, I.T. & Muthusamy, K.A., 2016. A review of sleep and its disorders in patients with Parkinson's disease in relation to various brain structures. *Frontiers in Aging Neuroscience*, 8(MAY), pp.1–17.
- Hatcher, J.M., Pennell, K.D. & Miller, G.W., 2008. Parkinson's disease and pesticides: a toxicological perspective. *Trends in Pharmacological Sciences*, 29(6), pp.322–329.
- Hopkins, A.L., 2008. Network pharmacology: the next paradigm in drug discovery. *Nature Chemical Biology*, 4(11), pp.682–690.
- Kaestli, L.-Z. et al., 2008. Use of Transdermal Drug Formulations in the Elderly. *Drugs & Aging*, 25(4), pp.269–280.
- Klein, C. & Westenberger, A., 2012. Genetics of Parkinson's Disease. , pp.363–369.
- Maiti, P. et al., 2017. Current understanding of the molecular mechanisms in Parkinson's disease: Targets for potential treatments. *Translational Neurodegeneration*, 6(1), pp.1–35.
- Maresova, P. et al., 2016. Alzheimer's and Parkinson's Diseases: Expected Economic Impact on Europe-A Call for a Uniform European Strategy. *Journal of Alzheimer's disease*, 54(3), pp.1123–1133.
- Mariani, E. et al., 2005. Oxidative stress in brain aging, neurodegenerative and vascular diseases: An overview. *Journal of Chromatography B*, 827(1), pp.65–75.
- Oertel, W.H., 2017. Recent advances in treating Parkinson's disease. *F1000Research*, 6, p.260.
- Okimoto, N. et al., 2009. High-Performance Drug Discovery: Computational Screening by Combining Docking and Molecular Dynamics Simulations D. Case, ed. *PLoS Computational Biology*, 5(10), p.e1000528.
- Parhi, P., Mohanty, C. & Sahoo, S.K., 2012. Nanotechnology-based combinational drug delivery: An emerging approach for cancer therapy. *Drug Discovery Today*, 17(17–18), pp.1044–1052. Available at: <http://dx.doi.org/10.1016/j.drudis.2012.05.010>.
- Ravichandran, R., 2009. Nanoparticles in drug delivery: Potential green nanobiomedicine applications. *International Journal of Green Nanotechnology: Biomedicine*, 1(2).
- Rodriguez-Aller, M. et al., 2015. Strategies for formulating and delivering poorly water-soluble drugs. *Journal of Drug Delivery Science and Technology*, 30, pp.342–351. Available at: <http://dx.doi.org/10.1016/j.jddst.2015.05.009>.

Shah, S., Prabhu, P. & Gundad, S., 2011. Formulation development and investigation of domperidone transdermal patches. *International Journal of Pharmaceutical Investigation*.

Ullah, N. et al., 2018. Dexibuprofen nanocrystals with improved therapeutic performance: Fabrication, characterization, in silico modeling, and in vivo evaluation. *International Journal of Nanomedicine*, 13, pp.1677–1692.

## CHAPTER 2

### 2. Background on Domperidone

#### 2.1 Introduction

Parkinson's disease, also known as originally known as “shaking palsy” is the second most common degenerative disorder, which embodies a growing burden known to have affected more than 7 million people worldwide with an average age of 60 years, showing it to be prevalent among the aged (Lewis 2012; Zampieri et al. 2010). Parkinson's disease is a movement disorder with dopamine producing neurons and substantia nigra undergoing degeneration. And its progressive adult onset disease and it gets more common with age affecting about 1% of people over 60 years (Tysnes & Storstein 2017).

Most of the time there is no known cause but in a few cases there might be a genetic cause like mutation and currently there are eight genes (PINK 1, PARKIN, LRRK2, SNCA, DJ-1, ATP13A2, EIF4G1 and VPS35) (Kong et al. 2014; Erer et al. 2016). It is widely accepted that genetic factors combined with environmental risk factors make for the risk factors. Figure 2.1 portrays effects various risk factors that are associated with PD.

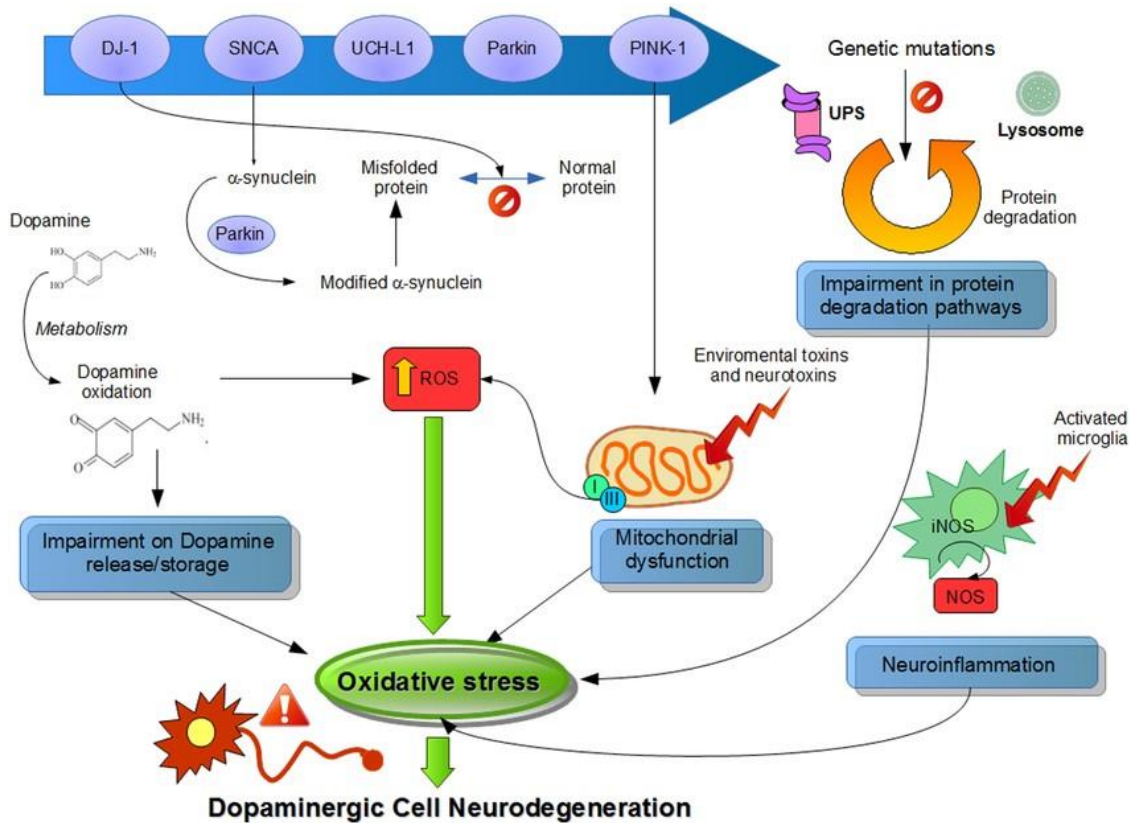


**Figure 2.1:** A diagram of Risk factors that are associated with Parkinson’s disease. The diagram shows multiple factors that exacerbate oxidative stress and thus resulting in Dopaminergic Cell Neurodegeneration.

Presently, the pharmacological and non-pharmacological (surgical and electrodes e.t.c.) regiments endorsed for PD offer only symptomatic relief for patients. As these regiments are not able to halt or reverse the neurodegenerative process, PD remains incurable. The motor symptoms can be reduced by many drugs that increase the DA level in the central nervous system (CNS) or mimic its effects. The gold standard for the treatment of PD nowadays is Levodopa, a DA precursor (Politis & Lindvall 2012). The prodrug that adequately addresses motor symptoms. Figure 2.2 shows some of the key medicines that are used individually or as adjuncts in treating PD symptoms.

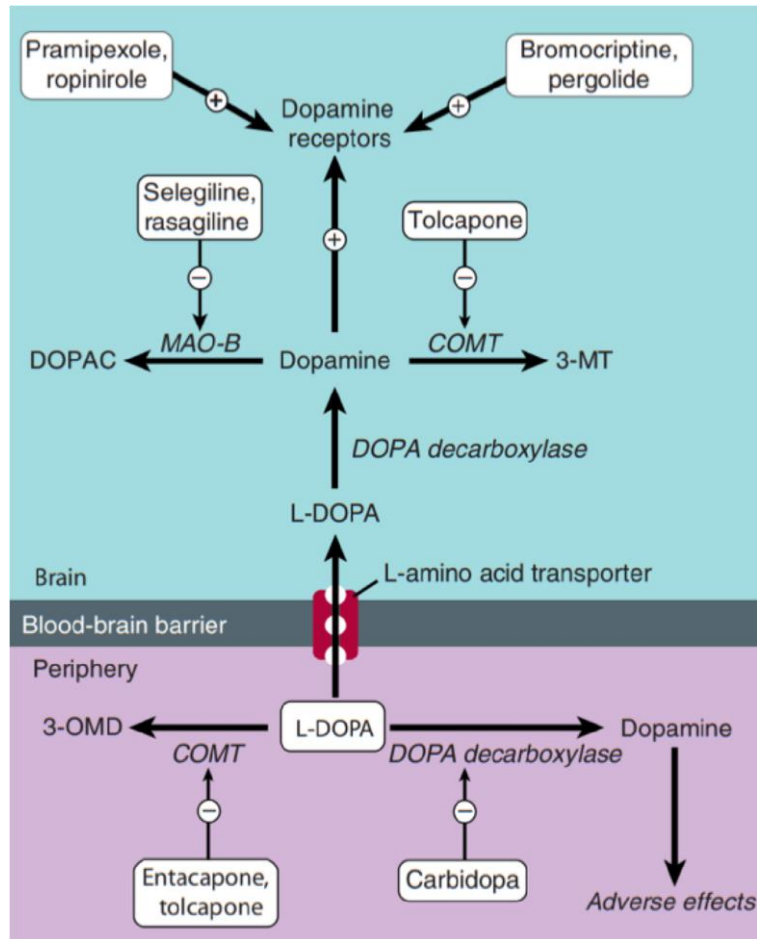


**Figure 2.2:** The key drugs in the Parkinson's symptoms .

Parkinson's disease is thought to be caused by too little of a naturally occurring substance (dopamine) in the brain (Fernandez 2012). Levodopa changes into dopamine in the brain, helping to control movement. Carbidopa prevents the breakdown of levodopa in the bloodstream so more levodopa can enter the brain. Carbidopa can also reduce some of levodopa's side effects such as nausea and vomiting (Olanow et al., 2014)(Figure 2.3).

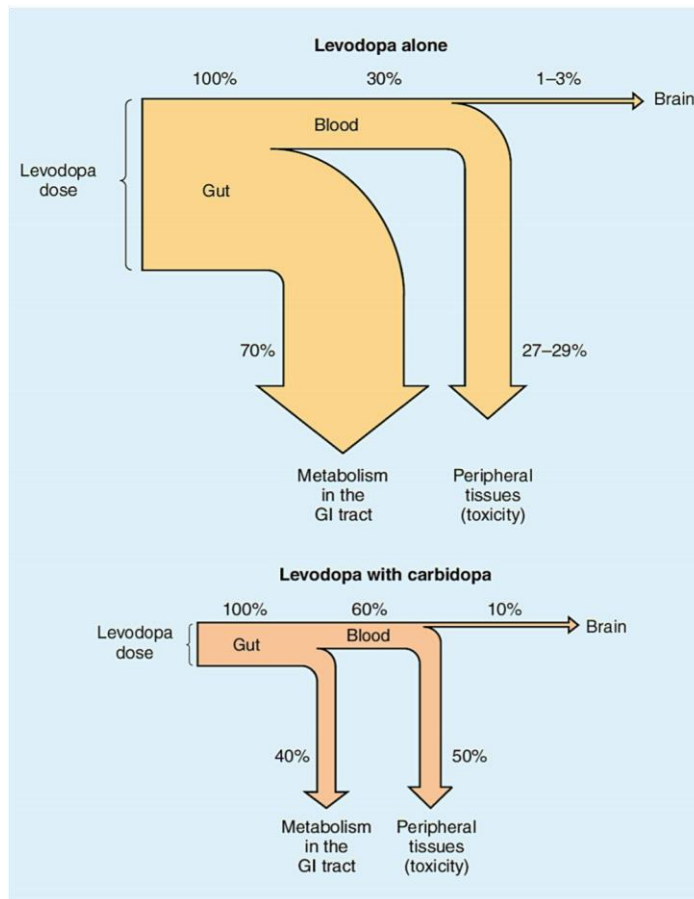


**Figure 2.3:** Complete diagram of the distribution and metabolism of Levodopa and Levodopa/Carbidopa. Levodopa alone yields less dopamine than Levodopa administered with carbidopa into the brain thus Levodopa with Carbidopa is more efficacious.

Literature throughout the medical field confirms PD is caused by the deficiency of naturally occurring dopamine in the brain, which regulate movement. Carbidopa counteracts the catabolism of levodopa's side effects (Zibetti et al., 2014). Unfortunately these peripheral inhibitors do not sufficiently curb side effects caused by Levodopa, metoclopramide and other centrally acting dopamine.

## 2.2 Discovery and structure of Domperidone

From the time of its synthesis in 1974 by Janssen pharmaceuticals Domperidone has been employed as an antiemetic, gastroprokinetic agent and galactagogue (Smolina et al., 2016). Figure 2.4 projects the structure of this unique dopamine antagonist. It was confirmed that domperidone is in circulation in 58 countries,

encompassing Canada, and there is a global ordeal in using this agent, both as a remedy for gastroparesis as well as a general antiemetic. A cogent antidote to nausea and vomiting associated with the peripheral formation of dopamine due to Parkinson's treatment, namely levodopa and bromocriptine. Although both metoclopramide and domperidone have similar anti-emetic properties, domperidone has a greater advantage than metoclopramide in that it does not cross the blood-brain barrier, therefore it has reduced central nervous system effects like drowsiness and therefore preferred to metoclopramide. The clinical use of metoclopramide, particularly for chronic treatment, is additionally dwindled by its capability of unfavorable effects like drowsiness, akathisia, restlessness syndrome, insomnia, lassitude, and fatigue. The unique structure of has a bearing on its more tolerable effects that are yet to be computationally investigated using quantitative structure-activity relationship.

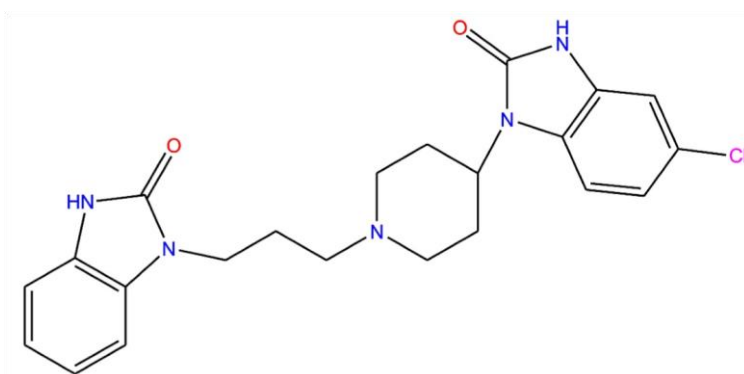


**Figure 2.4:** The 2D structure of Domperidone

### ***2.3 Domperidone's Unique Mechanism Of Action***

Domperidone is a unique peripheral *Dopamine*<sub>2</sub>-receptor (DA<sub>2</sub>) antagonist which is related to haloperidol and other butyphenone tranquilizers, but different to the benzamides such as metoclopramide and cisapride. Its manner of action and chemistry separate it from other gastrokinetic drugs. As such it is an adherent to D2 subtype receptors in the brain and stomach. Regardless of its nominal level of CNS action, domperidone is a potent antiemetic. Such potency is indicative of its action at the (CTZ), which is situated in the fourth ventricle of the brain yet external to the blood-brain barrier (Reddymasu et al., 2007a) (Figure 2.5).

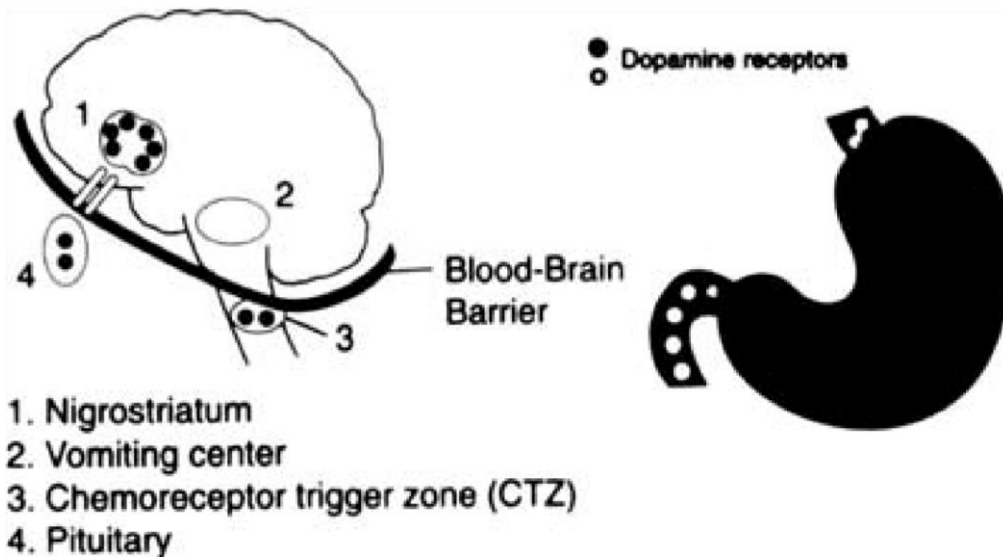


**Figure 2.5:** Mechanisms of action of domperidone (Reddymasu et al., 2007b)

***2.4 Domperidone is a drug with multiple uses in the field of medicine:***

Many of the mainstream PD drugs, namely Levodopa, bromocriptine, Ropinirole, Pramipexole, Carbergoline and other centrally acting drugs .Therefore , Domperidone has many uses within the pharmaceutical arena. Over the past decades it has been employed as an antiemetic and prokinetic. Its use as a galactagogue is still under investigation in many countries where it has been accepted. Figure 2.6 demonstrates the many medical conditions in which DOMP is utilized.

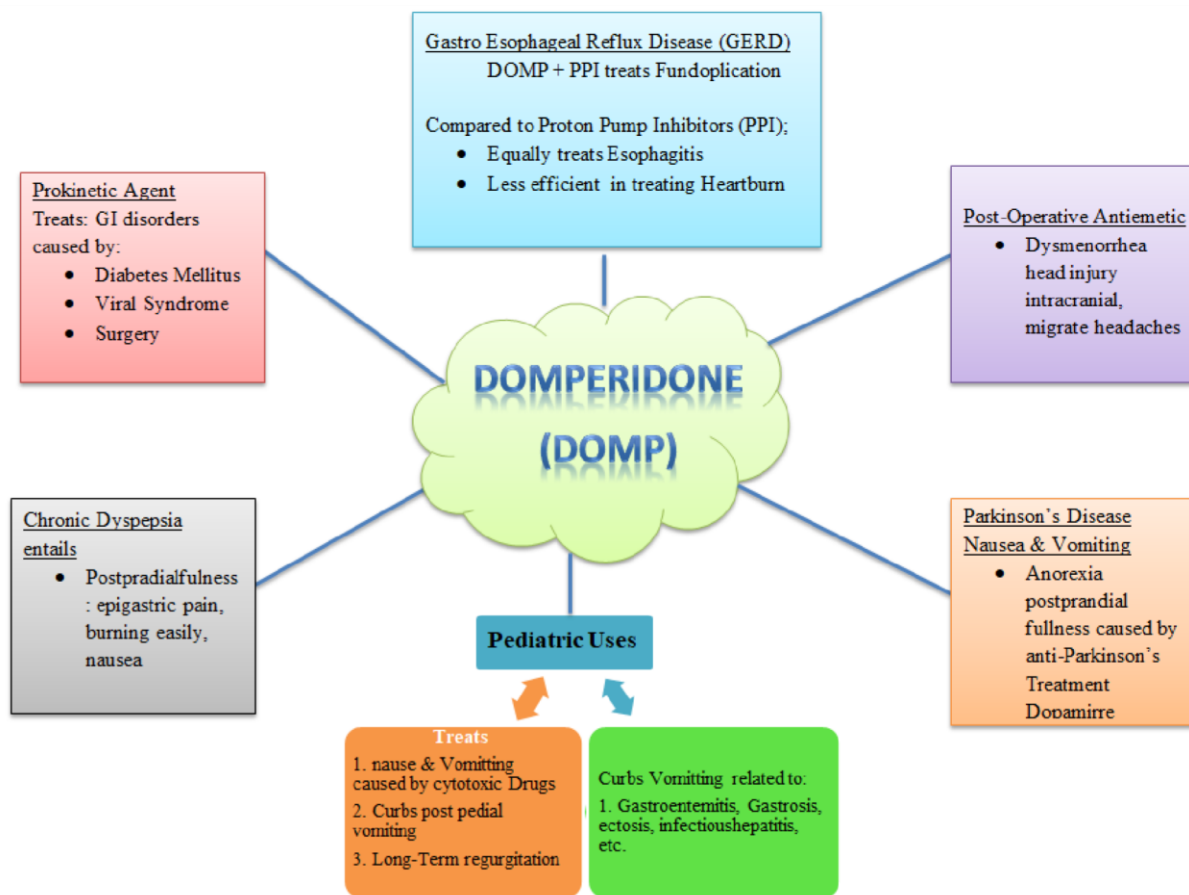


**Figure 2.6 :** Known mainstream uses of Domperidone (Prepared by author).

### ***2.5 Physicochemical properties of DOMP and its effects on various routes of administration***

Domperidone has been availed all over the world in sundry dosage forms namely oral tablet, oral solution and rectal suppository (Palem et al., 2013). It wields a molecular weight of 425.9. Time taken to reach plasma peak levels ranges from 10 to 30min reliant on whether it is given by intramuscular (IM) or oral administration (30min). Even though the bioavailability of IM administration is high the anti-emetic has been proven to present intense adverse effects such as dystonia, galactorrhoea, and gynaecomastia at high concentrations especially with parenteral administrations (Brück 2002). When given by injection has also been associated with convulsions, arrhythmias, and cardiac arrest (Rocha & Barbosa 2005). Such fatalities have restricted these routes of administration. On the other hand, the oral route of administration has a trifling bioavailability of 13-17%, and limited plasma half-life 7-9 hrs. This is likely to be caused by

inadequate assimilation coupled with a first pass effect with oral dispensation. For the relief of nausea and vomiting in PD patients, domperidone is taken for up to 12 weeks, which necessitates sustained regimen (Shazly et al., 2018; Palem et al., 2013).

### 2.6 Transition of DOMP-nanopolymers from transdermal to oral route of administration

On the basis of the promising outcomes transdermal patches of nausea and vomiting, the domperidone oral administration can be adopted as a controlled drug delivery system for medication of the same symptoms in PD (Ahmed et al., 2018). The investigation of the transdermal polymeric delivery using patches has already shown through *in vitro* cellophane and *in vivo* rabbit formulations that a release of more than 32.50% can easily be attained within a 24 h period. Even though work has already been made towards the advancement of domperidone transdermal patches, there is a great demand to transition to oral delivery intense pharmacokinetic and pharmacodynamics research would be necessary to launch the usefulness of oral delivery (Shah et al., 2011). Fig 2.9 below gives a snippet of advantages and disadvantages, thus validating emergent move reconsider adoption of oral administration for DOMP nanopolymers.

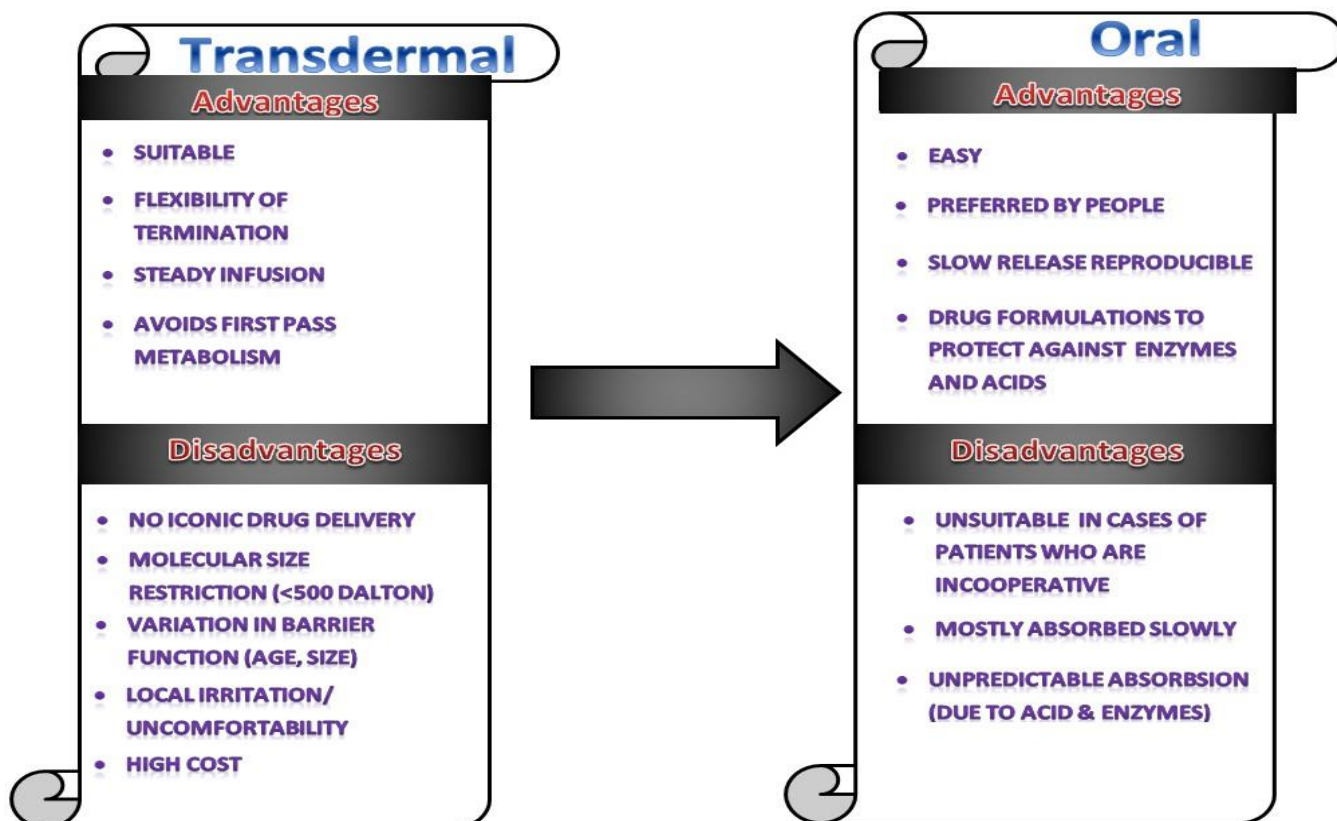


**Figure 2.7:** Summary of considerations to be made upon transition to oral administration of drugs (Prepared by Author).

## 2.7 Adverse effects and low solubility of Domperidone

Domperidone is deemed a choice prospect since it is the most tolerable drug among the antiemetics largely due to its action being restricted to the peripheral nervous system, while metoclopramide has a great deal of blockade interaction with  $D_2$ -Receptors (Prajapati & Patel 2010; Paradkar et al. 2016). Even though its effects do not result from the central nervous system CNS they still pose significant concern since they affect patient adherence and have been suspected to have deleterious effects on the cardiac system among other adverse effects (van Noord et al. 2010; Hashmi & Al-Salam 2015; Boyce et al. 2012). Figure 2.8 highlights some of the adverse effects that are associated with Domperidone.

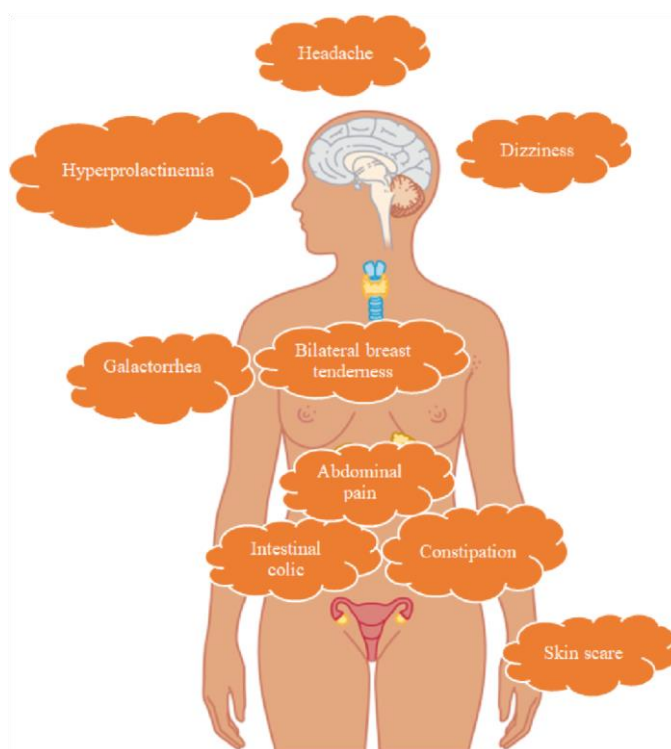


**Figure 2.8:** Adverse effects of Domperidone (Prepared by Author).

## 2.8 The emergence of polymers salvaging the drug crisis in Parkinson's disease

Both in the near- and medium-duration, we can anticipate the boom of a plethora of drug Nano-polymeric delivery transport utilization(Ullah et al. 2018). Even as both organic and inorganic science is work in progress, controlled-release polymer tools and liposomes will possibly persist to have the most immense clinical influence for the near future. It is broadly believed that with continued resources, medicine and the area of drug transport will be a significant recipient of nanotechnology for years to come(RodriguezAller et al. 2015).

Deficient aqueous solubility is the critical limiting area of plenty of drug candidates in their developing initiative in the world market regardless of having promising pharmacokinetic action. The low water solubility of drug issues into low dissolution rate with consecutive limited and irregular absorption and eventually bounds the clinical efficiency(Rodriguez-Aller et al. 2015). The advancement of polymers is the new arsenal to the pathways of pharmaceutical companies. Employing nanotechnology makes it attainable to boost the transport of insufficiently water-soluble medicine; intended relay of drugs in a cell- or tissue-precise approach; transcytosis of drugs beyond tight epithelium and endothelial membranes(Alam et al. 2010); transport large macromolecule drugs to intracellular areas of operation; multi-transport of drugs or curative approach for joint therapy; determination of locations of drug transport by joining curative agents with the imaging approaches; and real-time read on the *in vivo* efficiency of a therapeutic agent. The above are some of the many compelling rationales that nanotechnology carries immense possibilities for drug transport (Farokhzad & Langer n.d.).

There are sundry characteristics that are essential for profitable enhancement and production of targeted drug transport carriers that are employed in the treatment of neurodegenerative disease among others (Gu et al. 2008; Decuzzi et al. 2009). Figure 2.9 demonstrates three of the most essential qualities of any given polymeric nanoparticle for use in pharmaceutical formulations.

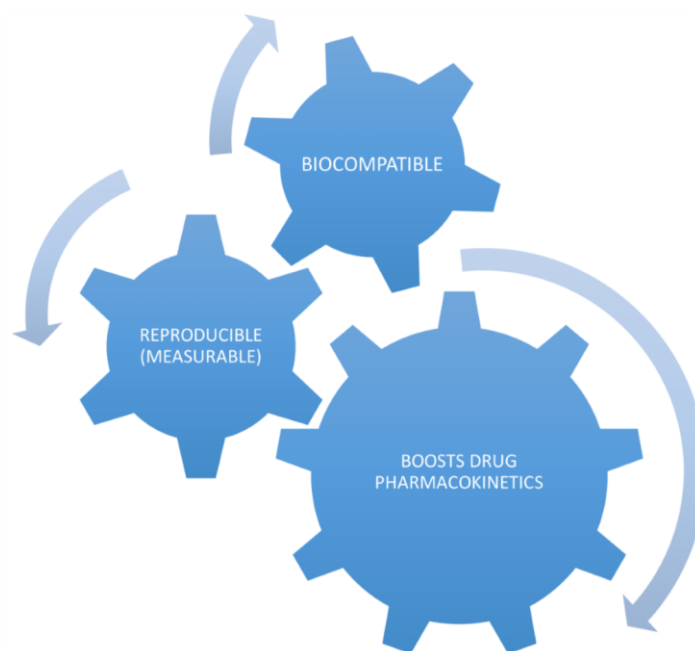


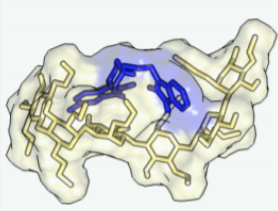
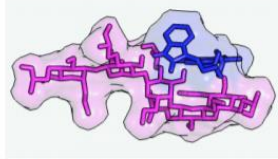
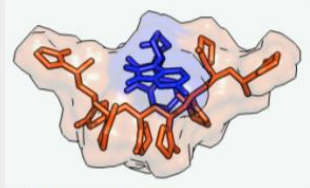
**Figure 2.9:** Essential qualities of polymeric nanoparticle in formulations (Prepared by Author)

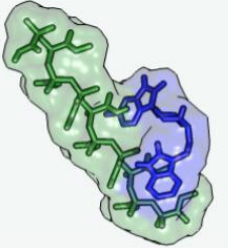
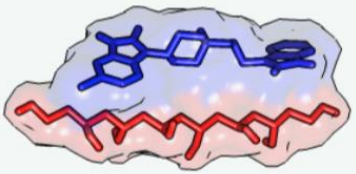
The advancement of polymeric nanoparticles (NPs) for targeted transport and controlled drug discharge likely boosts the therapeutic index (beneficial range) of medicines (Masood 2016). Such an enhancement is particularly important when dispensing low solubility drugs that have toxicities that usually reduce their dose, resulting in suboptimal efficiency (Rodriguez-Aller et al. 2015).

### ***2.9 The inevitable merge of Nano polymers with computational chemistry***

Nano-drug transport methods are performing a vital task in conquering these obstacles and ushers to fresh avenues for effective therapy in neurodegenerative disease. Domperidone, a poorly water-soluble  $d_2$ receptor antagonist, has long been reported to have antiemetic properties a broad spectrum of nanoparticles has been refined and used efficiently (Venkatesh et al., 2006). Diversified forms of lipophilic and hydrophilic parkinsonian drugs can be conjugated with assorted nanoparticles. The unification of molecular modeling with experimental verdict has been largely embraced in biomedical research, containing material science (Silindir Gunay et al., 2016). The molecular modeling implements are capable of providing more morphological acumen into polymer-target interactions when experimental methods fail to operate large molecular complexes (Ullah et al., 2018).

**Table 2.1: Showing choice polymers and their properties**

Names of Polymers	Qualities and Advantages	Approved /Not Approved History of Usage
 <p><b>Figure 1: Ethocel</b></p>	<ul style="list-style-type: none"> <li>• Ethyl cellulose is a cellulose derivative</li> <li>• Flexible; Organosoluble,</li> <li>• Thermoplastic polymer</li> <li>• Thin film to accommodate</li> <li>• swelling-shrinking transitions</li> </ul>	<ul style="list-style-type: none"> <li>• Approved to improve the strength and appearance of tablets and capsules</li> <li>• Showed good results in controlled release of Ibuprofen</li> </ul>
 <p><b>Figure 2: HPMC</b></p>	<ul style="list-style-type: none"> <li>• Mixed with ethers of cellulose able to by-pass the stomach and discharge the loaded medicine</li> <li>• Protective lining shields drug from early release in gastric intestinal system.</li> </ul>	<ul style="list-style-type: none"> <li>• Research shows HPMC to boost the bioavailability of poorly soluble albendazole and nilvadipine</li> </ul>
 <p><b>Figure 3: PVP</b></p>	<ul style="list-style-type: none"> <li>• Regarded harmless (with few allergic reactions)</li> <li>• therefore, naturally passes through the body.</li> <li>• Binder in pharmaceutical tablets and in normal dose.</li> <li>• Possess good water solubility and thus improved wetting and eventually enhanced dissolution</li> </ul>	<ul style="list-style-type: none"> <li>• FDA approved-</li> <li>• Regarded as non-toxic when given orally</li> <li>• E.g. Improves dissolution rate of Flufenamic acid</li> </ul>

 <p><b>Figure 4: Eudagrit (EUD)</b></p>	<ul style="list-style-type: none"> <li>• Able to by-pass first-pass effect exceptional encapsulation efficacy of roughly 94-98%</li> <li>•</li> <li>• Protective lining shields stomach release</li> </ul>	<ul style="list-style-type: none"> <li>• Approved</li> <li>• Eudagrit L boosted the bioavailability of Griseofulvin and Spirolactone</li> </ul>
 <p><b>Figure 5: Pluronic</b></p>	<ul style="list-style-type: none"> <li>• Possess a handy amphiphilic structure</li> <li>• ability to hike the solubility of hydrophobic and oily materials</li> <li>• Gelling behavior – namely, sol- gel transition (can be influenced by salts and alcohols)</li> </ul>	<ul style="list-style-type: none"> <li>• Approved</li> <li>• Increased the dissolution of Cefixime (BSC IV) in a rat experiment.</li> <li>• (Pluronic cefixime)</li> </ul>
 <p><b>Figure 6: PVA</b></p>	<ul style="list-style-type: none"> <li>• Hydrophilic man-made polymer:</li> <li>• adhesive qualities efficient in film; odorless and non-toxic impervious to grease</li> <li>• lofty tensile strength and elasticity</li> </ul>	<ul style="list-style-type: none"> <li>• Approved film for food and pharmaceuticals.</li> <li>• PVA in a drug /nicotinamide/polymer of 1:3: 1 dissolved 20times faster than the drug alone.</li> </ul>

The use of polymeric nanocrystals in molecular modelling is young and developing branch, however it is not an entirely new. There is enough work that has been done to confirm the enormous potential this arena has in combination with molecular modelling and computational chemistry (Ullah et al., 2018). In combined experimental and computational chemistry study, all of the above mentioned polymeric nanoparticles (PVA,PVP,HPMC, EUD, Pluronic and Ethocel researchers proved to have a lofty dissolution rate and significant boost therapeutic on the potential was achievable even with a drug of low solubility (BSC II)(Gulzar et al. 2015; Ndlovu et al., 2019). This research will provide molecular insight into methods of binding of optimal polymers to the surfaces of domperidone.

## **References 2.10**

- Ahmed, S. et al., 2018. Experimental and molecular modeling approach to optimize suitable polymers for fabrication of stable fluticasone nanoparticles with enhanced dissolution and antimicrobial activity. *Drug Design, Development and Therapy*, 12, pp.255–269.
- Alam, M.I. et al., 2010. Strategy for effective brain drug delivery. *European Journal of Pharmaceutical Sciences*, 40(5), pp.385–403.
- Boyce, M.J., Baisley, K.J. & Warrington, S.J., 2012. Pharmacokinetic interaction between domperidone and ketoconazole leads to QT prolongation in healthy volunteers: A randomized, placebo-controlled, double-blind, crossover study. *British Journal of Clinical Pharmacology*, 73(3), pp.411–421.
- Brück, C., 2002. Drug interactions in the treatment of Parkinson 's disease. , pp.24–29.
- Decuzzi, P. et al., 2009. Intravascular delivery of particulate systems: Does geometry really matter? *Pharmaceutical Research*, 26(1), pp.235–243.
- Erer, S. et al., 2016. Mutation analysis of the PARKIN, PINK1, DJ1, and SNCA genes in Turkish earlyonset Parkinson's patients and genotype-phenotype correlations. *Clinical Neurology and Neurosurgery*, 148, pp.147–153.
- Farokhzad, O. & Langer, R., Impact of Nanotechnology on Drug Discovery & Development *Pharmanext.* , 3(1), pp.16–20.
- Fernandez, H.H., 2012. Updates in the medical management of Parkinson disease. *Cleveland Clinic Journal of Medicine*, 79(1), pp.28–35.
- Gu, F. et al., 2008. Precise engineering of targeted nanoparticles by using self-assembled biointegrated block copolymers. *Proceedings of the National Academy of Sciences*, 105(7), pp.2586–2591.
- Gulzar, A. et al., 2015. Stimuli responsive drug delivery application of polymer and silica in biomedicine. *Journal of Materials Chemistry B*, 3(44), pp.8599–8622.
- Hashmi, S. & Al-Salam, S., 2015. Acute myocardial infarction and myocardial ischemia-reperfusion injury: A comparison. *International Journal of Clinical and Experimental Pathology*, 8(8), pp.8786– 8796.

- Kong, S.M.Y. et al., 2014. Parkinson's disease-linked human PARK9/ATP13A2 maintains zinc homeostasis and promotes  $\alpha$ -Synuclein externalization via exosomes. *Human Molecular Genetics*, 23(11), pp.2816–2833.
- Lewis, P.A., 2012. James Parkinson: The man behind the Shaking Palsy. *Journal of Parkinson's Disease*, 2(3), pp.181–187.
- Masood, F., 2016. Polymeric nanoparticles for targeted drug delivery system for cancer therapy. *Materials Science and Engineering C*.
- Ndlovu, S.T. et al., 2019. Domperidone nanocrystals with boosted oral bioavailability: fabrication, evaluation and molecular insight into the polymer-domperidone nanocrystal interaction. *Drug Delivery and Translational Research*, 9(1), pp.284–297.
- van Noord, C. et al., 2010. Domperidone and Ventricular Arrhythmia or Sudden Cardiac Death. *Drug Safety*, 33(11), pp.1003–1014.
- Olanow, C.W. et al., 2014. Continuous intrajejunal infusion of levodopa-carbidopa intestinal gel for patients with advanced Parkinson's disease: A randomised, controlled, double-blind, double-dummy study. *The Lancet Neurology*, 13(2), pp.141–149.
- Palem, C.R. et al., 2013. Oral transmucosal delivery of domperidone from immediate release films produced via hot-melt extrusion technology. *Pharmaceutical Development and Technology*, 18(1), pp.186–195.
- Paradkar, M., Gajra, B. & Patel, B., 2016. Formulation development and evaluation of medicated chewing gum of anti-emetic drug. *Saudi Pharmaceutical Journal*.
- Politis, M. & Lindvall, O., 2012. Clinical application of stem cell therapy in Parkinson's disease. *BMC Medicine*, 10, pp.1–7.
- Prajapati, B.G. & Patel, D. V., 2010. Formulation and optimization of domperidone fast dissolving tablet by wet granulation techniques using factorial design. *International Journal of PharmTech Research*, 2(1), pp.292–299.
- Reddymasu, S.C., Soykan, I. & McCallum, R.W., 2007a. Domperidone: Review of pharmacology and clinical applications in gastroenterology. *American Journal of Gastroenterology*.

- Reddymasu, S.C., Soykan, I. & McCallum, R.W., 2007b. Domperidone: Review of Pharmacology and Clinical Applications in Gastroenterology. *The American Journal of Gastroenterology*, 102(9), pp.2036–2045.
- Rocha, C.M.G. & Barbosa, M.M., 2005. QT Interval Prolongation Associated with the Oral Use of Domperidone in an Infant. *Pediatric Cardiology*, 26(5), pp.720–723.
- Rodriguez-Aller, M. et al., 2015. Strategies for formulating and delivering poorly water-soluble drugs. *Journal of Drug Delivery Science and Technology*, 30, pp.342–351.
- Shah, S., Prabhu, P. & Gundad, S., 2011. Formulation development and investigation of domperidone transdermal patches. *International Journal of Pharmaceutical Investigation*.
- Shazly, G.A. et al., 2018. Development of Domperidone Solid Lipid Nanoparticles: In Vitro and In Vivo Characterization. *AAPS PharmSciTech*, 19(4), pp.1712–1719.
- Silindir Gunay, M., Yekta Ozer, A. & Chalon, S., 2016. Drug Delivery Systems for Imaging and Therapy of Parkinson's Disease. *Current Neuropharmacology*, 14(4), pp.376–391.
- Smolina, K. et al., 2016. Postpartum domperidone use in British Columbia: a retrospective cohort study. *CMAJ Open*, 4(1), pp.E13–E19.
- Tysnes, O.-B. & Storstein, A., 2017. Epidemiology of Parkinson's disease. *Journal of Neural Transmission*, 124(8), pp.901–905.
- Ullah, N. et al., 2018. Dexibuprofen nanocrystals with improved therapeutic performance: fabrication, characterization, in silico modeling, and in vivo evaluation. *International Journal of Nanomedicine*, 13, pp.1677–1692.
- Venkatesh, D.N. et al., 2006. Dissolution Enhancement of Domperidone Using Water Soluble Carrier By Solid Dispersion Technology. , 100(100), pp.221–226.
- Zampieri, C. et al., 2010. The instrumented timed up and go test: Potential outcome measure for disease modifying therapies in Parkinson's disease. *Journal of Neurology, Neurosurgery and Psychiatry*, 81(2), pp.171–176.
- Zibetti, M. et al., 2014. Levodopa/carbidopa intestinal gel infusion in advanced Parkinson's disease: A 7 year experience. *European Journal of Neurology*, 21(2), pp.312–318.

## CHAPTER 3

### 3.1 Introduction

Computational chemistry is a field in chemistry which deals with the use of mathematical theories using computer simulation of chemicals and biochemical systems with the intent of acquiring solutions to medical challenges. This allows scientists to study chemical reactions virtually through the use of computers as opposed to empirical chemical reactions in a laboratory. Computational chemistry encompasses a variety of methods and theories, which contribute to solving problems in chemistry. This means atomic interactions can be portrayed in two ways: quantum mechanics (QM) and molecular mechanics (MM)(Jensen n.d.; Gil et al., 2011). Quantum mechanics solely focuses on electrons, and electron distribution is used to model the interaction between atoms. Whereas Molecular Mechanics uses atoms and focuses on classical Newtonian mechanics; modeling atomic interactions as a function of bond angles and bond length, non-bonded forces, and dihedral angles. This chapter gives an introduction to the computational and theoretical tools applied in this study. Theories used in MM and molecular dynamics (MD) applicable to the current study namely Schrödinger equation, the Born-Oppenheimer approximation and potential surface energy (PES).

### 3.2 Quantum Mechanics

Quantum Mechanics is a theory that describes the wave-like motion of sub-atoms particles, having discovered that electrons did not follow the Newtonian motion. Quantum Mechanics (QM) is one of the most well-decorated aspects of physics. The fundamentals of QM were laid down on Matrix Mechanics in the 20th century by a group of German scientists and later, in 1926 Erwin Schrödinger advanced wave mechanics, which is presently a key player in explaining quantum phenomena. The quantum theory interprets the behavioural characteristics of sub-atomic particles, namely electrons at a nanoscopic level. (Shrodinger1926). The electrons of an atom are considered as small sachets of energy i.e. quantum particles. Different energy states are correlated with peculiar quantum numbers. The allocation of quantum numbers is guided by particle properties such as; the spin of particle and electronic state of each molecule. Whether by release or addition, the shift in energy ensues in the form of a photon which is computed into a wave. The investigation of a biomolecule by QM involves the layout of nuclei with analogous electrons, in a three-dimensional zone. The electrons are profiled using the continuous electron density method, and the energetics quantified were expounded by the Schrödinger equation whereas Born-Oppenheimer approximation coupled with the Hartree-Fock self-consistent field which maps density of the system.

#### 3.2.1 The Schrödinger equation

Regular Newtonian physics is insufficient in explaining or describing the behavior of small particles such as nuclei and electrons. Schrodinger's equation is elementary to modern physics; it describes the conduct

of electrons in a molecule as wave-like action and how the molecular system transcends time (wave mechanics). QM explains Schrödinger's equation and displays the interaction in terms of a wave-like function, which is a mathematical function that is used to estimate the electron distribution. Using electron distribution other characteristics of a molecule can be concluded, e.g. the part of the molecule that is prone to nucleophilic or electrophilic attack. In the realm of computational chemistry, the time-dependent equation is the most widely used among Schrödinger's equations, which is dependent on time and average of a system (time-dependent wave operation,  $\Psi$ ). The plainest expression of the Schrödinger equation is given as a sum of its operators:

$$H\Psi = E\Psi \quad (3.1)$$

$$H = T + V \quad (3.2)$$

Where H is the Hamiltonian operator (total energy of a system), T is the kinetic energy operator of the system and V is the potential energy operator. The Hamiltonian operator can also be detailed as:

$$H = \left[ -\frac{\hbar^2}{8\pi^2} \sum_i \frac{1}{m_j} \left( \frac{\partial^2}{\partial x^2} + \frac{\partial^2}{\partial y^2} + \frac{\partial^2}{\partial z^2} \right) \right] + \sum_i \frac{e_i e_j}{r_{ij}} \quad (3.3)$$

The Schrödinger equation is highly complicated, and it constitutes a multitude of mathematical equations and cannot be solved for a molecular system, nevertheless, an answer can be given by a compensatory Born-Oppenheimer approximation.

### 3.2.2 Born-Oppenheimer Approximation Theory

Max Born and J Robert Oppenheimer, who were physicists in their own right, submitted the Born-Oppenheimer approximation, which solves the perceived problem of segregation of nuclei wave function to that of the electrons. Electrons are considered to be lighter weight to that of nuclei, thus possessing increasing velocity and move rapidly to nuclei motion (Pisana et al. 2007). Therefore, the location of electrons molecules is determined by the location of the nuclei. This gives room for the Schrödinger equation to be solved for the kinetic energy of the electrons alone since the kinetic energy for the nuclei will remain steady. (Woolley, 1991; Gu et al, 2008; Wudka, 1990; Bludman, 1954). The disparity in velocities of nuclei and electrons permits the use of the Born-Oppenheimer approximation, reducing the complexity of the wave function of the Hamiltonian equation.

The simplified wave function:

$$\Psi(r_{elec}) = \Psi(r_{elec}) (\Psi(r_{nucl})) \quad (3.4)$$

Equation (4) is converted:

$$H_{EN} \Psi(r_{elec}) = E_{EN} \Psi(r_{elec}) \quad (3.5)$$

Whereby  $H_{EN}$  articulates a contrast between terms based interaction with fixed nuclear positions ( $V_{NN}$ )

or their interaction with the non-fixed electron positions. Eq. (3.6) shows  $E_{EN}$ , which is derived from 2 sources being the oscillating electron co-ordinates and fixed nuclear coordinates.

$$(H_{el} + V_{NN}) \Psi(r_{el}) = E_{EN} \Psi(r_{el}) \quad (3.6)$$

The most plausible explanation of the electron motion within a molecule is given by the electronic Schrödinger equation, which is most accurate when applied to the ground electronic states. Evaluation of equilibrated states and construction of the potential energy surface curve may only be done when the equation has been resolved (Deslauriers & Wieman 2011).

### 3.2.3 Potential Energy Surface

The potential energy surface is a mathematical connection, often presented graphically, between the energy of a molecule with its geometry by working out solutions to the time-dependent Schrödinger equation. This theory birthed the Born-Oppenheimer approximation described above, where electrons differ in accordance with the positional state of the nuclei such a way that the potential energy surface is taken as the potential of atoms to collide with each other in a molecule (Peter W. Atkins n.d.) (Woolley 1991). A potential energy surface exhibits high potential energy domain, implying high-energy nuclear or molecular conformations and low energy domains implying low energy conformations. The potential energy surface is employed in computational chemistry to investigate the lowest energy state and the positional geometry of a molecule at this state (Peter W. Atkins n.d ; Elsayy et al., 2005).

The potential energy function is therefore described as follows:

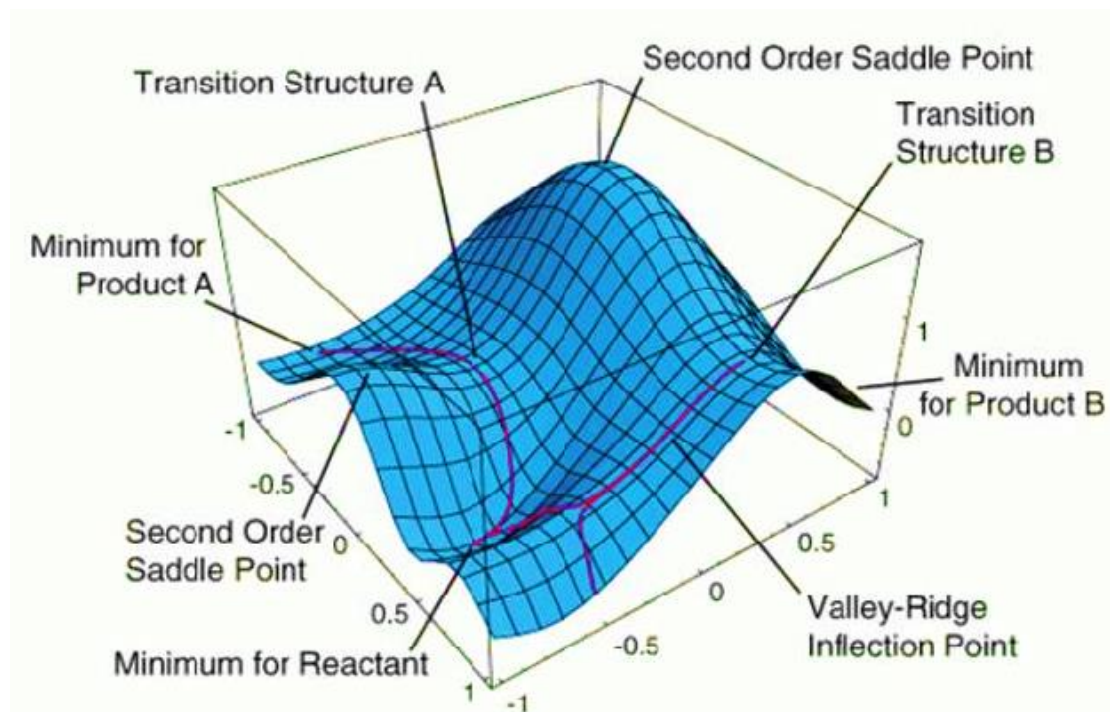


**Figure 3.1:** Graphical representation of a 2-D potential energy surface (PES).

### 3.3 Molecular docking

Molecular docking is conventionally used in structure-based drug design to determine the accurate configuration of ligand to the polymer targets and to surmise the stability of polymer-ligand interaction. Molecules such as inhibitors or other drug competitors are analyzed in the active sites of macromolecules. A macromolecule is described as a very large molecule as a colloidal particle, protein or especially a polymer composed of hundreds or thousands of atoms. The ligand-receptor binding is calculated as follows:

$$E_{binding} = E_{target} + E_{ligand} + E_{target-ligand} \quad (3.7)$$

There are ample molecular docking tools that are employed for academic and commercial purposes. There are two primary steps in docking:

1. Sampling configurations of a ligand in the binding site of the receptor molecule. Numerous conformations of the docked complex can be sampled using different algorithms to attain results.

The "lock and key" model describes the ligand-receptor as rigid structures, or the ligand may show flexibility by irregular or simulation-based methods. The latter algorithm is the most commonly used approach since it permits a more rational fit of the ligand to the polymer (Zhang et al. , 2008).

2. Using scoring functions to rank different conformations. The scoring function may be based on contracts that are more statistically favored, MM force fields or pre-existing protein-ligand binding affinities (Geng et al., 2013).

Molecular docking is associated with many discrepancies; as such docked compounds are often criticized due to incorrect binding sites or choice of the docked complex. Due to these matters, all docked complexes in this study were substantiated with MD simulations and the stability of the ligand at the binding site was displayed.

### 3.4 Molecular Mechanics

Molecular mechanics (MM) is an experimental approach whose fundamentals are revealed from the classical laws of physics in the forecasting of chemical characteristics of molecules. MM is usually employed in enormous molecular systems to estimate molecular structures and corresponding potential energies of molecular arrangements.(Case et al., 2005; Peter W. Atkins n.d.; Schrodinger, 1926). The electrons in the particular systems are absolutely ignored; however, each atom rather, specifically the atomic nuclei and related electrons are considered as a single particle. Definitive removal of electrons in the system is validated on the grounds of the Born –Oppenheimer approximation, which claims that the

electronic and nuclear motions can be disjointed from one another and accounted for individually. Energy differences between conformations are more consequential in such calculations than absolute potential energy values.

Molecular mechanics can easily be regarded as a ball-and-spring model of atoms and molecules with classical forces separating them. The aforesaid forces can be considered by the potential energy functions concerning structural aspects being bond length, bond angle, and torsional angles. The potential energies are armed with parameters tailored to duplicate experimental qualities (Jaquet 2002). The total potential energy of a molecule is defined as the sum of bond-stretching energy ( $E_{str}$ ), the bond angle-bending energy ( $E_{bend}$ ), torsion energy ( $E_{tor}$ ) and energy of interactions between non-bonded atoms ( $E_{nb}$ ). The energy contributions of the latter constitute van der Waals and electrostatic interactions, such that:

$$E_{tot} = E_{str} + E_{bend} + E_{tor} + E_{vdw} + E_{elec} \quad (3.8)$$

Where  $E_{tot}$  stands for the total potential energy,  $E_{str}$  the bond-stretching energy,  $E_{bend}$  the bond angle-bending energy,  $E_{tor}$  the torsional energy,  $E_{vdw}$  the van der Waals forces and  $E_{elec}$  the electrostatic forces separating atoms which are chemically non-bonded. Energy inputs from hydrogen bonding and stretch-bend pairing interactions are also explained in molecular mechanics.

### 3.4.1 Force Field

A force field is a mathematical framework, which describes complement of the energy of a system to the proportion of its particles. The commonly used sets of the parameter in bimolecular simulations are AMBER (Case et al. 2005), CHARMM, GROMOS (Christen et al., 2005), and NAMD (Fromageau et al., 2003) force fields. Customarily, parameters are captured from the data of experimental source, ab initio or semi-empirical QM. Molecules are expressed as atomic sets held by elastic forces and the force field reduces the actual potential a plain model relevant to the area that is being simulated. A vast array of force fields is investigated each with a singular degree of intricacy and each set up to treat different kinds of systems. Different force fields have pros and cons analogous to the data and the implemented strategy in its framework, depending on selective malfunction at hand. Nonetheless, they ought to be adjusted to gain a global fitting; hence force fields gravitate towards showing similar results. Herein, the AMBER force field (Pearlman et al., 1995) was applied whereby the General AMBER Force Field was applied for the ligand and the standard AMBER force field to compensate for the protein.

### 3.5 Molecular Dynamics

Molecular dynamics (MD) is a computer simulation process for analyzing the kinetics of atoms and molecules. Properties of assemblies of molecules in terms of their structure and the microscopic can be

expounded using MD simulations. In MD, complex systems are modelled at atomic level and the equations of motion are mathematically solved to indicate the time of evolution of a specific system, thus allowing a derivation of its kinetic energy and thermodynamic properties through the application of computational tools (Peter Atkins, Julio De Paula 2009; Case et al. 2005). Atomic trajectories are generated through the integration of Newton's equations of motion for atoms on an energy surface. This can be illustrated by the equation below:

$$F_1 = m_1 \frac{d^2 r_1(t)}{dt^2} \quad (3.9)$$

Where  $r_i(t)$  is the particle position vector,  $t$  is time-evolution,  $m$  is the mass of the particle and  $F_1$  depicts the interacting force on the particle.

Molecular dynamics can be categorized into four (4) continuous technical steps that are repeated numerous to generate a trajectory. The categories can be summarized by:

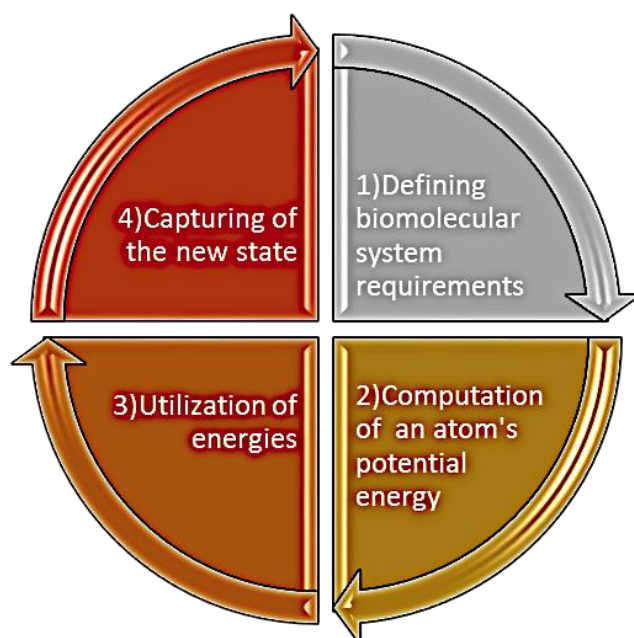


**Figure 3.1:** Cycle of molecular dynamics steps (prepared by author).

The steps are outlined below:

- 1) The fundamental requirements of the biomolecular system are defined:
  - The co-ordinates of each atom
  - The bond characteristics between each atom
  - The acceleration of atoms
- 2) Each atom's potential energy is computed.
- 3) The energies from step are then utilized to solve the equation of motion.
- 4) The new state of the system needs to be saved, and the atoms' co-ordinates changed, and

step forward in the simulation taken. The cycle then restarts from step 1.

### 3.5.1 Molecular Dynamics Post-Analysis

Molecular post-dynamic techniques and calculations have been used to describe the protein features in studies conducted in this thesis. Molecular dynamic trajectories are a product of the run molecular dynamic simulation. They can be defined as sequential snapshots characterized by both positional coordinates and velocity vectors (Shao et al., 2007). In this study, post dynamic analysis of the trajectories is critical for determining the:

- 1) Energetic and conformational stability of the biomolecular system.
- 2) The characteristics of the system's small molecule binding landscape and the thermodynamic energy fluctuations along the system's clustered trajectory.
- 3) Dynamic conformational features or variability of the biomolecular system.

#### 3.5.1.1 System Stability

##### **Convergence:**

Convergence is an empirical description of protein dynamics. It specifically describes protein dynamics based on bond types and bond angle vibrations during the unfolding of a protein. This fusion toward equilibrium and portrayal of a conclusive plateau is impertinent for a MD trajectory to be accurate and reproducible. At this plateau, the protein-ligand system displays energetically stable conformations (Galindo-Murillo et al., 2015) .

##### **Root Mean Square Deviation (RMSD):**

Spatial difference between two static structures of the same trajectory measure the deviation of a complex (Brüschweiler 2003). The RMSD of a trajectory is defined as:

$$\text{RMSD} = \frac{\sum N (R_1 - R_1^0)^2}{N} \quad (3.10)$$

##### **Root Mean Square Fluctuation (RMSF):**

The root mean fluctuation (RMSF) of a protein measures residue's  $C\alpha$  atom fluctuations is based on the average protein structure along the system's trajectory. The RMSF captures the fluctuation for each atom around its average position (Margreitter & Oostenbrink,2017; Martínez, 2015). It is calculated using the equation below:

$$\text{sRMSF} = \frac{(RMSF_1 - RMSF)}{\sigma(RMSF)} \quad (3.11)$$

Where:  $RMSF_1$  is the RMSF of the  $i$ th residue, from which the average RMSF is subtracted. This is then divided by the RMSF's standard deviation to yield the resultant standardized RMSF.

### 3.5.1.2 Binding Free Energy

Binding free energy calculations are significant in ligand-polymer systems interactions and construction, and also in other facets of computational drug design discovery (Kollman 1993 ; Kamerlin et al., 2009; Homeyer & Gohlke, 2012). Calculations of computer-based free binding energies of macromolecules and other differing molecular systems are estimated using either the Molecular Mechanics/Poisson-Boltzmann Surface Area (MMPB-SA) or Molecular Mechanics/Generalized Born Surface Area (MMGBSA) facilities (Wang et al. 2001; Kollman et al., 2000; Wang et al., 2006), which couple MM with the continuum solvation at low computational price (Wang et al., 2006). In the following studies, MMPBSA free energy calculations were used for differing molecular systems in question (Kar & Knecht, 2012). Additional explanation on free binding energy calculations has been described herein (see Chapters 3-4)

### 3.6 References

- Bludman, S. & Daitch, P.B., 1954. Validity of the Born-Oppenheimer approximation. *Physical Review*, 95(3), pp.823–830.
- Brüschweiler, R., 2003. Efficient RMSD measures for the comparison of two molecular ensembles. *Proteins: Structure, Function and Genetics*, 50(1), pp.26–34.
- Case, D.A. et al., 2005. The Amber biomolecular simulation programs. *Journal of Computational Chemistry*, 26(16), pp.1668–1688.
- Christen, M. et al., 2005. The GROMOS software for biomolecular simulation: GROMOS05. *Journal of Computational Chemistry*, 26(16), pp.1719–1751.
- Decuzzi, P. et al., 2009. Intravascular delivery of particulate systems: Does geometry really matter? *Pharmaceutical Research*, 26(1), pp.235–243.
- Deslauriers, L. & Wieman, C., 2011. Learning and retention of quantum concepts with different teaching methods. *Physical Review Special Topics - Physics Education Research*, 7(1), pp.1–6.
- Elsawy, K.M., Hodgson, M.K. & Caves, L.S.D., 2005. The physical determinants of the DNA conformational landscape: An analysis of the potential energy surface of single-strand dinucleotides in the conformational space of duplex DNA. *Nucleic Acids Research*, 33(18), pp.5749–5762.
- Farokhzad, O. & Langer, R., *Impact of Nanotechnology on Drug Discovery & Development Pharmedx*, 3(1), pp.16–20.
- Fromageau, J. et al., 2003. Characterization of {PVA Cryogel for Intravascular Ultrasound Elasticity Imaging. *IEEE transactions on ultrasonics, ferroelectrics, and frequency control*, 50(10), pp.1318–1324.
- Galindo-Murillo, R., Roe, D.R. & Cheatham, T.E., 2015. Convergence and reproducibility in molecular dynamics simulations of the DNA duplex d(GCACGAACGAACGAACGC). *Biochimica et Biophysica Acta - General Subjects*, 1850(5), pp.1041–1058.
- Geng, Y. et al., 2013. Bioassay-guided isolation of DPP-4 inhibitory fractions from extracts of submerged cultured of *Inonotus obliquus*. *Molecules*, 18(1), pp.1150–1161.
- Gu, F. et al., 2008. Precise engineering of targeted nanoparticles by using self-assembled biointegrated block copolymers. *Proceedings of the National Academy of Sciences*, 105(7), pp.2586–2591.

Hernandez, M., Ghersi, D. & Sanchez, R., 2009. SITEHOUND-web: A server for ligand binding site identification in protein structures. *Nucleic Acids Research*, 37(SUPPL. 2), pp.413–416.

Homeyer, N. & Gohlke, H., 2012. Free energy calculations by the Molecular Mechanics Poisson-Boltzmann Surface Area method. *Molecular Informatics*, 31(2), pp.114–122.

Jaquet, R., 2002. Introduction to potential energy surfaces and graphical interpretation. <http://www.tc.chemie.uni-siegen.de/jaquet/Copy-of-introPEStexpowerlight.pdf>, (April).

Jensen, F., Introduction to computational chemistry, [Accessed June 19, 2018].

Kamerlin, S.C.L., Haranczyk, M. & Warshel, A., 2009. Progress in Ab initio QM/MM free-energy simulations of electrostatic energies in proteins: Accelerated QM/MM studies of pKa, redox reactions and solvation free energies. *Journal of Physical Chemistry B*, 113(5), pp.1253–1272.

Kar, P. & Knecht, V., 2012. Origin of decrease in potency of darunavir and two related antiviral inhibitors against HIV-2 compared to HIV-1 protease. *Journal of Physical Chemistry B*, 116(8), pp.2605–2614.

Kollman, P., 1993. Free Energy Calculations: Applications to Chemical and Biochemical Phenomena. *Chemical Reviews*, 93(7), pp.2395–2417.

Kollman, P.A. et al., 2000. Calculating structures and free energies of complex molecules: Combining molecular mechanics and continuum models. *Accounts of Chemical Research*, 33(12), pp.889–897.

Margreitter, C. & Oostenbrink, C., 2017. Europe PMC Funders Group MDplot : Visualise Molecular Dynamics. *The R Journal*, 9(1), pp.164–186.

Martínez, L., 2015. Automatic identification of mobile and rigid substructures in molecular dynamics simulations and fractional structural fluctuation analysis. *PLoS ONE*, 10(3), pp.1–10.

Pearlman, D.A. et al., 1995. AMBER, a package of computer programs for applying molecular mechanics, normal mode analysis, molecular dynamics and free energy calculations to simulate the structural and energetic properties of molecules. *Computer Physics Communications*, 91(1–3), pp.1–

Peter Atkins, Julio De Paula, J.K., 2009. Atkins' Physical Chemistry. In J. K. Peter Atkins, Julio De Paula, ed. *Atkins Physical Chemistry*. Oxford University Press, pp. 783–827.

Pisana, S. et al., 2007. Breakdown of the adiabatic Born-Oppenheimer approximation in graphene. *Nature Materials*, 6(3), pp.198–201.

Reddy Masu, S.C., Soykan, I. & McCallum, R.W., 2007a. Domperidone: Review of pharmacology and clinical applications in gastroenterology. *American Journal of Gastroenterology*.

Reddy Masu, S.C., Soykan, I. & McCallum, R.W., 2007b. Domperidone: Review of Pharmacology and Clinical Applications in Gastroenterology. *The American Journal of Gastroenterology*, 102(9), pp.2036–2045.

Schrodinger, E., 1926. Review. *Phys. Rev.*, 28(6), p.1049.

Screaton, G. et al., 2015. New insights into the immunopathology and control of dengue virus infection. *Nature Reviews Immunology*, 15(12), pp.745–759.

Shah, S., Prabhu, P. & Gundad, S., 2011. Formulation development and investigation of domperidone transdermal patches. *International Journal of Pharmaceutical Investigation*.

Shao, J. et al., 2007. Characterizing the Performance of Different Clustering Algorithms. *J. Chem. Theory Comput.*, 3(6), pp.2312–2334. University of California, Potential Energy Surface.

Wang, J., Hou, T. & Xu, X., 2006. Recent Advances in Free Energy Calculations with a Combination of Molecular Mechanics and Continuum Models. *Current Computer Aided-Drug Design*, 2(3), pp.287–306.

- Wang, W. et al., 2001. Biomolecular Simulations: Recent Developments in Force Fields, Simulations of Enzyme Catalysis, Protein-Ligand, Protein-Protein, and Protein-Nucleic Acid Noncovalent Interactions. *Annual Review of Biophysics and Biomolecular Structure*, 30(1), pp.211–243.
- Woolley, R.G., 1991. Quantum chemistry beyond the Born-Oppenheimer approximation. *Journal of Molecular Structure: THEOCHEM*, 230(C), pp.17–46.
- Wudka, J., 1990. Remarks on the Born-Oppenheimer approximation. *Physical Review D*, 41(2), pp.712–714.

## CHAPTER 4

### **Domperidone Nanocrystals with Boosted Oral Bioavailability: Fabrication, Evaluation and Molecular Insight into the Polymer-Domperidone Interaction**

Stalielson Tatenda Ndlovu<sup>1</sup>, Naseem Ullah<sup>2</sup>, Shahzeb Khan\*<sup>1,3</sup>, Pritika Ramharack<sup>1</sup>, Mahmoud Soliman<sup>1</sup>, Marcel de Matas<sup>1</sup>, Muhammad Shahid<sup>2</sup>, Muhammad Sohail<sup>3</sup>, Muhammad Imran<sup>4</sup>, Syed Wadood Ali Shah<sup>1</sup>, Zahid Hussain<sup>5</sup>

<sup>1</sup> Discipline of Pharmaceutical Sciences, College of Health Sciences, University of KwaZuluNatal, Durban, South Africa

<sup>2</sup> Department of Pharmacy, Abasyn University, Peshawar, KPK, Pakistan

<sup>3</sup> Department of Pharmacy, University of Malakand, Dir Lower Chakdara, KPK, Pakistan

#### **<sup>4</sup> Abstract**

The aim of this study was to employ experimental and molecular modelling approaches to use molecular level interactions to rationalise the selection of suitable polymers for use in the production of stable domperidone (DOMP) nanocrystals with enhanced bioavailability. A low energy method, anti-solvent precipitation was used for preparation and screening of polymers for stable nanocrystals of DOMP. Ethyl cellulose was found to be very effecient in producing stable

---

<sup>1</sup> SEDA Pharmaceutical development services, the BioHub at Alderley Park, Cheshire UK

<sup>2</sup> Department of Pharmacy Sarhad University of Science and Information Technology  
Peshawar, KPK, Pakistan

<sup>3</sup> Department of Pharmacy, COMSATS Institute of Information Technology, Abbottabad 22060,  
Pakistan

<sup>4</sup> HEJ, Research Institute of Chemistry, International Centre for Chemical and Biological  
Sciences, University of Karachi, Pakistan

<sup>5</sup> Department of Pharmaceutics, Faculty of Pharmacy, Universiti Teknologi MARA (UiTM)  
Selangor, Puncak Alam Campus 42300, Bandar Puncak Alam, Selangor, Malaysia

DOMP nanocrystals with particle size of  $130 \pm 3$  nm. Moreover, the combination of hydroxypropylmethylcellulose and polyvinyl alcohol was also shown to be better in producing DOMP nanocrystals with smaller particle size ( $200 \pm 3.5$  nm). DOMP nanosuspension stored at 2-8 °C and room temperature (25 °C) exhibited better stability compared to the samples stored at 40 °C. Crystallinity of the unprocessed and processed DOMP was monitored by Differential Scanning Calorimetry and Powder X-ray diffraction. DOMP nanocrystals gave enhanced dissolution rate compared to the unprocessed drug substance. DOMP nanocrystals at a dose of 20 mg/kg in rats showed enhanced bioavailability compared to the raw drug substance and marketed formulation. A significant increase in plasma concentration of 2.6 µg/mL with a significant decrease in the time (1 h) to reach maximum plasma concentration was observed for DOMP nanocrystals, compared to the raw DOMP. Molecular modelling studies provided underpinning knowledge at the molecular level of the DOMP-polymer nanocrystal interactions and substantiated the experimental studies. This included an understanding of the impact of polymers on the size of nanocrystals and their associated stability characteristics.

**Keywords:** Domperidone, Nanocrystals, Molecular modelling, Polymers, Dissolution; Enhanced bioavailability

## **1. Introduction**

The oral route of administration is one of the most convenient, useful and frequently used means to administer drugs (1). In this regard however, the poor aqueous solubility of drugs has been the leading factor, limiting the attractiveness of this route for some compounds and leading to low oral bioavailability and dissolution rate via this route. For drugs classified as class-II according to the

Biopharmaceutics Classification System (BCS), solubility and dissolution rate are of great importance and considered as the basic factors, which influence the rate and extent of drug absorption from GIT track (2). According to recent publications, approximately 40% of compounds in development are subject to poor water solubility (3). To reach the therapeutic plasma concentrations, poorly water soluble drugs are often given at high doses. With the variability in exposure, which is often observed for drugs of this nature, this provide risks of suboptimal efficacy and safety, particularly for drugs with low therapeutic index. In this regard, from a clinical perspective it is more desirable to use low doses of drugs having greater dissolution rate, better absorption and enhanced bioavailability. A number of well establishment strategies exist for enhancing the solubility and dissolution rates of drugs with low aqueous solubility. (4, 5).

In the current pharmaceutical drug delivery research domain, nanotechnology is an emerging field, where drugs with sub-micron particle size are increasingly being considered as a means to address the problem of poor aqueous solubility.. Owing to their significantly high surface area to volume ratio, the nanoparticles (6, 7) are believed to provide an excellent means to drive dissolution in the GI tract. Noyes–Whitney equation gives a sound basis for this dissolution rate enhancement with reduction of the particle size to the nano-sized range, enhancing the surface free energy and surface area leading to increases in water solubility and rate of dissolution (8).

In terms of methods for producing nanoparticulate drugs, two major techniques have been described, which include bottom-up and top-down methods. The typical top down methods include wet milling and high pressure homogenisation (9). Whereas, the bottom up methods are mainly

based on the principle of anti-solvent crystallisation (10). Nanosuspensions are the preparations composed of suspended particles in nanoform, stabilised by polymers and surfactants. The patented solvent displacement method was first used by Fessi et al for the preparation of nano suspensions (11).

Domperidone is pharmacological antagonist of dopamine-2 receptor and belongs to class-II of the BCS (Biopharmaceutical Classification System) (Figure 1). DOMP is used as antiemetic as well as prokinetic representative by producing its effect on chemoreceptor trigger zone and also motor function of small intestine and stomach. This drug has poor aqueous solubility (0.986mg/L) while oral bio-availability is 12 to 18% percent during fasting and 24% after food

(12). The poor water solubility seems to be one of the probable causes for its low bioavailability

(13). The conversion of DOMP into stable nanocrystals could potentially be one of the promising solutions to address this issue.

This study focused on the production of stable nanocrystals of DOMP and investigated using molecular dynamics simulation studies the polymer drug nanocrystal interactions underpinning use of the low energy antisolvent precipitation for nanocrystal manufacture. A number of studies have reported the impact of polymers on particle sizes of drug nanoparticles. Despite these learnings, the molecular level interactions of polymers and drug nanocrystals is still an interesting issue yet to be fully resolved (14). In this study, extensive molecular modelling was coupled with the experimental results to investigate and evaluate the correlation between molecular interactions and drug and stabilisers and nanoparticle properties. The traditional experiments cannot provide the molecular insight of the nanocrystal- polymer interactions in isolation. (15, 16). The comprehensive molecular level understanding gained from this study will be useful going forward

for nanoformulation scientists to optimise polymer selection for stable nanocrystals production for a range of different APIs.

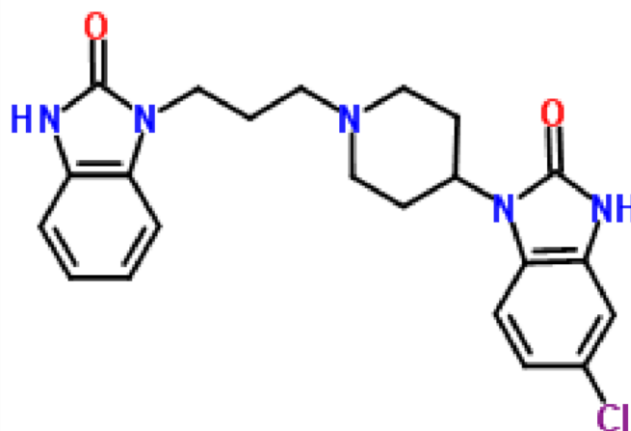


**Figure 1:** Chemical structure of Domperidone

## 2. Materials and Methods

### 2.1. Materials

DOMP was gifted by Stanley Pharma having batch no. BDOM /1302036 Vasodha Pharma Chem Lab 78/A Vengal Rao Nagar Hyderabad-38 Andra Pardish India, ethanol and n-hexane china, Poly vinyl pyrrolidone (PVP) CAS number: 9003-39-8 and hydroxypropylmethylcellulose (HPMC) 9004-65-3 USA were also gifted by Stanley Pharma. Sprague-Dawley rats (150-200 g) were used for bioavailability studies.

### 2.2. Preparation of DOMP nanosuspension

A low energy anti-solvent precipitation method was employed for production of stable nanocrystals of DOMP (14). The DOMP solution (10mg/ml) was prepared in

dimethylformamide (DMF) then filled into the syringe and with the help of a syringe pump the solution was quickly injected at a constant flow rate of 2-8 mL/min into the polymer solutions that served as antisolvent phase, with continuous stirring rate at 600 -1000 rpm. Different polymers and subsequent combinations thereof were used to evaluate their impact on produced nanocrystals of DOMP. The polymer solutions were composed of 1% (w/v) of each of the polymers which included PVP, Ethyl cellulose, HPMC and PVA, Pluronic F127, and Eudragit (EUD). Ethocel was dissolved in drug solutions in DMF then injected into the water. The produced DOMP nanocrystals were filtered and vacuum dried.

### *2.3. Physicochemical characterization*

#### *2.3.1. Particle size Measurements*

Particle size and associated polydispersity index (PI) measurements of the produced nanoparticles of DOMP were carried out in triplicate using dynamic light scattering (Zetasizer® NanoS, Malvern Instruments, UK), which measures the hydrodynamic diameter including the solvation layer around each particle.

#### *2.3.2. Morphological studies*

##### *2.3.2.1. Scanning electron microscope (SEM)*

The principle used in the operation of scanning electron microscopy (SEM) is light reflection microscopy. Reflection of electrons occur as a result of incident light striking the surface of the powder sample and colliding with particle surfaces. The reflected electrons are picked up by the detector and are then transformed into an image by algorithm. Scanning electron microscopy is

applied for the description of surface morphology of the powder sample and provides good resolution down to scale of several nanometers.

Surface morphology studies of the unprocessed DOMP was carried out by placing the sample on a grid covered with gold sputter coater (SPI, USA) using Jeol JSM5910 scanning electron microscope at an operating voltage of 30mA for duration of 2 minutes and an accelerating voltage of 20Kv.

#### *2.3.2.2. Transmission Electron Microscopy (TEM)*

The size and appearance of the produced DOMP nanoparticles were evaluated using TEM (TEM-1200Ex; Japan Electron Optics Laboratory Corporation, Tokyo, Japan). The images of DOMP nanoparticles were taken at 120 kV. The drops of DOMP nanosuspensions were deposited on 200 mesh copper grid followed by coating with formvar/carbon (code no: S162) and drying at room temperature. Owing to low conductivity of the produced samples, they were negatively stained using 2% solution of magnesium uranyl acetate.

#### *2.3.3. Differential scanning calorimetry (DSC)*

To investigate and evaluate the impact of particle size on the thermal profile of the produced DOMP nanoparticles, the comparative DSC studies were carried out. The samples were scanned using the Mettler Toledo Differential Scanning Calorimeter (MettlerToledo®, USA). Samples (2-3mg) of unprocessed and processed DOMP were weighed into separate aluminium pans, which were sealed and then analysed by heating from 30° to 300°C at a heating rate of 10°C min<sup>-1</sup> and nitrogen flow of 40 ml/min. Indium was used as a standard for calibration of the instrument.

#### *2.3.4. Powder X-Ray Diffraction Studies (PXRD)*

The prepared nanoparticles and unprocessed drug substance were subjected to testing for crystallinity using (PXRD) powder x-ray diffractometer (D8 ADVANCE, Bruker, Germany). The silicon-well sample holder was used for analysis of nanoparticle samples, while the plastic sample holder was used for raw drug substance. Nanoparticle sample and raw drug substance were scanned in triplicate in the range  $0^\circ \leq 2\theta \leq 70^\circ$  using copper  $K\alpha$  as the radiation source with 1mm slit at 1.542 Å wavelength. Step size was  $0.05^\circ$  and the time lapse between the steps was 2 seconds.

#### *2.4. Stability studies*

The stability of nanoparticles, particularly those produced by bottom up method is very important, especially because agglomeration and particle growth can occur quickly, leading to the loss of rapid dissolution performance. In this study, produced DOMP nanosuspensions was subjected to testing of physical stability over a duration of 90 days following storage at 2-8°C, 25°C and 40 °C. This study was designed to monitor the rate and extent of particle growth with measurements of particle size being made using dynamic light scattering.

#### *2.5. Computational methods*

##### *2.5.1. Molecular Docking of polymers and DOMP*

A short MD run was performed on the polymers to obtain relaxed energy conformers prior to docking. The Molecular docking software utilized included Raccoon (17), Autodock Graphical user interface supplied by MGL tools (18) and AutoDockVina (19) with default docking parameters. Prior to docking, Gasteiger charges (20) were added to polymers as well as

Domperidone and the non-polar hydrogen atoms were merged to carbon atoms. The gridbox was set to cover the entire polymer to allow for the best-docked pose. The optimal geometric conformation bearing the best binding energy was picked from the View Dock feature on Chimera(21) and the complex saved with the reference polymers. The polymer-domperidone for each system was prepared using Chimera and MMV molecular modeling suites (22) and later subjected to molecular dynamic simulations.

### *2.5.2. Molecular Dynamic Simulations*

GPU version of the PMEMD engine in Amber14 software package was utilized to execute unrestrained all-atom MD simulations. The Restrained Electrostatic Potential (RESP) and the General AMBER Force Field (GAFF) (23) systems were used by ANTECHAMBER (24) to generate the atomic partial charges for the polymers and domperidone. The systems were solvated in a cubic box of TIP3P water, such that all atoms were within 10 Å of a box edge. Long-range electrostatic interactions were treated with the Ewald method and a van der Waals cut-off of 12 Å. Each of the systems were minimized for 1000 steps (500 steepest descent followed by 2500 steps of the conjugate gradient). The langevin thermostat, with a collision frequency of 1.0 ps<sup>-1</sup> with harmonic restrained of 5 kcal/mol on the solutes, was applied during the gradual heating of the systems to a temperature of 300 K in the canonical ensemble for 50 ps. This was followed by 50 ps of density equilibration in NPT ensemble and a final 500 ps equilibration at 300 K, 1 bar pressure and a coupling constant of 2 ps, and the by a MD production run of 50 ns. System coordinates were then saved every 1 ps and analyzed using the PTRAJ module employed in AMBER14 (25) . The Root mean square deviation (RMSD) was employed to establish the stability of the 12 systems over the 50 ns trajectory.

### 2.5.3. Binding free energy calculation

Calculations of free binding energies were engaged using the Molecular Mechanics/GB Surface

Area method (MM/GBSA) (26) . This was carried out to evaluate the binding affinities of each system. Binding free energies were then averaged over 5 000 snapshots extracted from the 50 ns trajectory. Figure 2 depicts free binding energy ( $\Delta G$ ), which was computed by the MM/GBSA method for each molecular species (complex, ligand and polymer).

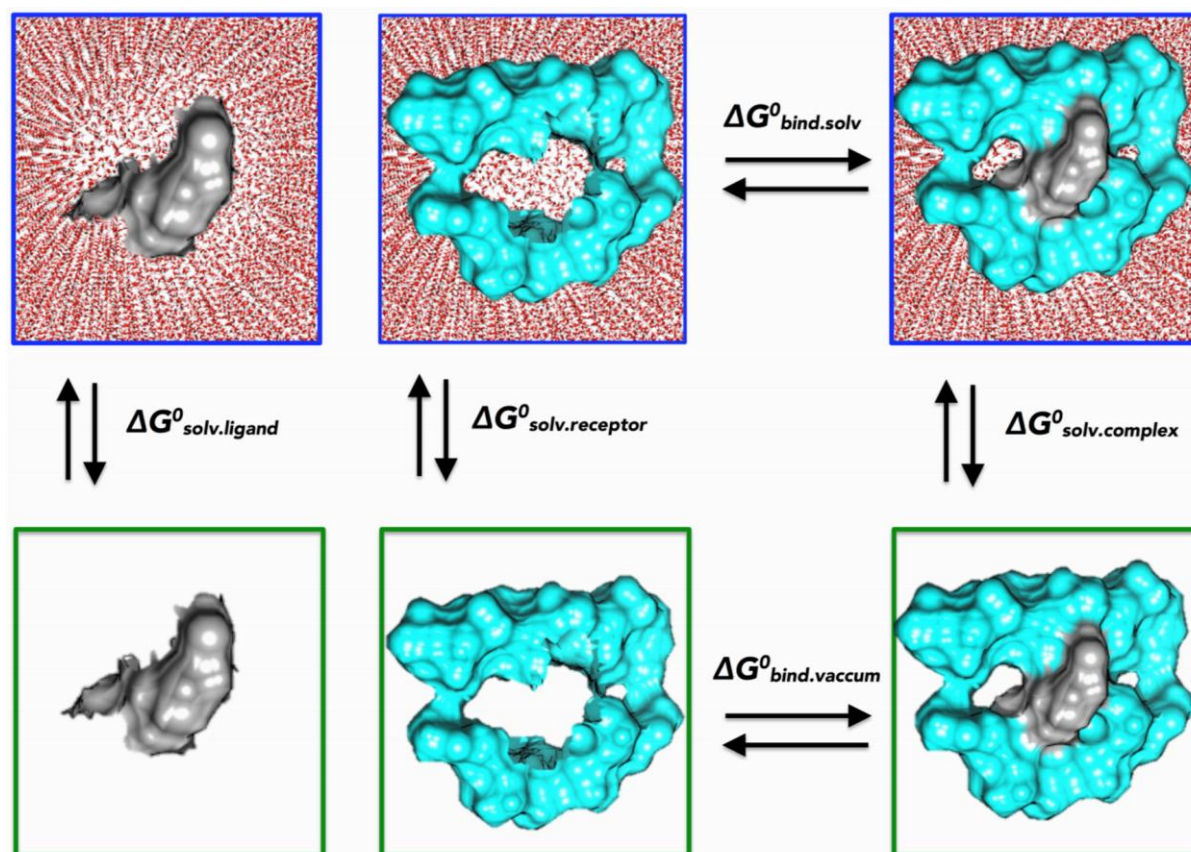


**Figure 2:** Diagrammatic representation of thermodynamic calculation (MM/GBSA) used in the study (Prepared by Author)

### 2.6. Bioavailability studies

The pharmacokinetics studies of unprocessed domperidone, its fabricated nanocrystals (DomNano), prepared solid dosage form (Dom-Nano dosage form) and marketed formulations were carried out using rats as the animal model. Sprague-Dawley rats (150-200 g) were administered with an oral dose of 10 mg/kg of domperidone, its nanoparticles, its nano-dosage form, and marketed drug and blood was collected after 0.25, 0.5, 1, 2, 3, 4, 6, 8, 10 and 12 hrs postadministration ( $n = 6$  rats each for different time periods). The collected blood samples were centrifuged and plasma was obtained. The blood plasma was quantified for DOMP using a reported HPLC method (27). The pharmacokinetics parameters in the plasma were determined using the pharmacokinetic software WinNonLin (v 4.0; Pharsight Software, Mountain View, CA, USA). The pharmacokinetics parameters determined include maximal plasma concentration ( $C_{\max}$ ), time to reach maximal plasma concentration ( $T_{\max}$ ), half-life ( $t_{1/2}$ ), and the area under the concentration-time curve (AUC).

### *2.7. Dissolution studies*

Dissolution studies on pure DOMP as well as the nanoparticles prepared EPN was performed using two separate dissolution tests, both using the U.S. Pharmacopoeia (USP) tablet dissolution test apparatus 2 (6 station) with the paddle rotating at 50 rpm in 900 ml of both pH 1.2 (0.1N HCl) media and in a separate test 6.8 pH phosphate buffer at  $37 \pm 0.5^\circ\text{C}$ . All drugs equivalent to 10 mg of DOMP were used as samples for the dissolution test. At 10 min, 30 min and 60 minutes intervals, 5 ml samples were withdrawn, filtered through a 0.1  $\mu\text{m}$  membrane filter and assayed for DOMP content by measuring the absorbance at 284 nm using UV -Visible spectrophotometer (Shimadzu UV-1700). Fresh medium (5 ml), pre-warmed at  $37 \pm 0.5^\circ\text{C}$ , was added to the

dissolution medium after each sampling to maintain a constant volume throughout the test. Dissolution studies were performed in triplicate (n=3) [15].

### *2.8. Statistical analysis*

All the tests were run in triplicate and results were given as mean $\pm$  standard mean error (SEM). Mean values were compared using Anova-test and differences were considered statistically significant at level ( $p < 0.05$ ) using Statistics 8.1 software.

## **3. Results and discussion**

### *3.1. Preparation of DOMP nanosuspension using antisolvent precipitation method*

Nanosuspensions of DOMP were produced by antisolvent precipitation. The particle size of nanosuspensions produced using this method are given in Table 1. There were used different polymer solutions as anti-solvent phase having different combination of polymers to investigate the impact of the polymers on particle sizes of the produced DOMP nanocrystals. There was observed that Ethocel was the most suitable single polymer to produce DOMP nanocrystals with small particle size  $130.0\pm 3.0$  (Table 1 and Figure 3). This shows that ethocel strongly adsorbed onto the surface of DOMP nanocrystals to establish the steric stabilisation with subsequent small particle size and low PDI value. In addition, HPMC was also found comparatively effective single polymer to control the size of DOMP nanocrystals ( $300\pm 4.0$ ) (Table 1). However, when HPMC was combined with PVA in antisolvent phase, the impact became more predominant in terms of controlling the particle size. The combination of HPMC-PVA produced DOMP nanocrystals with particle size ( $200\pm 3.5$ ). DOMP nanoparticles produced at optimised conditions were quickly recovered by vacuum evaporation of all solvent and antisolvent using a rotary evaporator and were

the washed and dried. The resulted PDI was was below 0.5, which shows homogenous particle size distribution of the suspended particles (28, 29).

**Table 1.** Impact of polymers on particle sizes and PDI values of DOMP nanosuspension.

<b>DOMP-Polymer complexes</b>	<b>Particle size <math>\pm</math> SD</b>	<b>PDI <math>\pm</math> S.D</b>
Ethocel	130.0 $\pm$ 3.0	0.15 $\pm$ 0.01
Pluronic	1200 $\pm$ 7.5	0.85 $\pm$ 0.06
PVP	950.0 $\pm$ 5.0	0.77 $\pm$ 0.05
PVA	400.0 $\pm$ 4.5	0.50 $\pm$ 0.03
EUD	1175 $\pm$ 7.0	0.80 $\pm$ 0.06
HPMC	300 $\pm$ 4.0	0.40 $\pm$ 0.02
EUD-PVA	775 $\pm$ 6.0	0.65 $\pm$ 0.04
EUD-PVP	985 $\pm$ 5.7	0.80 $\pm$ 0.05
HPMC-PVA	200 $\pm$ 3.5	0.20 $\pm$ 0.02
HPMC-PVP	570.0 $\pm$ 5.0	0.52 $\pm$ 0.03
HPMC-EUD	550 $\pm$ 6.5	0.60 $\pm$ 0.04
PVA-PVP	650 $\pm$ 5.2	0.40 $\pm$ 0.02

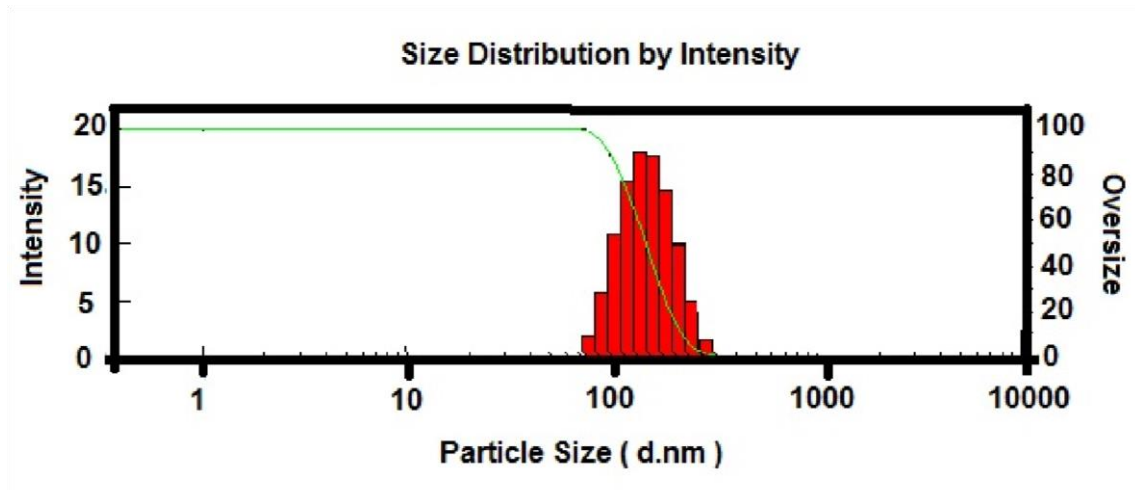


**Figure 3:** Particle size distribution of DOMP nanoparticles.

The highly concentrated drug solutions injected into anti solvent phase can potentially produce high levels of supersaturation and consequently nanoparticles with small particle size. The (SAS) ratio is a very important process parameter, which should be optimised during APSP production of nanoparticles, whereby the barrier for the existing species to be grown during mixing of the solvent anti-solvent phases is affected by this parameter. In this study, it has been observed that DOMP nanoparticles with small particle size ( $130.00\text{nm} \pm 3.0$ ) were produced using a high SAS ratio (Figure 3), while using the antisolvent phase with etocel. At low SAS ratio the available diffusion distance for the growing species is low and can potentially lead to high nucleation with subsequent comparatively large particle sizes being produced (30, 31).

### 3.2. Morphological examination

The morphology studies of raw and processed DOMP were carried out by SEM and TEM respectively. SEM observation showed some differences in size and shape of the unprocessed DOMP particles (Figure 4 (A)). The average particle size was found to be 10-15 micron and most of the particles were shown to be cuboidal and prism like. Some traces of oval shape particles were also observed although, all particles are appeared to demonstrate regular crystalline morphologies (Figure 4 (B)). TEM images of the DOMP nanoparticles demonstrated that most of the particles were spherical in shape with some traces of the triangular shape particles. In addition, the TEM results exhibited that all the nanoparticles were homogenously distributed with no clumps or aggregates. The particle size was shown to be approximately 100.0nm in good agreement with DLS data. The minor difference in the particle size measured using DLS and TEM is related to the difference in the principles of the two techniques. In DLS, the electrical double layers surrounding the individual particle could are also measured, whereas,

TEM only measures the actual particles (29).

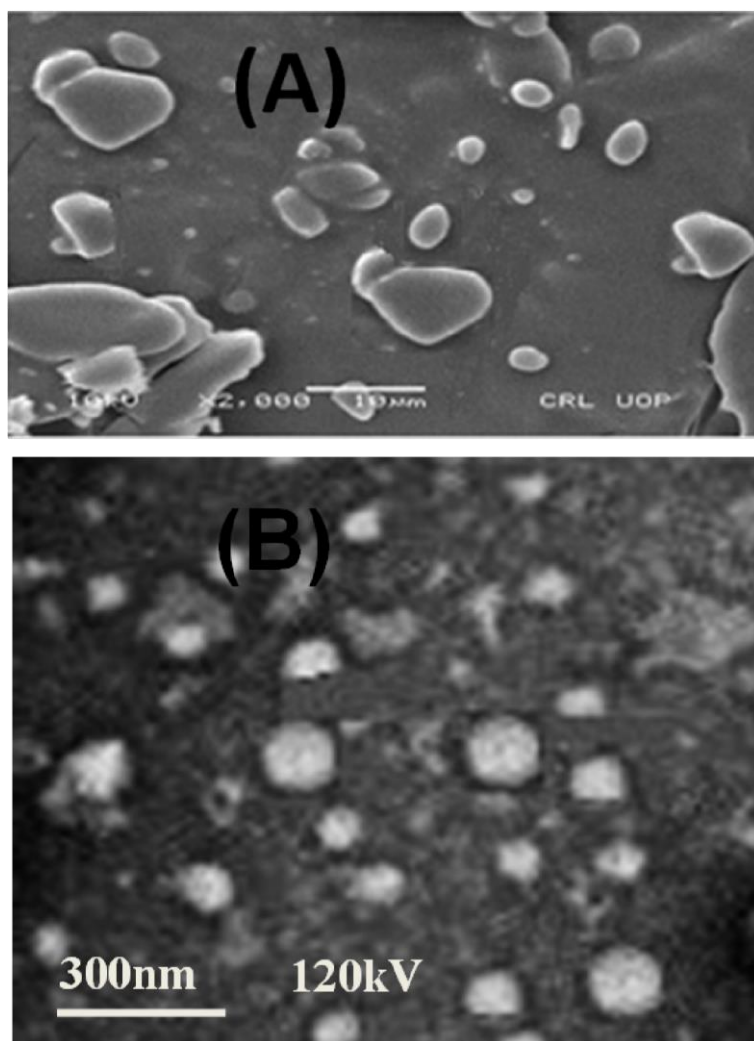


**Figure 4.** SEM image of raw DOMP (A) and TEM micrographs of processed DOMP particles (B)

### *3.3. PXRD analysis*

PXRD analysis was carried out for raw and DOMP nanoparticles. PXRD diffractograms show that raw DOMP sharp peaks of high intensity compared to the DOMP nanoparticles (Figure 5 A). The

nano formulation gives lower intensity, broader peaks, which are typically of crystalline particles with low particle size peaks (Figure 5 (B)). X-ray diffractograms with lower peak intensities and the absence of some peaks have also been previously been reported by other researchers for crystalline nanoparticles (32-34). Furthermore, nanoparticles can result in broadening and disappearance of some peaks in X-ray diffractograms. Owing to small angular reflection by the smaller particles, the peak intensity of X-ray diffractograms is reduced. For domperidone nanoparticles, the small sample sizes were with fewer particles can also result in lower intensity reflections.

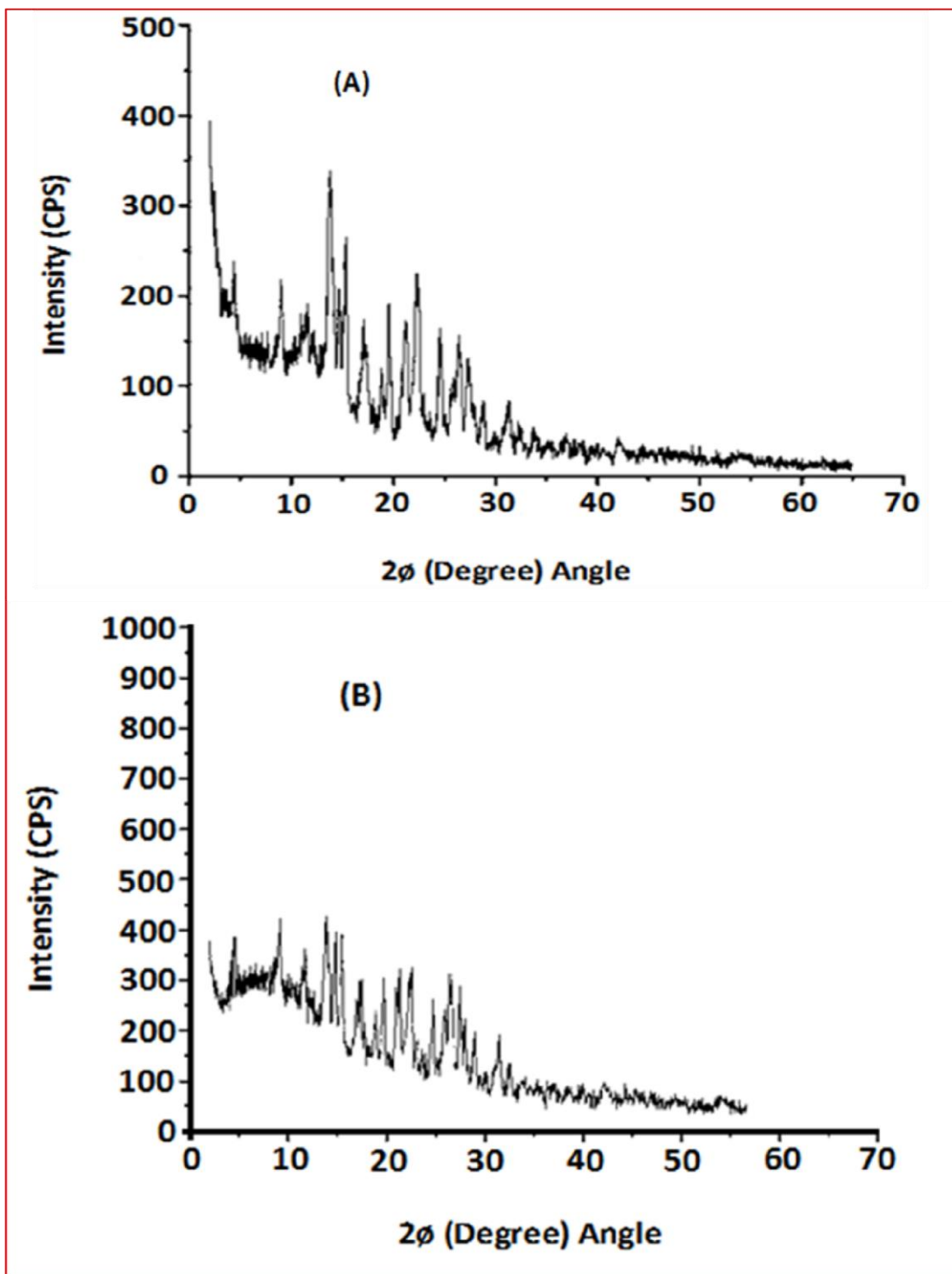


**Figure 5:** PXRD patterns of Unprocessed (A) and DOMP nanoparticles (B).

#### 3.4. DSC analysis

DSC thermograms of pure DOMP and the prepared nanocrystals are shown in Figure 6. There appeared an intense endothermic peak at approximately 238°C for unprocessed DOMP. It is known that crystalline structure will give a peak at the melting point temperature with high heat enthalpy ( $\Delta H$ ) values compared to that of amorphous structures of the same materials. The produced nanocrystals have low values of the  $\Delta H$  representing reduction in crystallinity of the resulted nanocrystals. The produced nanocrystals have shown melting point peak at lower temperature compared to the unprocessed DOMP, which is typical of nanocrystalline materials.

The endothermic peak of the processed DOMP was broadened, which is potentially be caused by the packing density of the produced nanoparticles, incorporating traces of stabilising polymers (35).

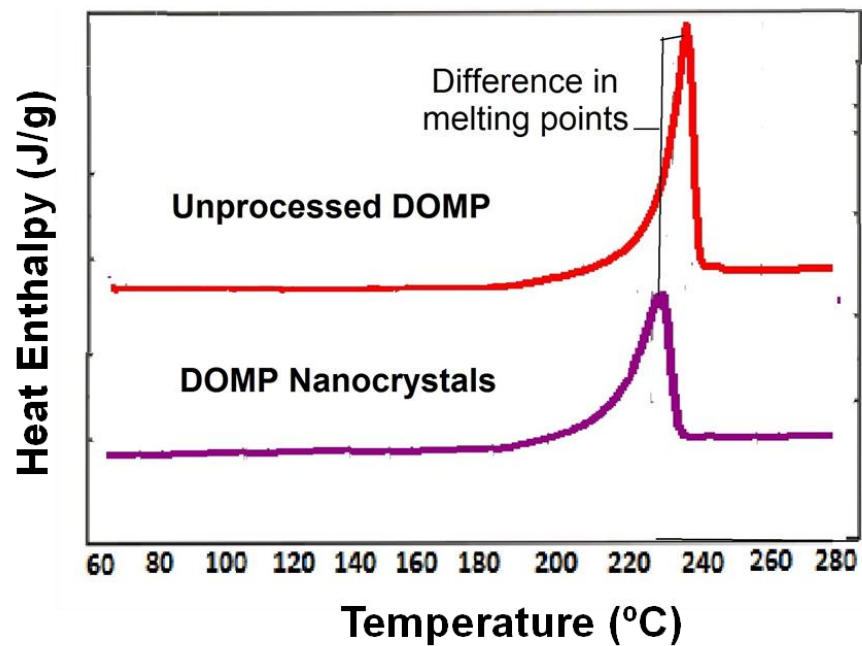


**Figure 6:** DSC Thermograms of Unprocessed DOMP and DOMP nanocrystals.

### 3.5. Molecular docking and conformational analysis of polymer systems

Molecular docking is a conventional method in computational chemistry, which is utilized in the prediction of optimized geometric conformations of a ligand within an appropriate binding site (36). Of the docked polymer-DOMP complexes (Figure 7 and 8), the highest binding affinity was observed for the HPMC-EUD co-polymer (-6.0 kcal/mol). Of the mono-polymer complexes, PVP demonstrated the highest binding affinity (-5.2kcal/mol).

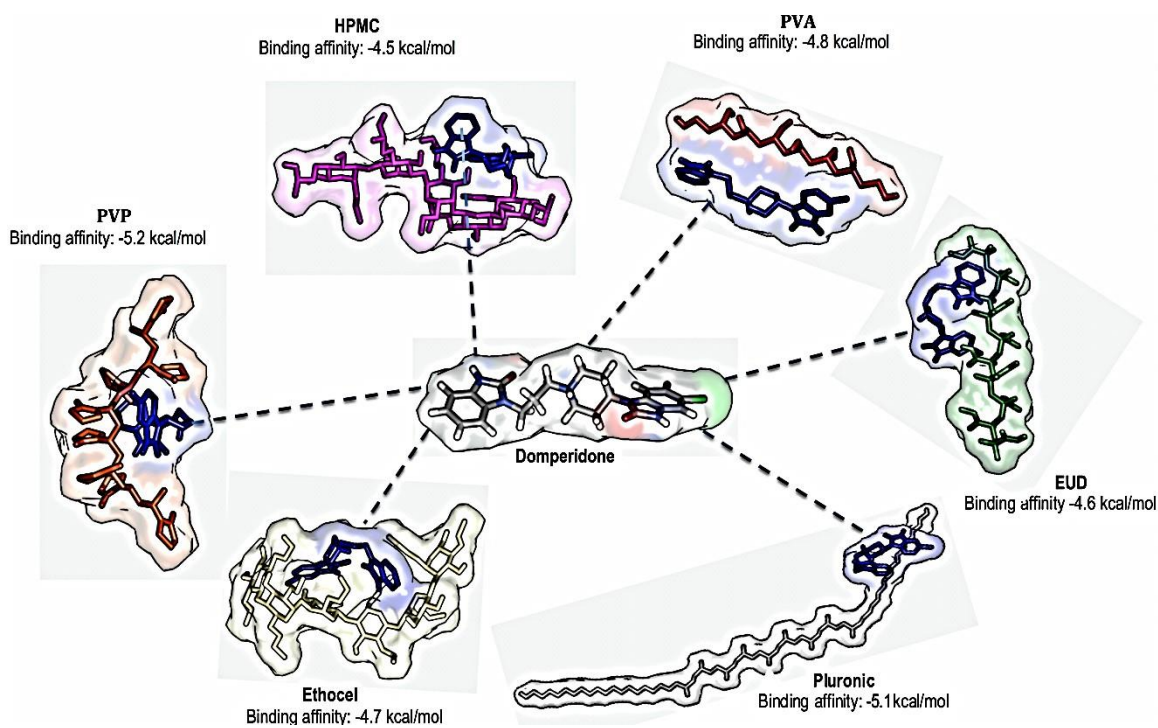


**Figure 7:** Binding affinity results from molecular docking of domperidone-monomer complexes.

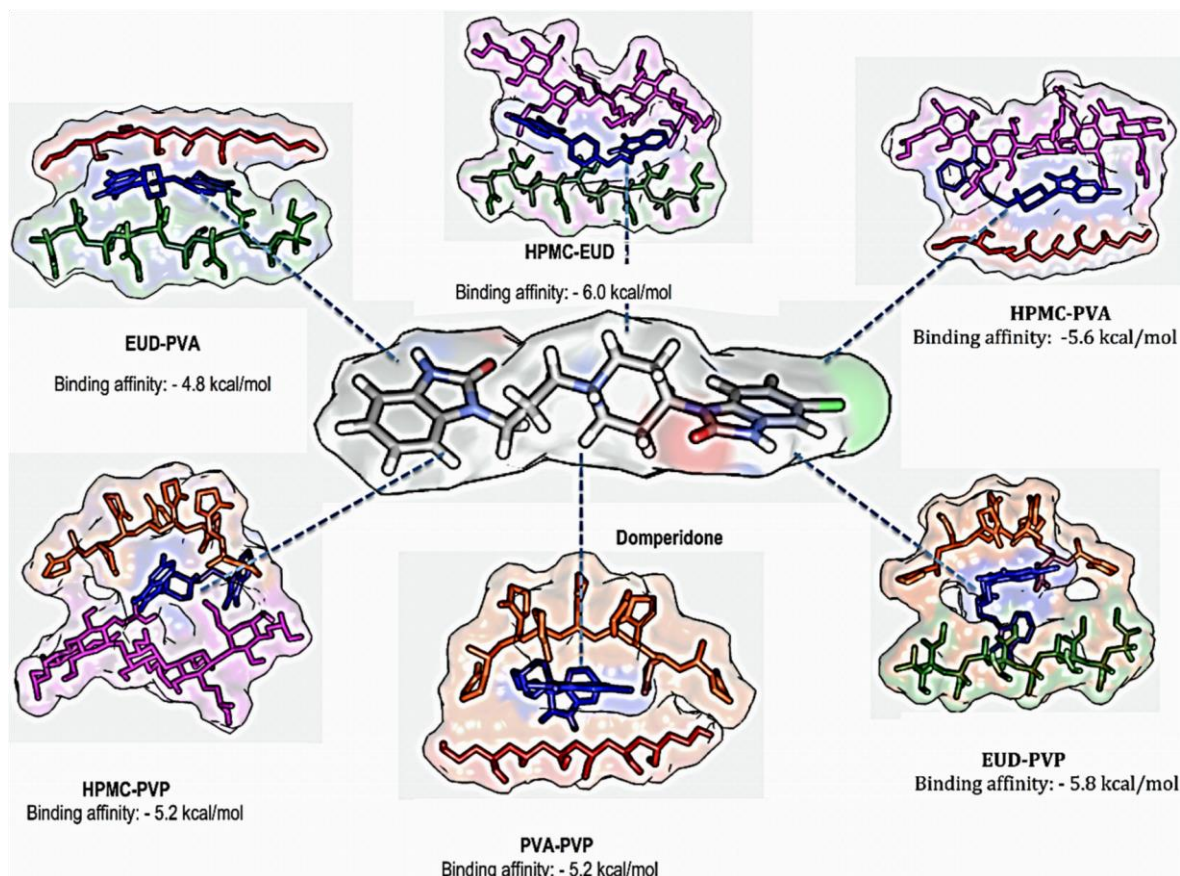


**Figure 8:** Binding affinity results from molecular docking of domperidone –copolymer complexes.

The molecular docking results, however, only take into account the geometric orientation of domperidone when bound to suitable regions of the polymers and thus may be inconclusive when identifying the forces that stabilize domperidone to the polymers. To overcome any binding mode ambiguities, molecular dynamics were carried out to simulate the interaction of domperidone with the polymers over a 50ns trajectory. After allowing domperidone to equilibrate with the polymers, the binding mechanism and stabilizing intra-molecular forces were investigated using binding free energy calculations.

### 3.6. Polymer systems stability through molecular dynamic simulations

The stability of trajectories that was identified using root mean square deviation (RMSD) over the 50ns simulation, the potential energy of the polymer-domperidone remained stable during the MD trajectories and convergence was reached at approximately 20ns.

### 3.7. Thermodynamic energy analysis

The total binding free energy for each of the 12 polymer-domperidone complexes were calculated using the MM/GBSA approach to better understand the various energy contributions stabilizing the polymer to domperidone and to assess which polymer-complex showed the most favorable intermolecular interactions. Based on Table 2, a conformational analysis was performed to distinguish between the most favorable polymer-domperidone complexes.

Calculating the thermodynamic energy between a polymer and drug gives the approximate intensity and stability of interactions between the molecules, thus a higher binding interaction will result in a more stable polymer-drug complex (37).

1 **Table 2.** Binding free energy analysis (kcal/mol) for polymer-domperidone complexes.

2

Energy Components (kcal/mol)						3
Single Polymer Systems						4
Complex	$\Delta E_{vdW}$	$\Delta E_{elec}$	$\Delta G_{gas}$	$\Delta G_{solv}$	$\Delta G_{bind}$	5
<hr/>						6

<b>Ethocel</b>	$-30.37 \pm 0.24$	$-6.95 \pm 0.43$	$-37.32 \pm 0.43$	$10.06 \pm 0.33$	$-27.26 \pm 0.247$
<b>Pluronic</b>	$-3.69 \pm 0.05$	$0.29 \pm 0.079$	$-3.40 \pm 0.96$	$2.19 \pm 0.09$	$-1.20 \pm 0.54^8$
<b>PVP</b>	$-5.52 \pm 2.68$	$-20.94 \pm 1.12$	$-26.46 \pm 1.87$	$18.75 \pm 0.52$	$-7.72 \pm 1.95$
<b>PVA</b>	$-31.77 \pm 5.23$	$-25.19 \pm 11.32$	$-56.96 \pm 12.24$	$38.08 \pm 8.33$	$-18.88 \pm 6.39$
<b>EUD</b>	$-4.10 \pm 2.09$	$-5.55 \pm 0.60$	$-9.64 \pm 1.84$	$7.73 \pm 0.31$	$-1.91 \pm 1.97$
<b>HPMC</b>	$-20.35 \pm 0.92$	$-22.42 \pm 0.79$	$-42.77 \pm 1.04$	$20.04 \pm 0.43$	$-22.73 \pm 0.82$
					14

---

**Dimer Systems**

15

<b>Complex</b>	$\Delta E_{vdW}$	$\Delta E_{elec}$	$\Delta G_{gas}$	$\Delta G_{solv}$	$\Delta G_{bind}^{16}$
<b>EUD-PVA</b>	$-13.83 \pm 0.34$	$0.00 \pm 0.00$	$-13.83 \pm 0.34$	$4.33 \pm 0.10$	$-9.50 \pm 0.36$
<b>EUD-PVP</b>	$-10.78 \pm 0.73$	$-5.08 \pm 0.43$	$-15.87 \pm 0.56$	$9.19 \pm 0.33$	$-6.67 \pm 0.64$
<b>HPMC-PVA</b>	$-39.84 \pm 0.74$	$-12.88 \pm 0.85$	$-42.72 \pm 1.00$	$17.50 \pm 0.62$	$-25.22 \pm 0.79$
<b>HPMC-PVP</b>	$-15.15 \pm 1.37$	$-24.91 \pm 0.71$	$-40.06 \pm 1.19$	$24.46 \pm 0.44$	$-15.60 \pm 1.13$
<b>HPMC-EUD</b>	$-13.17 \pm 0.81$	$-27.93 \pm 0.78$	$-41.10 \pm 0.85$	$27.00 \pm 0.40$	$-14.10 \pm 0.84$
<b>PVA-PVP</b>	$-26.09 \pm 1.23$	$-12.77 \pm 1.11$	$-28.86 \pm 1.53$	$16.09 \pm 0.56$	$-12.77 \pm 0.60$

Upon analysis of Table 2, the most favorable interactions were observed in the Ethocel system ( $-27.26$  kcal/mol), while the Pluronic complex showed the least favorable binding free energy ( $1.20$  kcal/mol). It was also interesting to note that the inclusion of EUD significantly lowered the thermodynamic energy of the co-polymer complexes, as the addition of EUD to PVA decreased

the free binding energy by 9.38 kcal/mol. This trend was also observed in both the HPMC and PVP complexes. This confirms that molecular docking demonstrates only the “geometric fit” of two molecules and free energy binding calculations are still required when estimating molecular interactions (38). As observed in the HPMC-PVA complex, significant improvements were noted in the thermodynamic energy upon inclusion of HPMC compared to the monopolymer PVA complex (Figure 9 and Figure 10). This may have been a result of increased intermolecular surface area based on the interaction size of HPMC. The above characteristic features may also be used to explain the high binding energy of the Ethocel complex (Figure 11). Increased molecular surface area due to the conformational flexibility of Ethocel may have allowed for greater hydrophobic interactions with domperidone. As a general trend, greater stability was seen in the polymers that showed enhanced interactive binding surfaces such as HPMC and Ethocel.

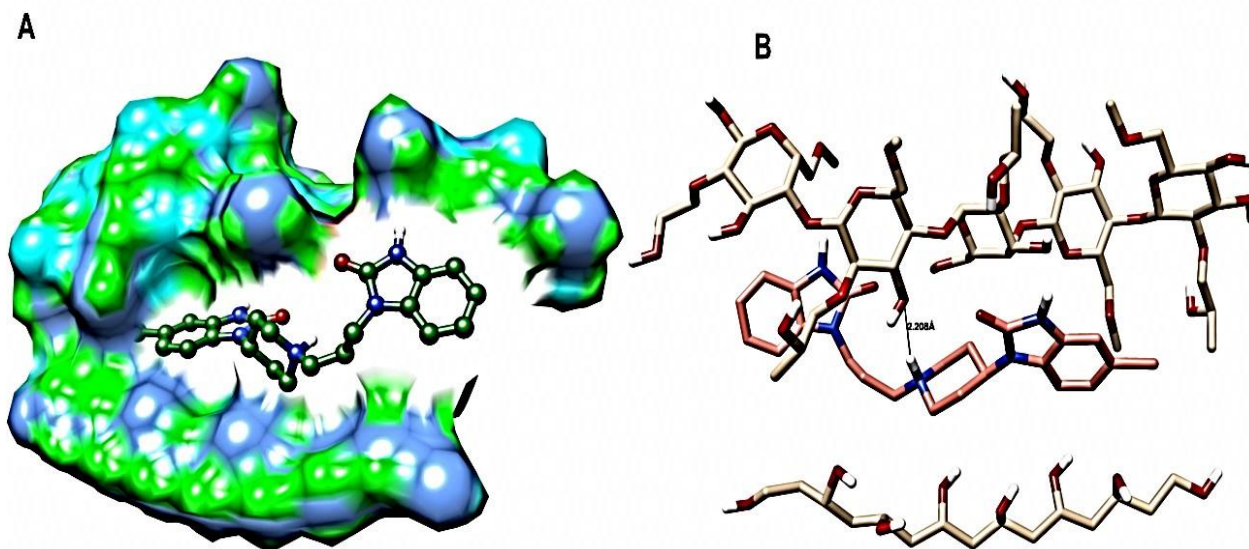


**Figure 9:** The lowest energy conformation of HPMC-PVA-DOMP complex (-25.25 kcal/mol); (A) depicts the molecular surface of HPMC-PVA encapsulating DOMP, (B) displays the hydrogen bond interaction between DOMP and HPMC.

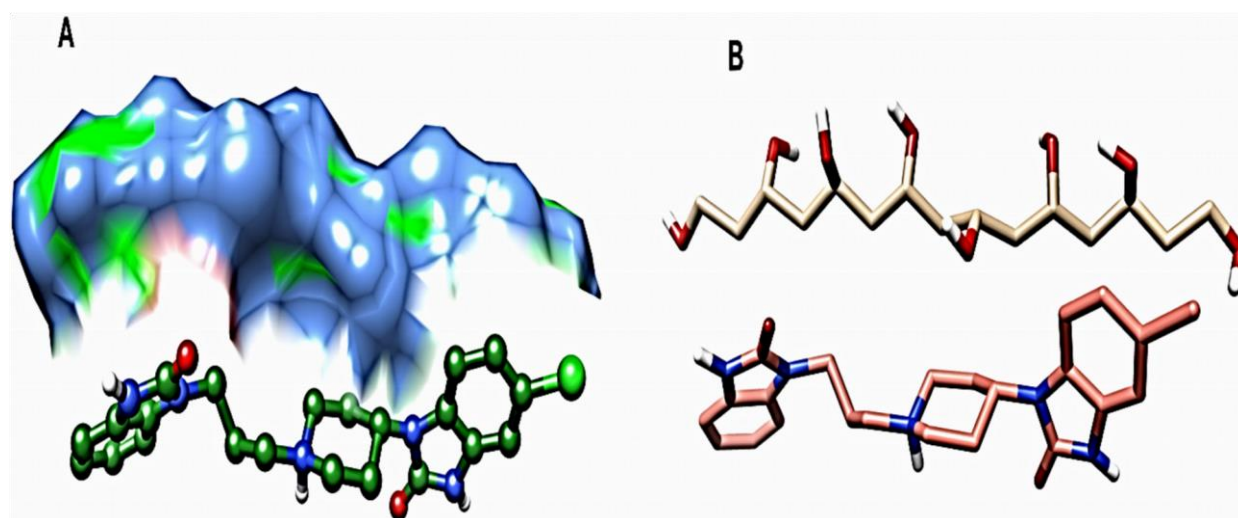


**Figure 10:** The PVA-DOMP complex (-18.88kcal/mol) (A) Molecular surface interaction between PVA and DOMP, (B) graphical representation of the lack of hydrogen bonds between PVA and DOMP.

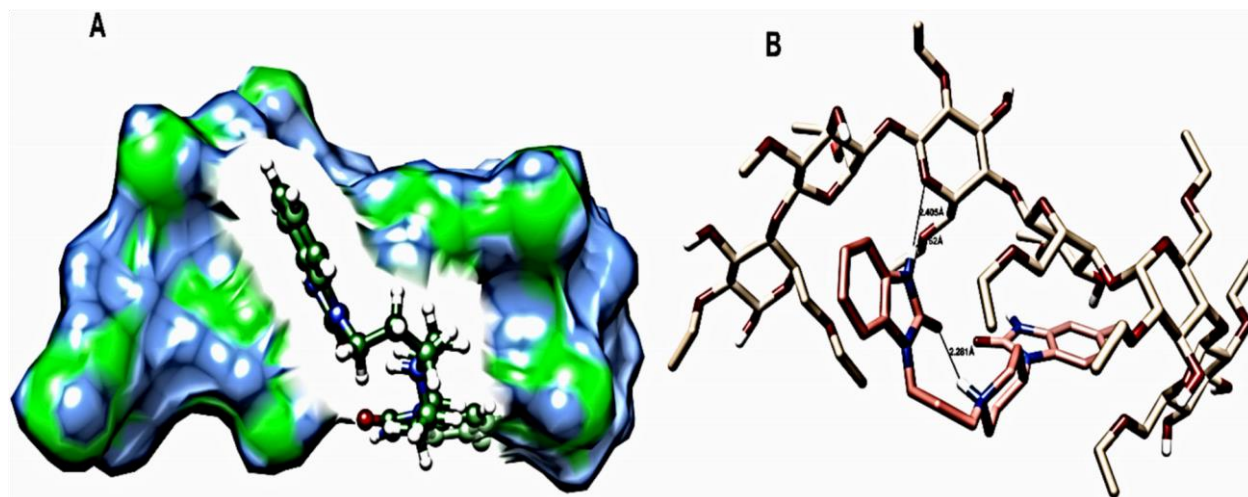


**Figure 11:** The lowest energy conformation of Ethocel-DOMP complex (-27.26kcal/mol) after molecular dynamic simulations; (A) molecular surface interaction between Ethocel and DOMP, (B) presents three stabilizing hydrogen bonds of the Ethocel-DOMP complex.

### 3.8. Bioavailability studies

The pharmacokinetic profile of domperidone in plasma after oral administration of 10mg/kg dose of DOMP, its nanocrystals, tablets having DOMP in annoform and marketed product (Motilium®) via oral administration is shown in Figure 12.

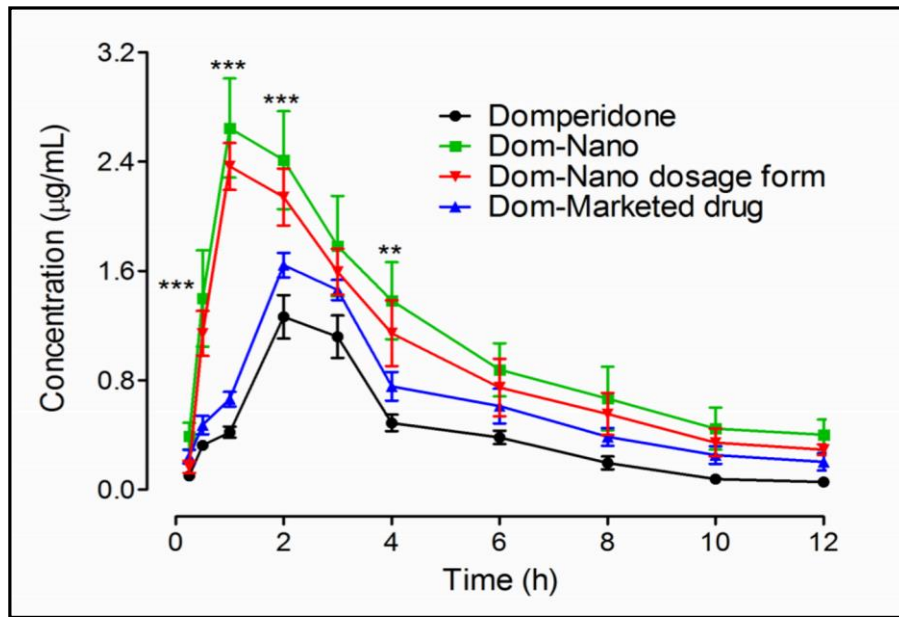


**Figure 12:** Comparative *in-vivo* Pharmacokinetic profile of (Domperidone) ( $n = 6, \pm SD$ )  $**P < 0.01$ ,  $***P < 0.001$ .

Numerous pharmacokinetic parameters, including area under the concentration-time curve, maximal plasma concentration, time to reach maximal plasma concentration, and biological half-life, are shown in Table 3.

**Table 3:** Summary of pharmacokinetic parameters for domperidone.

Sample	Pharmacokinetic Parameters			
	$T_{1/2}$ (h)	$T_{max}$ (h)	$C_{max}$ ( $\mu\text{g/mL}$ )	AUC <sub>0-t</sub> ( $\mu\text{g h/mL}$ )
Raw DOMP	4.182±0.43	2.0±0.11	1.3±0.26	4.91±0.31
DOMP Nanocrystals	13.34±0.32***	1.0±0.07**	2.6±0.18**	13.3±0.44***
Tablets (DOMP- Nanocrystals)	8.334±0.71***	1.0±0.09**	2.4±0.21**	11.3±0.39***
DOMP marketed formulation	6.451±0.52*	2.0±0.16	1.6±0.31	7.73±0.37*

( $n = 6$ ,  $\pm\text{SD}$ ) \* $P < 0.05$ , \*\* $P < 0.01$ , \*\*\* $P < 0.001$

Administration of domperidone at a dose of 20 mg/kg showed an elimination phase from 10 to 12 h with an elimination half-life of 4.18 h with a clearance of 4051.3 mL/h. The distribution phase was observed from 6 to 8 h with an observed volume of distribution of 24470.8 mL. The absorption phase was noted from 0.3 h to 4 h. The maximum plasma concentration was observed as 1.3  $\mu\text{g/mL}$  at 2 h. 4.9  $\mu\text{g h/mL}$  was the area under the concentration-time curve from time 0 to 12 h. Marked

changes in the pharmacokinetics of nanoparticles were observed. Administration as nanoparticles increased the plasma concentration of domperidone throughout the study; however, a noteworthy escalation has been noted at 0.5 h ( $P < 0.01$ ), 1-2 h ( $P < 0.001$ ) and at 4 h ( $P < 0.05$ ). The nanoparticles formulations resulted in a decreased elimination rate of domperidone as reflected from a significant increase in the half-life of 13.34 h ( $P < 0.001$ ). A significant increase plasma concentration of 2.6  $\mu\text{g/mL}$  ( $P < 0.01$ ) with a significant decrease ( $P < 0.01$ ) in the time (1 h) to reach maximum plasma concentration was observed compared to domperidone treated rats. The nanoparticles increased the plasma exposure of domperidone as a significant increase in the AUC from time zero to 12 h was observed (13.3  $\mu\text{g h/mL}$ ,  $P < 0.001$ ). Similarly, the nano dosage form also showed an enhancement in the pharmacokinetic parameters i.e. half-life (8.3 h,  $P < 0.001$ ), maximal plasma concentration (2.4  $\mu\text{g/mL}$ ,  $P < 0.01$ ), time to reach maximal plasma concentration (1.0 h,  $P < 0.01$ ) and AUC (11.3  $\mu\text{g h/mL}$ ,  $P < 0.001$ ), as compared to domperidone treatment. For the marketed drug, a significant increase in the apparent half-life (6.45 h,  $P < 0.05$ ) and AUC (7.73  $\mu\text{g h/mL}$ ,  $P < 0.05$ ) was observed compared to the domperidone alone treated animals

### 3.9. Stability studies

The physical stability studies of DOMP nanosuspensions stored at 2-8 °C, 25 °C and 40 °C for 90 days showed that nanosuspensions stored at 2-8 °C and 25 °C (Figure 13A and 13B) were stable compared to the samples stored at 40 °C (Figure 13C). The nanosuspension stored at 2-8°C exhibited adequate stability (Figure 13A) with no marked changes in key nanosuspension characteristics. The nanosuspensions stored at 2-8 °C and 25 °C maintained their PDI values and there was no significant difference ( $P > 0.05$ , paired t-test, one way ANOVA) difference in the mean values of particle size after 90 days storage, which confirms that a homogenous particle size

distribution of DOMP nanocrystals has been achieved and consequently the Ostwald ripening process which is very common in the nanosuspensions could be hindered.

Among the different factors influencing physical stability of nanosuspensions, temperature has been reported the major factor to be controlled for production of stable nanoparticles (14, 39). At high temperature, kinetic energy of the suspended particles increases which results in strong van der Waals forces and increased attraction among the particles followed by agglomeration and destabilisation of the suspensions. For maximum stabilisation of nanoparticles, a temperature range of 2-8°C has been recommended by Frietz and Muller. In addition, increases in temperature and high intensity of light radiation can cause rapid particle growth. Nucleation is the key step in anti-solvent crystallisation methods which can be manipulated for tailoring particle size and shape of crystallised materials (40, 41). Moreover, the polymeric media and associated stabilising agent is also considered very important and is known to facilitate surface stabilisation and consequent control of particle size during the nucleation process (42). 0.5% ethocel was found the most suitable single polymer to effectively control the growth of the DOMP nanocrystals, which remained stable for 90 days (Table 4). This study demonstrated that sufficient adsorption of the polymers occurred onto the surfaces of the produced DOMP nanocrystals which resulted into strong repulsion of the particles and subsequent colloidal stabilization. The molecular Modeling studies also substantiated the experimental results and suggested that Ethocel gave higher binding free energy ( $-27.26 \pm 0.24$  kcal/mol) compared to other complexes which in turn provided higher levels of surface polymer adsorption and more effective stabilisation. In addition, DOMP nanocrystals produced by 1% HPMC were also shown to be stable compared to other single polymers. This binding free energies resulted for DOMP nanocrystals and HPMC ( $-22.73 \pm 0.82$  kcal/mol) also suggest that HPMC could be effectively adsorbed onto the surface of DOMP nanocrystals with subsequent controlled particle

growth. In the case of polymer combinations, the combination of HPMC-PVA was found the most suitable combination to retard the particle growth, because of its higher binding free energy ( $-25.22 \pm 0.79$  kcal/mol) compared to other counterparts.

**Table 4:** Stability study of DOMP optimised nanocrystals as a function of time.

DOMP-polymer complexes	Average Particle Sizes of DOMP Nanocrystals with $\pm$ SD						
	Day 0	Day 15	Day 30	Day 45	Day 60	Day 75	Day 90
Ethocel-DOMP	130.0 $\pm$ 2.5	135 $\pm$ 3.0	140 $\pm$ 4.0	143 $\pm$ 3.5	144 $\pm$ 4.5	145 $\pm$ 3.8	147 $\pm$ 3.5
Pluronic-DOMP	1200 $\pm$ 4.5	1280 $\pm$ 5.0	1385 $\pm$ 3.5	1450 $\pm$ 4.5	1600 $\pm$ 5.5	1730 $\pm$ 6.5	1850 $\pm$ 6.0
PVP-DOMP	950.0 $\pm$ 5.0	980 $\pm$ 5.5	1070 $\pm$ 6.0	1200 $\pm$ 4.5	1280 $\pm$ 4.0	1390 $\pm$ 7.0	1470 $\pm$ 7.5
PVA-DOMP	400.0 $\pm$ 4.5	440 $\pm$ 3.0	455 $\pm$ 2.7	470 $\pm$ 3.2	490 $\pm$ 2.4	520 $\pm$ 3.5	545 $\pm$ 2.8
EUD-DOMP	1175 $\pm$ 7.0	1220 $\pm$ 3.7	1260 $\pm$ 3.5	1325 $\pm$ 3.7	1410 $\pm$ 2.5	1500 $\pm$ 2.0	1610 $\pm$ 3.0
HPMC-DOMP	300 $\pm$ 4.0	325.0 $\pm$ 2.0	338 $\pm$ 2.7	350 $\pm$ 2.0	370 $\pm$ 3.0	385 $\pm$ 3.5	392 $\pm$ 2.5
EUD-PVA-DOMP	775 $\pm$ 6.0	800 $\pm$ 5.4	860 $\pm$ 5.5	930 $\pm$ 4.0	1020 $\pm$ 6.4	1100 $\pm$ 5.6	1170 $\pm$ 6.0
EUD-PVP-DOMP	985 $\pm$ 5.7	1015 $\pm$ 6.5	1090 $\pm$ 5.5	1210 $\pm$ 7.0	1300 $\pm$ 6.5	1410 $\pm$ 7.5	1515 $\pm$ 5.8
HPMC-PVA-DOMP	200 $\pm$ 3.5	210 $\pm$ 2.5	217 $\pm$ 2.0	230 $\pm$ 2.4	240 $\pm$ 3.0	245 $\pm$ 2.7	250 $\pm$ 2.5
HPMC-PVP-DOMP	570.0 $\pm$ 5.0	600 $\pm$ 2.8	645 $\pm$ 3.5	680 $\pm$ 3.0	730 $\pm$ 3.7	790 $\pm$ 3.0	830 $\pm$ 3.2
HPMC-EUD-DOMP	550 $\pm$ 5.5	575 $\pm$ 4.5	615 $\pm$ 5.0	650 $\pm$ 4.0	690 $\pm$ 4.5	710 $\pm$ 5.5	750 $\pm$ 6.0
PVA-PVP-DOMP	650 $\pm$ 5.2	695 $\pm$ 5.5	730 $\pm$ 6.0	780 $\pm$ 6.5	830 $\pm$ 5.0	900 $\pm$ 4.5	945 $\pm$ 6.5

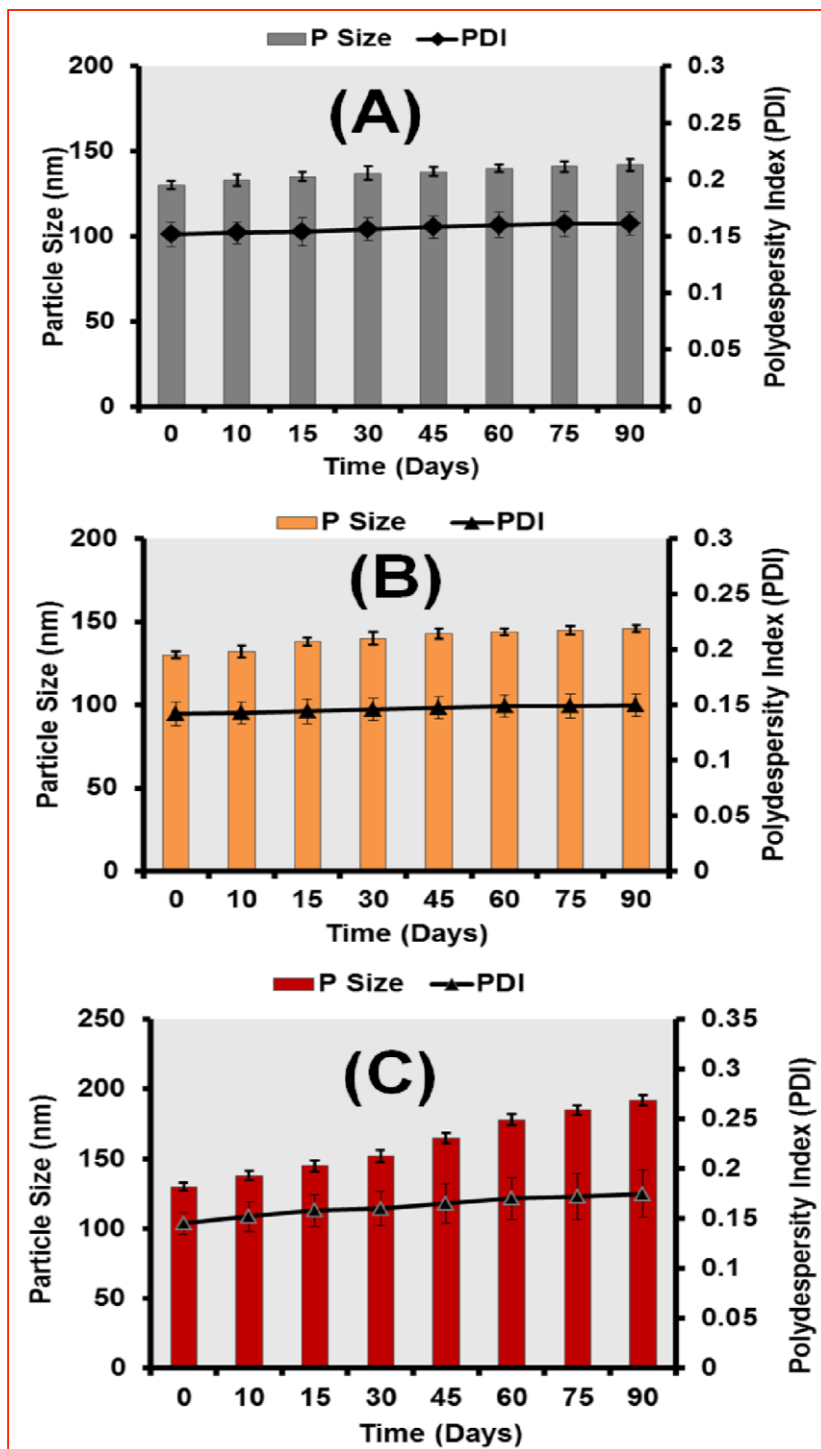


**Figure 13:** Stability studies of DOMP nanoparticles stored at 2-8 °C (A), 25 °C (B) and 40 °C.

### *3.10. Dissolution studies*

Figure 14 clearly shows that dissolution of DOMP has been increased enormously with the conversion of pure/raw DOMP to the nanocrystals prepared by EPN method. The difference in dissolution profiles of the produced DOMP nanocrystals forms in acidic and basic media is attributed to its physicochemical attributes. DOMP is basic in nature, therefore it dissolves efficiently in acidic media; [23]. The dissolution study of DOMP conducted in a buffer (pH 6.8) medium resulted in approximately 80% and 20% release of the drug within first ten minutes, from nanocrystals and raw DOMP formulations respectively. In addition, the dissolution studies conducted at acidic pH (0.1M HCL), also resulted in enhanced dissolution rate for DOMP nanocrystals (38%) compared to the raw DOMP. Dissolution has been reported as being the rate limiting step for BCS II class drug compounds, because they have high permeability but low dissolution rate (43). Owing to increased dissolution rate of DOMP nanocrystals, the bioavailability could also potentially be enhanced, which is substantiated by the oral bioavailability studies in rates. Furthermore, nanocrystals have increased surface area and improved adhesiveness to the cell membrane which subsequently leads to high bioavailability (44). The dissolution studies confirmed that the produced DOMP nanocrystals maintained their surface area and particle size.

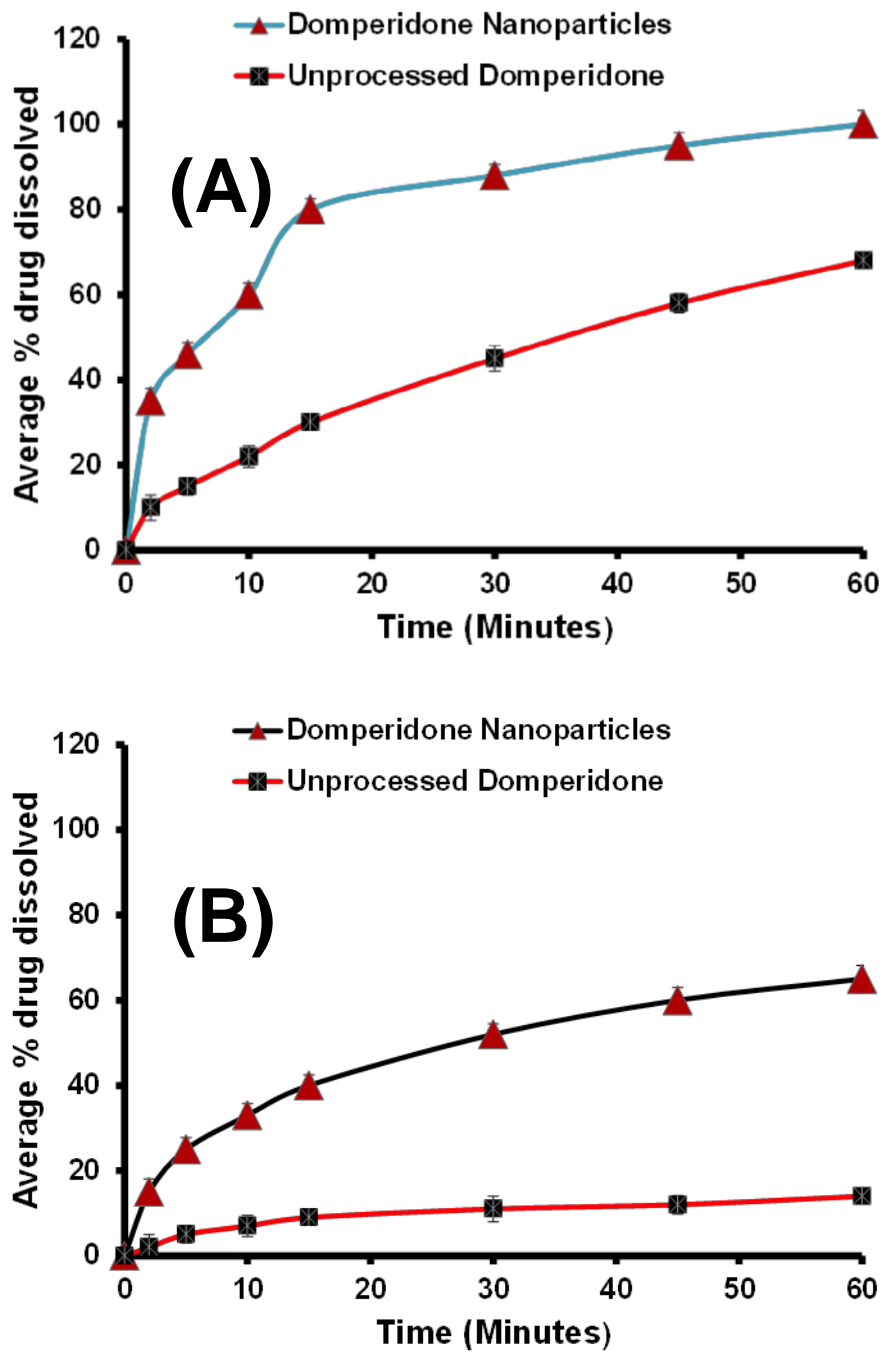


**Figure 14:** Comparative dissolution profile of unprocessed and DOMP nanoparticles at acidic pH: 0.1MHCL (A) and phosphate buffer pH: 6.8 (B).

#### **4. Conclusion**

This study concluded that polymers play an important role in the production of stable nanocrystals using the anti-solvent precipitation method. This study provided molecular insight into the interactions between polymers and drugs at nanocrystal surfaces, knowledge which is not easily accessible through experiment. Ethocel was found the most effective polymer to control the particle size of DOMP nanocrystals ( $130.0 \pm 2.5$ ). Furthermore, the 1% (w/v) HPMCPVA combination also showed strong binding potential with DOMP nanocrystals demonstrating particle size ( $200.0 \pm 3.5$ ). The molecular modelling studies provided molecular level insight into polymer drug interactions underpinning the mode of binding of polymers with DOMP at the surfaces of nanocrystals. This has provided an opportunity for the formulation scientist to rationally select suitable polymers, most likely to achieve desirable particle size control for nanocrystals and deliver stable formulations which deliver optimal in-vivo performance.

DOMP nanocrystals showed enhanced dissolution rate at both acidic and basic pH conditions compared to the unprocessed form of DOMP. The dissolution enhancement for this BCSII class drug compound can potentially provide the opportunities to develop a more cost effective dosage form having the same therapeutic performance, but at much lower dose compared to the existing marketed drug product. Pharmacokinetic studies in rat have shown that the improved dissolution performance leads to markedly improved rate and extent of drug absorption in-vivo. Future studies will be focussed on transforming the prototype formulations tested in this project into drug products suitable for clinical testing and commercialisation.

#### **Acknowledgement**

The authors acknowledge Abdullah Jan at Central Research laboratory, University of Peshawar for Scanning Electron Microscope, Differential Scanning Calorimetry and Fourier Transform

Infrared Spectroscopy instrumentation time and assistance by Mr. Saddiq Afridi at Pakistan Council of Scientific and Industrial Research laboratory Peshawar KP. The authors also extend thanks to Mr. Iqbal Central Research Laboratory Peshawar University for his contribution in carrying out the X-ray Diffraction analysis.

### **Conflict of interest**

The authors report no conflicts of interest in this work.

### **References**

1. Sastry SV, Nyshadham JR, Fix JA. Recent technological advances in oral drug delivery— a review. *Pharmaceutical Science & Technology Today*. 2000;3(4):138-45.
2. Kawabata Y, Wada K, Nakatani M, Yamada S, Onoue S. Formulation design for poorly water-soluble drugs based on biopharmaceutics classification system: basic approaches and practical applications. *International Journal of Pharmaceutics*. 2011;420(1):1-10.
3. O'driscoll C, Griffin B. Biopharmaceutical challenges associated with drugs with low aqueous solubility—the potential impact of lipid-based formulations. *Advanced Drug Delivery Reviews*. 2008;60(6):617-24.
4. Sarkar N. Mifepristone: bioavailability, pharmacokinetics and use-effectiveness. *European Journal of Obstetrics & Gynecology and Reproductive Biology*. 2002;101(2):113-20.
5. Dressman JB, Reppas C. In vitro–in vivo correlations for lipophilic, poorly water-soluble drugs. *European Journal of Pharmaceutical Sciences*. 2000;11:S73-S80.

6. Salah N, Habib SS, Khan ZH, Memic A, Azam A, Alarfaj E, et al. High-energy ball milling technique for ZnO nanoparticles as antibacterial material. *International Journal of Nanomedicine*. 2011;6:863.
7. Seo WS, Lee JH, Sun X, Suzuki Y, Mann D, Liu Z, et al. FeCo/graphitic-shell nanocrystals as advanced magnetic-resonance-imaging and near-infrared agents. *Nature Materials*. 2006;5(12):971.
8. Kesisoglou F, Panmai S, Wu Y. Nanosizing—oral formulation development and biopharmaceutical evaluation. *Advanced Drug Delivery Reviews*. 2007;59(7):631-44.
9. Verma S, Gokhale R, Burgess DJ. A comparative study of top-down and bottom-up approaches for the preparation of micro/nanosuspensions. *International Journal of Pharmaceutics*. 2009;380(1-2):216-22.
10. Chan H-K, Kwok PCL. Production methods for nanodrug particles using the bottom-up approach. *Advanced Drug Delivery Reviews*. 2011;63(6):406-16.
11. Jacobs C, Müller RH. Production and characterization of a budesonide nanosuspension for pulmonary administration. *Pharmaceutical research*. 2002;19(2):189-94.
12. Saritha D, Sathish D, Rao YM. Formulation and Evaluation of Gastroretentive Floating Tablets of Domperidone Maleate. *Journal of Applied Pharmaceutical Science*. 2012;2(3):68.
13. Reddymasu SC, Soykan I, McCallum RW. Domperidone: review of pharmacology and clinical applications in gastroenterology. *The American journal of gastroenterology*. 2007;102(9):2036.

14. Ullah N, Khan S, Ahmed S, Govender T, Faidah HS, de Matas M, et al. Dexibuprofen nanocrystals with improved therapeutic performance: fabrication, characterization, in silico modeling, and in vivo evaluation. *International Journal of Nanomedicine*. 2018;13:1677.
15. Anwar J. From virtual molecule to formulate medicine; A review of the potential of molecular simulation in drug delivery and formulation. *LPT*. 2007;10(7):66-72.
16. Seedat N, Kalhapure RS, Mocktar C, Vepuri S, Jadhav M, Soliman M, et al. Coencapsulation of multi-lipids and polymers enhances the performance of vancomycin in lipid– polymer hybrid nanoparticles: in vitro and in silico studies. *Materials Science and Engineering: C*. 2016;61:616-30.
17. Cosconati S, Forli S, Perryman AL, Harris R, Goodsell DS, Olson AJ. Virtual screening with AutoDock: theory and practice. *Expert opinion on drug discovery*. 2010;5(6):597-607.
18. Morris GM, Huey R, Lindstrom W, Sanner MF, Belew RK, Goodsell DS, et al. AutoDock4 and AutoDockTools4: Automated docking with selective receptor flexibility. *Journal of Computational Chemistry*. 2009;30(16):2785-91.
19. Seeliger D, de Groot BL. Ligand docking and binding site analysis with PyMOL and Autodock/Vina. *Journal of computer-aided molecular design*. 2010;24(5):417-22.
20. Selvi BR, Batta K, Kishore AH, Mantelingu K, Varier RA, Balasubramanyam K, et al. Identification of a novel inhibitor of CARM1-mediated methylation of histone H3R17. *Journal of Biological Chemistry*. 2009:jbc. M109. 063933.

21. Yang Z, Lasker K, Schneidman-Duhovny D, Webb B, Huang CC, Pettersen EF, et al. UCSF Chimera, MODELLER, and IMP: an integrated modeling system. *Journal of structural biology*. 2012;179(3):269-78.
22. Kusumaningrum S, Budianto E, Kosela S, Sumaryono W, Juniarti F. The molecular docking of 1, 4-naphthoquinone derivatives as inhibitors of polo-like kinase 1 using Molegro Virtual Docker. *J App Sci*. 2014;4:47-53.
23. Özpınar GA, Peukert W, Clark T. An improved generalized AMBER force field (GAFF) for urea. *Journal of molecular modeling*. 2010;16(9):1427-40.
24. Wang J, Wang W, Kollman PA, Case DA. Antechamber: an accessory software package for molecular mechanical calculations. *J Am Chem Soc*. 2001;222:U403.
25. Galindo-Murillo R, Robertson JC, Zgarbová M, Sponer J, Otyepka M, Jurečka P, et al. Assessing the current state of AMBER force field modifications for DNA. *Journal of Chemical Theory and Computation*. 2016;12(8):4114-27.
26. Godschalk F, Genheden S, Söderhjelm P, Ryde U. Comparison of MM/GBSA calculations based on explicit and implicit solvent simulations. *Physical Chemistry Chemical Physics*. 2013;15(20):7731-9.
27. Alhumayyd M, Bukhari I, Almotrefi A. Effect of piperine, a major component of black pepper, on the pharmacokinetics of domperidone in rats. *J Physiol Pharmacol*. 2014;65:785-9.
28. Shah SMH, Ullah F, Khan S, Shah SMM, de Matas M, Hussain Z, et al. Smart

nanocrystals of artemether: fabrication, characterization, and comparative in vitro and in vivo antimalarial evaluation. *Drug design, development and therapy*. 2016;10:3837.

29. Ali HS, York P, Blagden N. Preparation of hydrocortisone nanosuspension through a bottom-up nanoprecipitation technique using microfluidic reactors. *International Journal of Pharmaceutics*. 2009;375(1-2):107-13.
30. Kakran M, Sahoo N, Li L, Judeh Z, Wang Y, Chong K, et al. Fabrication of drug nanoparticles by evaporative precipitation of nanosuspension. *International Journal of Pharmaceutics*. 2010;383(1-2):285-92.
31. Cao G. *Nanostructures & nanomaterials: synthesis, properties & applications*: Imperial college press; 2004.
32. O'Mahony M, Leung AK, Ferguson S, Trout BL, Myerson AS. A Process for the Formation of Nanocrystals of Active Pharmaceutical Ingredients with Poor Aqueous Solubility in a Nanoporous Substrate. *Organic Process Research & Development*. 2014.
33. Ali HS, York P, Ali AM, Blagden N. Hydrocortisone nanosuspensions for ophthalmic delivery: a comparative study between microfluidic nanoprecipitation and wet milling. *J Controlled Release*. 2011;149(2):175-81.
34. Khan S, Matas Md, Zhang J, Anwar J. Nanocrystal preparation: Low-energy precipitation method revisited. *Crystal Growth & Design*. 2013;13(7):2766-77.

35. Rahim H, Sadiq A, Khan S, Khan MA, Shah SMH, Hussain Z, et al. Aceclofenac nanocrystals with enhanced in vitro, in vivo performance: formulation optimization, characterization, analgesic and acute toxicity studies. *Drug design, development and therapy*.

2017;11:2443.

36. Mura C, McAnany CE. An introduction to biomolecular simulations and docking. *Molecular Simulation*. 2014;40(10-11):732-64.

37. Clark AJ, Gindin T, Zhang B, Wang L, Abel R, Murret CS, et al. Free energy perturbation calculation of relative binding free energy between broadly neutralizing antibodies and the gp120 glycoprotein of HIV-1. *Journal of molecular biology*. 2017;429(7):930-47.

38. Śledź P, Caflisch A. Protein structure-based drug design: From docking to molecular dynamics. *Current Opinion in Structural Biology*. 2018;48:93-102.

39. Plakkot S, De Matas M, York P, Saunders M, Sulaiman B. Comminution of ibuprofen to produce nano-particles for rapid dissolution. *International Journal of Pharmaceutics*. 2011;415(12):307-14.

40. Dalvi SV, Dave RN. Analysis of nucleation kinetics of poorly water-soluble drugs in presence of ultrasound and hydroxypropyl methyl cellulose during antisolvent precipitation.

*International Journal of Pharmaceutics*. 2010;387(1):172-9.

41. Voorhees PW. The theory of Ostwald ripening. *Journal of Statistical Physics*. 1985;38(12):231-52.
42. Anwar J, Khan S, Lindfors L. Secondary Crystal Nucleation: Nuclei Breeding Factory Uncovered. *Angewandte Chemie*. 2015.
43. Chavda H, Patel C, Anand I. Biopharmaceutics classification system. *Systematic reviews in pharmacy*. 2010;1(1):62.
44. Möschwitzer JP. Drug nanocrystals in the commercial pharmaceutical development process. *International Journal of Pharmaceutics*. 2013;453(1):142-56.

## CHAPTER 5

# Permeating The Blood Brain Barrier; Computational Exploration Of Chemotherapeutic Paradigms Towards Effective Treatment Of Parkinson's Disease

Stalielson Ndlovu<sup>1</sup>, Ransford Oduro Kumi<sup>1</sup>, Pritika Ramharack<sup>1</sup>, Manimbulu Nlooto<sup>2</sup>, Mahmoud E. S. Soliman<sup>1\*</sup>

<sup>1</sup> Molecular Bio-computation and Drug Design Laboratory, School of Health Sciences, University of KwaZulu-Natal, Westville Campus, Durban 4001, South Africa

<sup>2</sup> Discipline of Pharmaceutical Sciences, School of Health Sciences, University of KwaZulu-Natal, Westville Campus, Durban 4001, South Africa

**\* Correspondence:**

Mahmoud E.S. Soliman email:

soliman@ukzn.ac.za

**Keywords: Parkinson's treatment, drug revamping, polymeric drug delivery, computational drug discovery, Permeating blood brain barrier**

### Abstract

Parkinson's disease is marked by gradual loss of dopaminergic neurons and embodies an escalated health encumbrance, particularly in developed countries. Most clinically approved drugs used in Parkinson's treatment are specifically utilized for symptomatic relief and/or are associated with a plethora of adverse effects. The rarity of curative or effective treatment for Parkinson's in the medical sector is the key motivation of the growing studies for therapeutic alternatives. Currently a concoction of drugs shuttled by polymeric nanoparticles has proven advantageous. These "drug carriers" have recently sparked interest in the pharmaceutical domain due to increasing popularity in overcoming two common adverse effects of brain diseases: off-target binding and inability to pass the blood-brain-barrier. This study seeks to unravel some of the *In-silico* methodology that can be used to improve potential compounds and establish varying drug-polymer combinations that can traverse the blood brain barrier and bind effectively at a target site. The

establishment of this computational approach as a blueprint in increasing bioavailability and reducing adverse of anti-Parkinson's drugs will eventually prove useful in other neurodegenerative diseases.

## **Introduction**

Parkinson's disease (PD) is the second most common neurodegenerative disease devastating approximately 1-1.5% of the populace above 60 years old. At present the degenerative onslaught of PD cannot be cured (Leyva-Gómez et al., 2015). The difficulty of attaining curative therapy could be attributed to the complexity of its etiology. There are other highly efficient non-pharmacological treatments like deep brain stimulation (DBS) of the subthalamic nucleus (STN) with known curative potential and chance of side effects and surgical risks. However, our supreme focus will be pointed on pharmacological treatment of PD, whose potentiality is yet to be fully explored. The PD drugs that are available in the realm of approved medicines only replenish, regulate and imitate dopamine effects and alter motor behavior in varying ways. The dopamine precursor, Levodopa (L-dopa) is a gold standard that is renowned for its ability to improve the quality of life among PD patients. Levodopa/Carbidopa (Levocarb) formulation is the foremost treatment for PD symptoms. Yet contrary to its "golden" abilities, this dopamine precursor like other antiparkinsonian drugs as dopamine agonists, monoamine oxidase type B (MOA-B) inhibitors, amantadine and domperidone have differing adverse effect. It is these dilapidating effects and many drugs with limited solubility that have necessitated the *in-silico* investigating the approach for improvement of efficacy by modifying the structure and using novel drug delivery systems as polymeric nanoparticles (Loftsson and Brewster, 2010).

Usually symptoms of PD are akin to motor functions because dopamine is essential for conveying electrical signals for sustaining normal physical motion (Hovgaard and Brndsted, 1995). At initial stages of PD, the most commonly seen symptoms are movement-related such as bradykinesia, resting tremor, rigidity, and postural instability (DeMaagd and Philip, 2015; Silindir Gunay et al., 2016). As the disorder develops, thinking and behavioral problems may arise, and dementia can occur in the advanced stages of the disease (Hovgaard and Brndsted, 1995) . Additionally, depression can be seen as a psychiatric.

### ***The "Degenerative" Origin of PD***

Parkinson's disease results mainly due to complications of the basal ganglia, which mainly enables muscle tone, and ease of movement. This degeneration of the substantia nigra, essentially the loss of neurons in the

*pars compacta* of the substantia nigra results in reduced dopamine levels (Figure 1) cause the striatum fire out excessive unwanted signals namely tremors, which are most basic symptoms of Parkinsonism (Newland et al., 2015) .

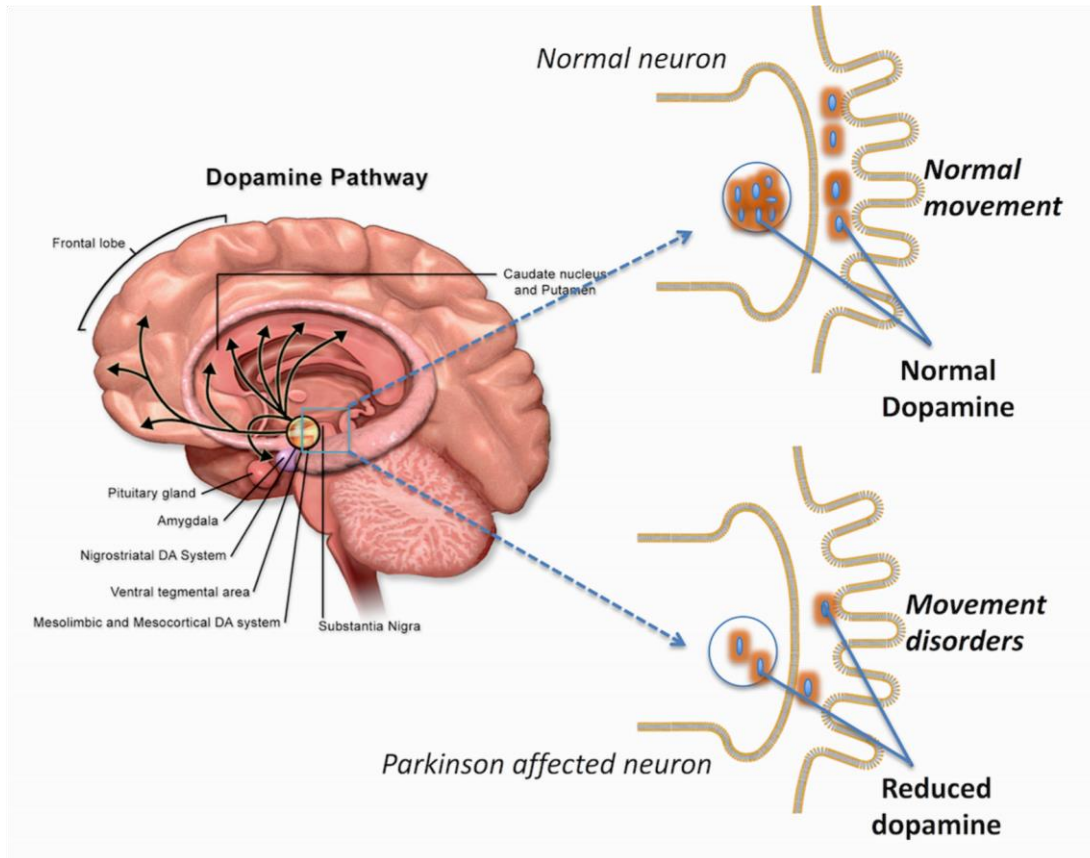


**Figure 1:** Pathologic degeneration of the dopamine pathway during Parkinson’s disease. Decreased dopamine levels lead to staggered or minimal excitement through peripheral neurons, thus resulting in movement disorders (created by Authors).

Deterioration in basal ganglia in the brain of PD patients fundamentally influences dopaminergic neurons in the substantia nigra, which concludes in dopamine insufficiency. In PD, the dyed neurons of the substantial nigra, locus caeruleus and other brain stem dopaminergic cells are vanished therefore reducing the production and transfer of dopamine within the nigrostriatal pathway. The death of neurons in the midbrain area is also closely linked with the formation of Lewy bodies which are strange proteins which develop inside nerve cells (Leyva-Gómez et al., 2015).

### ***The “Degenerative” Origin of PD***

The substantia nigra is depigmentation, neuronal loss and gliosis (within the substantia nigra). Pathogenesis probably involves apoptosis and necrosis of dopaminergic neurons. The death of neurons is supposedly due to protein misfolding, aggregation and toxicity, defective proteolysis, mitochondrial dysfunction or oxidative stress thus reduces dopamine. Other pathological hallmarks are Lewy bodies within the soma of the neurons, which are mainly made up of  $\alpha$ -synuclein bound to ubiquitin and other proteins (Leyva-Gómez et al., 2015).

### **Treatment Regimens Against Parkinson’s Disease: A Major Gap in Effectivity**

Presently, the variable treatment regimens endorsed for PD only present with symptomatic aid of sufferers. Therefore deemed incurable to inability to halt or attain reversal of the neurodegenerative progression (Schapira et al., 2014). The motor indicators are managed by a plethora of compounds that boost the DA level in the central nervous system (CNS) or mimic its effects. A DA precursor, namely, Levodopa for years now has been recognized as the gold standard for the treatment of PD. Additional regimens popularly recommended are DA receptor agonists, monoaminoxidase (MAO) 1 inhibitors (such as selegiline and rasagiline), amantadine, catechol-o-methyl-transferase (COMT) inhibitors and anticholinergic agents. These medicines are expected exert their effects of reducing symptoms to better patient lifestyle until a cure is discovered (Esposito et al., 2007).

Table 1 shown below shows some of the medicines that are already in the market or still undergoing clinical tests due to their potential antiparkinsonian effect. As highlighted earlier these drugs merely treat motor symptoms and non-motor symptoms which have devastating effects in individual, their life style and the general economy due to its implications on people who are part of a nation’s due to the demand on the public sector and tax payers to take care of PD related costs and supply (Kowal et al., 2013). Although there are ample treatment regimens for PD, none are fully effective while some have major adverse effects. Available treatment against PD is largely symptomatic since no drug has been found to slow down the degenerative process or worse even cure the disease.

This is because limited insight into the disease progression has been gathered. The most significant drug against the motor symptoms is levodopa. Even though it’s long term administration is known to induce motor complications the pro-drug is still the gold standard for symptomatic treatment, being the most tolerated among dopaminergic remedies (Silindir Gunay et al., 2016). *Dopamine agonists* have shown to have anti-parkinsonian activity; they exert their effects by acting directly on dopamine receptors and imitate

the endogenous transmitter. Originally, they were launched, as an adjunct to levodopa treatment in patients displaying fluctuating motor reaction and dyskinesia's associated with long-term use. Eventually, it has been proposed that the treatment should be introduced with a merger of low dose Levodopa and a dopamine agonist. MAO-B inhibitors were extensively employed for their proven efficiency in symptom recovery and assumed 'neuroprotective' influence. Entacapone among other *peripheral COMT inhibitors* is often given with levodopa/ADDC-inhibitor therapy, they inhibit peripheral and thus increase yield of dopamine in the neurons (Leyva-Gómez et al., 2015). The elementary PD indications arise from seriously diminished action of dopaminergic neurons due to apoptosis in the substantia nigra, specifically on pars compacta. There are five significant pathways whose names are indicative of each projection area of the brain (Mariani et al., 2005). They join other brain regions with the basal ganglia, namely, motor, oculomotor, associative, limbic and orbitofrontal circuits. The syndrome symptoms manifest due to the influence exerted by the disruption routes which largely carter for motion, attention and learning. Of all routes, the motor route experiences the most significant effects. The PD symptomatic regimen employed (Table 1), conversely may inessentially trigger action of dopamine, permitting for motion routines to respond at unseemly intervals and thus bearing dyskinesia's (Benitez-temino et al. 2008; Mariani et al., 2005)

(Table 1), conversely may inessentially trigger action of dopamine, permitting for motion routines to respond at unseemly intervals and thus bearing dyskinesia's.

Name of drugs	Target Protein	Lipophilicity (Predicted)	Log P	BBB Permeability	Side effects
Pramipexole	Selective dopamine receptor agonist	2.18	1.86	No	Headache, Nausea and vomiting, gambling, hyper sexuality, overeating.

Ropinirole	Suspected to be stimulation of postsynaptic dopamine D2-type receptors	2.3	2.7	Yes	dyskinesia, nausea, dizziness, somnolence, hallucinations, and orthostatic hypotension
Rotigotine	D2 dopamine Receptor Agonist	3.69	4.7	Yes	Vomiting, loss of appetite, diarrhea
Apomorphine	Non-selective dopamine agonist which activates D2 and D1 agonists.	2.57	3.1	Yes	Powerful emetic, its adverse effects limit its use.
Piribedile	Dopamine receptor agonist	2.88	1.8	Yes	Nausea and vomiting, flatulence, dizziness or confusion
Dihydro-ergocryptine	Dopamine receptor agonist	3.36	3.1	No	Nausea and Vomiting, Cardiac Arrhythmias, Postural hypotension
Pergolide	Dopamine receptor agonist	3.03	4.2	Yes	Withdrawn 2003 due to risk of Cardiac fibrosis; sex addiction, gambling addiction
Dopamine	Dopamine receptor agonist	1.08	-0.7	No	Bradycardia, Nausea, Vomiting

Opicapone	COMT Inhibitor	0.99	2.1	No	Dyskinesia, Dizziness, Dry mouth, Constipation
Tolcapone	Inhibits Catechol O-methyltransferase  COMT Inhibitor	0.93	3.3	No	Lethal Liver insufficiency
Carbidopa	DOPA decarboxylase inhibitor	0.47	-2.2	No	DOPA decarboxylase inhibitor

Selegiline	Irreversible inhibition of MAO-B	2.7	2.8	Yes	Mouth sores, Exacerbates L-dopa related dyskinesia's
Rasagiline	Irreversible inhibition of MAO-B	2.51	1.8	No	Mild skin rash, dizziness, vomiting,
Lazabemide	Irreversible inhibition of MAO-B	1.07	0.2	No	Joint pain, mild headache, hair loss.
Carbapoline	Dopamine Receptor Agonists	2.6	3.4	Yes	Nervousness, stomach pain
Cycrimine	Anticholinergic- blocks acetyl Choline in central and peripheral nervous system	3.58		Yes	Lethargy, psychosis, orthostatic dizziness, blurred vision.
Benserazide	DOPA Decarboxylase Inhibitor (DDC)	0.72	-1.3	No	Nausea and Vomiting paranoia and depression
Benzatropine	Anticholinergic	3.56	4.5	Yes	Blurred vision, Cognitive changes, Dry Mouth
Tropatepine	Anticholinergic	3.55	4.8	Yes	Glaucoma
Chlorphenoxamine	Anticholinergic	4.1	3.73	Yes	Constipation, decreased coordination

Amantadine	Increases dopamine release and Blocks dopamine re-uptake	2.18	2.44	Yes	Irritability, Ataxia
------------	---	------	------	-----	----------------------

Budipine	NMDA receptor antagonist promotes the synthesis of dopamine.	3.61	5.2	Yes	Dizziness, dry mouth and loss of appetite.
----------	--	------	-----	-----	---

### **Permeating the blood–brain barrier; Hindering PD therapy**

A particular challenge in the pharmacologic remedies of neurodegenerative diseases, such as PD, is that of neurodegenerative conditions is trouble in crossing the BBB (Figure 2) and relaying a sufficient dose to the brain without metabolism (Silindir Gunay et al., 2016). Such challenges emanate from the protective blockades immediate to the brain such as the BBB and the blood-cerebrospinal fluid, which restrict transport of compounds and necessitate the creation and employment of novel methods. This is because there is a limited amount of regimens that can infiltrate due to lipophilic membranes and junctions embedding the barriers; namely the blood–brain (BBB) and placental (Devnarain et al., 2017).

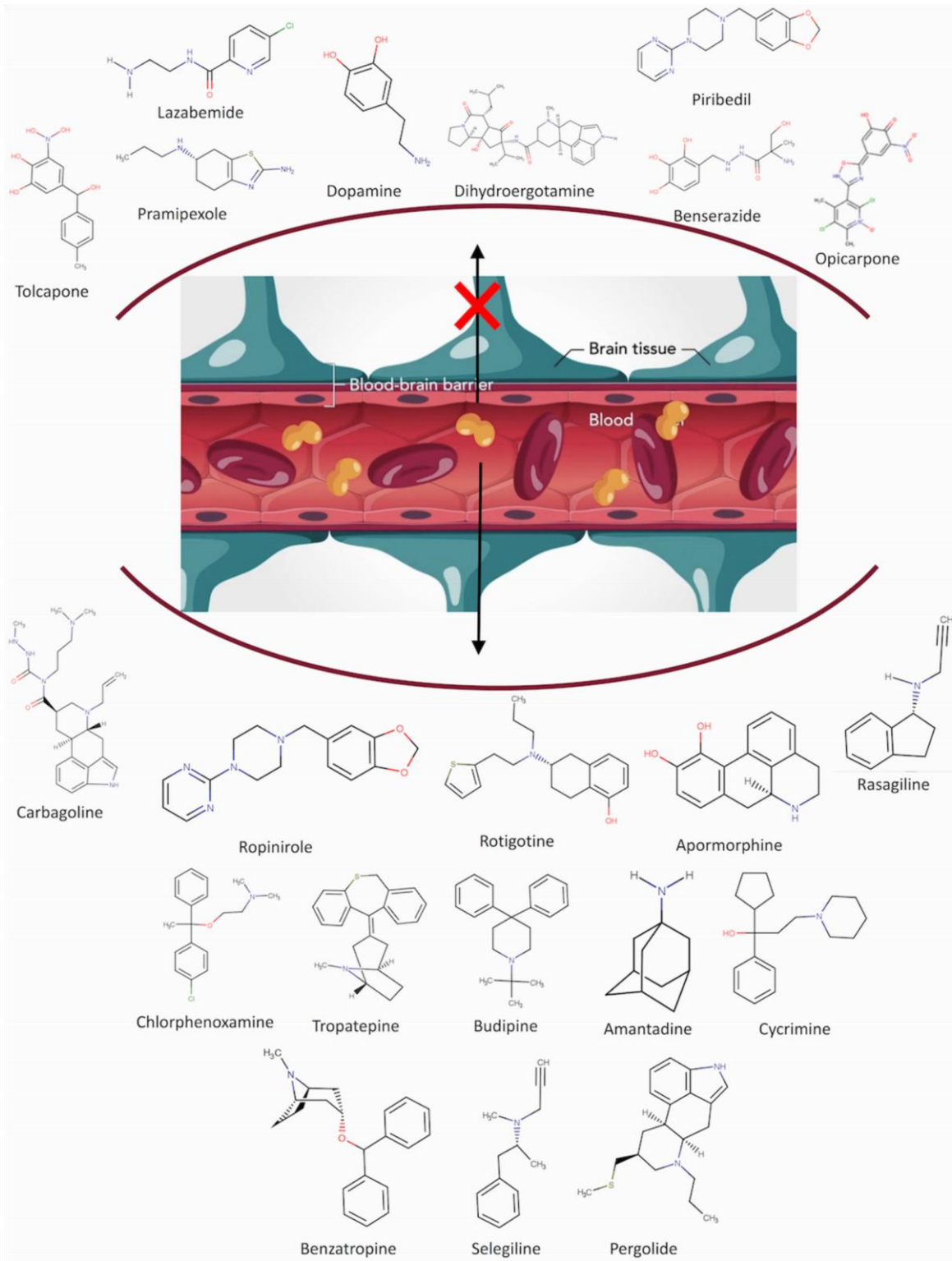


**Figure 2:** Anti-Parkinson's drugs that can pass the blood-brain-barrier, versus drugs that cannot.

### Systemic interventions to unstitch the obstacle in the treatment of PD

To overcome this setback in the treatment of PD, the drugs have to be transported across the BBB to elicit their full potential. This could be attained through drug delivery systems where pre-BBB impermeable drugs are “carried” or modified to permeate the BB. Two strategies: (1) ameliorate the inhibitor and (2) convey the cargo to enhance the delivery of PD drugs across the BBB is further elaborated in this review (Figure 3).

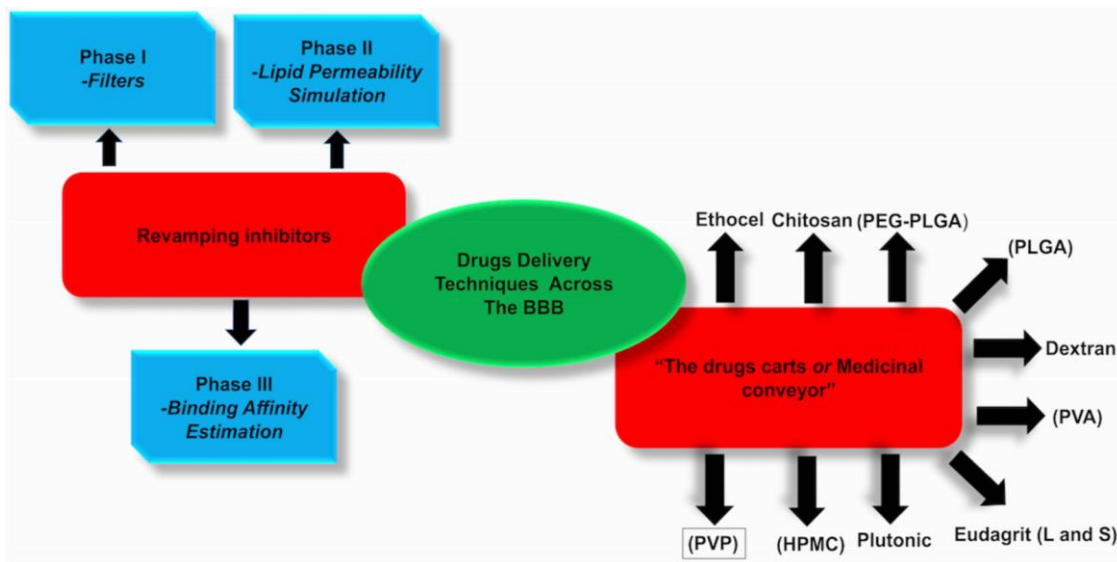


**Figure 3:** Graphical representation of interventions to unstitch the obstacle in the treatment of PD.

#### *Revamping inhibitors*

In this procedure, computational apparatus may be utilized to image and hone likely compounds, followed by compound manufacture and organic trials. These have been categorized into three phases; Phase I, II and III

**Phase I** entails targeted collection of possible anti-Parkinson's compounds. This encompasses screening for likely compounds with distinct physicochemical properties and anti-Parkinson's action operating chemical databases, including adoption of absorption, distribution, metabolism, excretion (ADME) indicator devices namely, Swiss ADME and quantitative structure-activity relationship (QSAR) models, for the sake of altering out compounds that possess the qualities of traversing the BBB while maintaining or improving anti-PD efficacy (Oksel and Wang, 2013). The capacity of an active ingredient to penetrate the BBB is determined by its extent of lipophilicity, the molecular properties of unstable and hydrophobic side-chains of the compound including molecular mass (Egido et al., 2015). The focal lipophilic attributes that should be pondered incorporate the Hansch constant ( $p$ ), hydrophobic fragmental constant ( $f$ ),  $\log P$ , capacity factor numbers from RPHPLC ( $\log k_w$ ), processed  $\log P$  values (CLOGP) and molecular lipophilic potential (MLP) (Oksel and Wang, 2013). Pertaining to the charge of the structure, only stable molecules can permeate the membrane to undergo re-protonation when it passes the membrane and enters the brain fluid (Egido et al., 2015). With increasing size of a compound, its aptitude to pervade the BBB dwindles (Arnott and Planey, 2012).

**Phase II** includes the forecast of lipid penetrability of the probable anti-PD compounds utilizing molecular dynamic imitations and Swiss ADME (3D modeled lipid simulations). Owing to the encircling lipid film of the BBB, it is essential to evaluate compound interfaces with the focal enzyme inside the lipid film (Rodriguez-espigares et al., 2014).

**Phase III** includes the computation of binding affinities between probable anti-Parkinson's substrates, which traverse the BBB, and areas of the brain affected by PD through binding free computations and molecular docking of specific compounds into the target receptor (Meng et al., 2011).

Subsequent to the course imagery, compound synthesis is a prerogative for additional examination. The development of the carbon structure and the removal/addition/transformation of side-chains are carried out

for the formation of a compound product. Ligand-binding tests are then done to verify the compound quality, the do target enzyme are mixed with compound of concern into diluent (e.g. water) to permit the compound to engage with the active site moieties of the enzyme (Hulme et al., 2010). Binding inquiries yield dependable analysis of binding affinities, errors and binding method (Hulme et al., 2010). Additional research involving biological examination will explore toxicity and efficacy of a compound, encompassing *in vitro* studies (cellular level), *in vivo* studies (organism level) and eventually clinical tests. Microscale thermophoresis (MST) might be employed for the sake of scrutinizing the interplay between the substrates and receptors, analytically, based on the regulated motion of particles across a slope of the temperature (Ali et al., 2012; Scheuermann et al., 2016) .

Research on treatment of Parkinson's disease has made some tremendous steps in exploring symptomatic treatment by graduating from the day a limited dopamine which could not pass the BBB to the discovery of ground breaking pro-drug Levodopa and the use accompaniment of enzyme inhibitors e.g. Carbidopa–Levodopa the most effective and well-tolerated pharmacological remedies on offer to patients, used for the treatment of rigidity and rest tremor (Brichta et al., 2013). Regardless of the various developments in approaches for treatment of this neurodegenerative disorder there are still challenges that restrain effective therapy, namely the shipment of drugs through the BBB to the target brain tissue and side effects noticed during long-term treatment. The use of drug delivery systems such as nanoparticles for more optimized therapy is being explored for PD therapy and is expected to help diminish adverse effects.

### ***“Drug Carts or A Medicinal Conveyor”***

The controlled drug release technology has evolved immensely over the last six decades (Figure 1). It commenced in 1952 with the introduction of the first sustained release preparation. Figure shows how. There is sundry PD research avenues that are prospective ground for future mediations including therapeutic centered either partly or completely, on Nano-polymer preparations. We are still face with the problems of “on-off” episodes, namely, dyskinesia's and poor drug solubility. Complementary to engineering new BBB-permeable medicines, the use of drug carriers have been effective in transporting medicines to the brain. This method removes the extra time and expenses necessitated to craft and formulate fresh medicines and drug carriers. A drug delivery system could be employed to transport a

BBB-impermeable drug to the brain and permit for the drug to execute its function against PD symptoms (Newland et al., 2015).

Throughout the development medicines of different routes in different certain benefits accompanied by challenges have been noticed and areas to be harnessed and a cause of concern respectively. Figure 4 highlights some of the characteristics to be noted in individual polymers while preparing various formulations to treat PD. The foremost prerogative for addressing the bioavailability and stability restraints of poorly soluble drugs is the diminution of particle size to nanoscale for improved solubility and drug targeting (Gigliobianco et al., 2018).

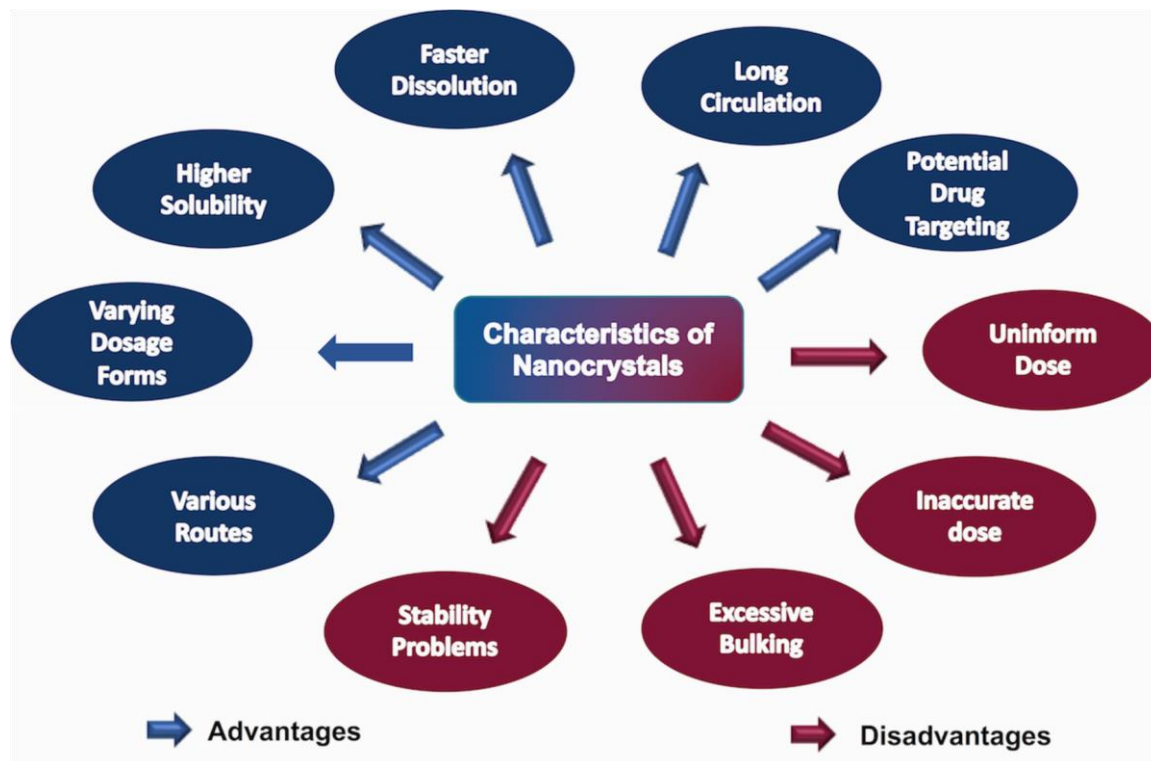


**Figure 4:** depiction of the major characteristics of nanocrystals (Prepared by author).

The drugs listed in (Table2) have been confirmed to deal with motor or non-motor symptoms of PD in secluded *in-vitro* testing. These include drugs such as dihydroergocryptine and pramipexole, however the drugs are unable to route through the BBB to thwart PD symptoms (Table 5.1). Traversing the blood BBB remains a major hindrance in development of efficient PD treatments and without a drug delivery system these molecules stay on the peripheral side of the BBB like cargo without a carrier and remain useless to the dopamine-starved brain cells.

**Table 2:** Properties exhibited by potential Parkinson’s drug carriers

Drug carrier	Drug Summary
Chitosan	Has shown to effectively transport Carbagoline effectively and accumulate high concentrations in brain through evoking paracellular drug transport  (Sharma et al., 2009).
Poly (ethylene glycol)-poly (colic-co-glycolic-acid) (PEG-PLGA)	PEG-PLGA are biodegradable with efficient transport of rotigotine across BBB for PD treatment (Wang et al., 2001).
Poly (butyl cyanoacrylate)	PBCA coated with polysorbate 80 enhances the efficiency of nerve growth factor and is shown to reverse MPTP induced PD in rats. (Kurakhmaeva et al., 2009)
Chitosan	<i>In-vitro</i> tests have affirmed that dopamine-loaded chitosan has diminished cytotoxicity of free dopamine. (Trapani et al., 2011)
PLGA	Levodopa nanoparticle encase benserazide PLGA microspheres favorably removed duskiness in rat. (Choudhury et al., 2017)
Dextran	Manageable equilibrium of expansion, mechanical tenacity and degradability.(Hovgaard and Brndsted, 1995)

Odorranalectin (OL) PEG-PLGA conjugated nanoparticles	The outcome implied that OL boosted the brain delivery of NPs. (Wen et al., 2011)
Polyvinyl alcohol (PVA)	Is impervious to grease oils, and solvents. It has a lofty tensile strength and elasticity, as well as steep oxygen and aroma blockade attributes (Fromageau et al., 2003).
PVP	It escalates the water solubility of hydrophobic substances. In normal doses naturally passes through the body with little to no harm when taken orally (Fromageau et al., 2003; Yoshida et al., 2008).
Pluronic	This sol- gel transition is can also be sensitive to concentration and temperature, is also affected by salts and alcohols by their influence on polymer hydration (Feilden et al., 2016).
HPMC	Given with Nifedipine in trial on rabbit specimen improved deficient solubility and dissolution speed of efficacious Ca antagonist(Yoshida et al., 2008; Ghosal et al., 2011).
Eudagrit (L and S)	The polymer only dissolves between a PH of 6 and 7, which enables it to resist the first-pass reactions in the stomach and liver which could potentially metabolize the loaded drug (Krögel and Bodmeier, 1999).
Ethocel	Ethyl cellulose materials are flexible, organosoluble, and thermoplastic polymers. Its pharmaceutically approved products cover the taste of sour medicines, improve the strength and empower controlled release mixtures (Decuzzi et al., 2009).

## **Discussion**

It is beyond any doubt that the computational tool kit is capable fulfilling the ordeal of identifying present properties, making required for current FDA approved drugs and giving reliable insight on the possibility of using the listed anti-Parkinson's drugs to eradicate or by the least manage the onslaught being perpetuated by PD globally. There is ongoing search on the cure and symptomatic treatment of PD and a significant foremost challenge lies with delivery across the BBB, side effects and low solubility of drugs. The approaches eluded in this review serve to deliver intelligence on additional studies on the design of drugs with improved BBB permeability profile for better curative and symptomatic treatment results, and less side effects for better patient adherence to medication.

## **Conflict of Interest**

The authors declare that the research was conducted in the absence of any commercial or financial relationships that could be construed as a potential conflict of interest.

## **Funding**

Details of all funding sources should be provided, including grant numbers if applicable. Please ensure to add all necessary funding information, as after publication this is no longer possible.

## **Acknowledgments**

This is a short text to acknowledge the contributions of specific colleagues, institutions, or agencies that aided the efforts of the authors.

## **Author Contributions**

The manuscript writing and image preparation was carried out by Ndlovu , ST and Kumi, RO. The conceptualization of the manuscript and editing was finalized by Ramharack, P and Soliman, ME.

Nloto, M, carried out supervision.

## References

- Ali, W., Williams, A. C., Rawlinson, C. F., Bennett, R. C., Brough, C., Miller, D. A., et al. (2012). Notice to Authors of JACS. *Int. J. Pharm.* 2, E18–E24. doi:10.1016/j.phymed.2007.11.019.
- Arnott, J. A., and Planey, S. L. (2012). The influence of lipophilicity in drug discovery and design. 909–921.
- Benitez-temino, B., Obeso, J. A., Rodri, M. C., Rodriguez, M., Blesa, F. J., and Guridi, J. (2008). Functional Organization of the Basal Ganglia : Therapeutic Implications for Parkinson’ s Disease. 23, 548–559. doi:10.1002/mds.22062.
- Brichta, L., Greengard, P., and Flajolet, M. (2013). Advances in the pharmacological treatment of Parkinson’ s disease : targeting neurotransmitter systems. *Trends Neurosci.* 36, 543–554. doi:10.1016/j.tins.2013.06.003.
- Choudhury, A., Vana, D., Varma R, J., Banerjee, T., Ramachandraravapu, A., and Adapa, D. (2017). *Cognitive and Psychological Anomalies in Parkinson’s Disease: An Insight into Non-Motor Characteristic Features.* doi:10.4172/Neuropsychiatry.1000317.
- Decuzzi, P., Pasqualini, R., Arap, W., and Ferrari, M. (2009). Intravascular delivery of particulate systems: Does geometry really matter? *Pharm. Res.* 26, 235–243. doi:10.1007/s11095-008-9697-x.
- DeMaagd, G., and Philip, A. (2015). Parkinson’s Disease and Its Management. 40, 504–511.
- Devnarain, N., Ramharack, P., and Soliman, M. E. (2017). Brain grants permission of access to Zika virus but denies entry to drugs: A molecular modeling perspective to infiltrate the boundary. *RSC Adv.* 7, 47416–47424. doi:10.1039/c7ra05918c.
- Egido, E., Müller, R., Li-blatter, X., Merino, G., and Seelig, A. (2015). Predicting Activators and Inhibitors of the Breast Cancer Resistance Protein ( ABCG2 ) and P-Glycoprotein ( ABCB1 ) Based on Mechanistic Considerations Predicting Activators and Inhibitors of the Breast Cancer Resistance Anna Seelig , PhD. doi:10.1021/acs.molpharmaceut.5b00463.
- Esposito, E., Di, V., Benigno, A., Pierucci, M., Crescimanno, G., and Di, G. (2007). Non-steroidal antiinflammatory drugs in Parkinson’ s disease. 205, 295–312. doi:10.1016/j.expneurol.2007.02.008.

- Feilden, E., Blanca, E. G. T., Giuliani, F., Saiz, E., and Vandeperre, L. (2016). Robocasting of structural ceramic parts with hydrogel inks. *J. Eur. Ceram. Soc.* 36, 2525–2533. doi:10.1016/j.jeurceramsoc.2016.03.001.
- Fromageau, J., Brusseau, E., Vray, D., Gimenez, G., and Delachartre, P. (2003). Characterization of PVA Crygel for Intravascular Ultrasound Elasticity Imaging. *IEE Trans. Ultrason. Ferroelectr. Freq. Control* 50, 1318–1324.
- Ghosal, K., Chakrabarty, S., and Nanda, A. (2011). Hydroxypropyl methylcellulose in drug delivery. *Der Pharm. Sin.* 2, 152–168. doi:10.5402/2011/651909.
- Gigliobianco, M. R., Casadidio, C., Censi, R., and Di Martino, P. (2018). Nanocrystals of poorly soluble drugs: Drug bioavailability and physicochemical stability. *Pharmaceutics* 10. doi:10.3390/pharmaceutics10030134.
- Hovgaard, L., and Brndsted, H. (1995). controlled release Dextran hydrogels for colon-specific drug delivery. 36, 159–166.
- Hulme, C., Wright, J., Crocker, T., Oluboyede, Y., and House, A. (2010). Non-pharmacological approaches for dementia that informal carers might try or access: A systematic review. *Int. J. Geriatr. Psychiatry* 25, 756–763. doi:10.1002/gps.2429.
- Kowal, S. L., Dall, T. M., Chakrabarti, R., Storm, M. V., and Jain, A. (2013). The current and projected economic burden of Parkinson's disease in the United States. *Mov. Disord.* 28, 311–318. doi:10.1002/mds.25292.
- Krögel, I., and Bodmeier, R. (1999). Floating or pulsatile drug delivery systems based on coated effervescent cores. *Int. J. Pharm.* 187, 175–184. doi:10.1016/S0378-5173(99)00189-1.
- Kurakhmaeva, K. B., Djindjikhvili, I. A., Petrov, V. E., Balabanyan, V. U., Voronina, T. A., Trofimov, S. S., et al. (2009). Brain targeting of nerve growth factor using poly ( butyl cyanoacrylate ) nanoparticles. 17, 564–574. doi:10.1080/10611860903112842.
- Leyva-Gómez, G., Cortés, H., Magaña, J. J., Leyva-García, N., Quintanar-Guerrero, D., and Florán, B. (2015). Nanoparticle technology for treatment of Parkinson's disease: the role of surface phenomena in reaching the brain. *Drug Discov. Today* 20, 824–837. doi:10.1016/j.drudis.2015.02.009.
- Loftsson, T., and Brewster, M. E. (2010). Pharmaceutical applications of cyclodextrins: Basic science and product development. *J. Pharm. Pharmacol.* 62, 1607–1621. doi:10.1111/j.20427158.2010.01030.x.

- Mariani, E., Polidori, M. C. C., Cherubini, A., and Mecocci, P. (2005). Oxidative stress in brain aging, neurodegenerative and vascular diseases: An overview. *J. Chromatogr. B* 827, 65–75. doi:10.1016/j.jchromb.2005.04.023.
- Meng, X., Zhang, H., Mezei, M., and Cui, M. (2011). Molecular Docking : A Powerful Approach for Structure-Based Drug Discovery. 146–157.
- Newland, B., Newland, H., Werner, C., Rosser, A., and Wang, W. (2015). Prospects for polymer therapeutics in Parkinson’s disease and other neurodegenerative disorders. *Prog. Polym. Sci.* 44, 79– 112. doi:10.1016/j.progpolymsci.2014.12.002.
- Oksel, C., and Wang, X. Z. (2013). “ Quantitative Structure - Activity Relationship ( QSAR ) models ” Purpose of Today.
- Rodriguez-espigares, I., Rami, J. M., Martinez-seara, H., Giorgino, T., and Selent, J. (2014). Structural bioinformatics MEMBPLUGIN : studying membrane complexity in VMD. 30, 1478–1480. doi:10.1093/bioinformatics/btu037.
- Schapira, A. H. V., Olanow, C. W., Greenamyre, J. T., and Bezdard, E. (2014). Slowing of neurodegeneration in Parkinson’s disease and Huntington’s disease: Future therapeutic perspectives. *Lancet* 384, 545–555. doi:10.1016/S0140-6736(14)61010-2.
- Scheuermann, T. H., Padrick, S. B., Gardner, K. H., and Brautigam, C. A. (2016). On the acquisition and analysis of microscale thermophoresis data. *Anal. Biochem.* 496, 79–93. doi:10.1016/j.ab.2015.12.013.
- Sharma, G., Mishra, A. K., Mishra, P., and Misra, A. (2009). Intranasal Cabergoline : Pharmacokinetic and Pharmacodynamic Studies. 10. doi:10.1208/s12249-009-9329-8.
- Silindir Gunay, M., Yekta Ozer, A., and Chalon, S. (2016). Drug Delivery Systems for Imaging and Therapy of Parkinson’s Disease. *Curr. Neuropharmacol.* 14, 376–391. doi:10.2174/1570159X14666151230124904.
- Trapani, A., Giglio, E. De, Cafagna, D., Denora, N., Agrimi, G., Cassano, T., et al. (2011). Characterization and evaluation of chitosan nanoparticles for dopamine brain delivery. *Int. J. Pharm.* 419, 296–307. doi:10.1016/j.ijpharm.2011.07.036.
- Wang, W., Donini, O., Reyes, C. M., and Kollman, P. A. (2001). Biomolecular Simulations: Recent Developments in Force Fields, Simulations of Enzyme Catalysis, Protein-Ligand, Protein-Protein, and Protein-Nucleic Acid Noncovalent Interactions. *Annu. Rev. Biophys. Biomol. Struct.* 30, 211– 243. doi:10.1146/annurev.biophys.30.1.211.

Wen, Z., Yan, Z., Hu, K., Pang, Z., Cheng, X., Guo, L., et al. (2011). Odorranalectin-conjugated nanoparticles: Preparation, brain delivery and pharmacodynamic study on Parkinson's disease following intranasal administration. *J. Control. Release* 151, 131–138. doi:10.1016/j.jconrel.2011.02.022.

Yoshida, K., Sakurai, Y., Kawahara, S., Takeda, T., Ishikawa, T., Murakami, T., et al. (2008). Anaphylaxis to polyvinylpyrrolidone in povidone-iodine for impetigo contagiosum in a boy with atopic dermatitis. *Int. Arch. Allergy Immunol.* 146, 169–173. doi:10.1159/000113522.

## CHAPTER 6

### Overall Conclusions and Recommendations for Future Studies

This Chapter provide a general conclusion, highlights the significance of the findings in the study and outlines recommendations for the future

#### 6.1. General conclusion

Since Parkinson's is envisioned to upset more lives in correspondence with a staggering increase in elderly population. There are growing conversations neurodegenerative tide of PD also poses non-motor symptoms and some of them are: autonomic dysfunctions, apathy, depressions, sleep disorders, fatigue, pain and dementia great deal of research pertaining to the treatment will be of necessity. The growth Insilico studies of polymer-drug structure and interaction is expected to bring about significant breakthrough to the research and medical arena in a year to come.

One of the major challenges that we encountered was with the establishing whether this improvement in this rate regulating solubility will result with in an intensification in bioavailability in *in-vivo* as in the *invitro* test. Therefore, the residual challenges in cementing the outcomes of both experimental and computational studies done on the interaction between polymeric nanoparticles and domperidone would be to establish the efficiency of the antiemetic drug in an animal specimen. Fortunately, the use of animals in testing for neurodegenerative diseases has become more conventional over the years. What also remains It is estimated that 90% of new drugs in the development pipeline can be classified as poorly soluble (Dennison 2016).

Given the great number of poorly soluble drugs, novel and appropriate formulations as well as technological solutions are needed to sufficiently increase drug bioavailability, accordingly to the administration route (Gigliobianco, Casadidio, Censi & Di Martino 2018) To date, the classical method for enhancing the dissolution rate of poorly soluble drugs is to reduce particle size, in particula through micronization (Gigliobianco *et al.*, 2018). However, it seems that further improvement in the drug dissolution rate and thus in bioavailability demands a shifting from micronization to nanonization. This requires various and innovative technological methods, as well as novel resolutions to overcome all of the physicochemical and stability problems linked with nanostructures.

Credits to the advanced process technologies and analytical methods harnessed in the last

decades, a considerable number of pharmaceutical nanocrystal formulations are now on the market and several are under development (Gigliobianco *et a.l.*, 2018). Nanocrystals consisting of pure drugs and a minimum of surface

Molecular modeling and computational pharmaceutics methods have been broadly adopted in drug discovery fields. A wide range of tools are being used to model or mimic the behavior of molecules and assist investigate formulation at the molecular level. Computational pharmaceutics enables us to understand and develop new pharmaceutical drug delivery systems. Regardless of plenty investigations on this field of research, restricted has been accounts on the oral therapy of this anti-Parkinson's drug, the gap in molecular modelling applications on antimicrobial drug delivery systems. Another disparity in the literature is the research that specifically aimed to explore the interactions between the nanoparticles and biological targets (proteins/enzymes), one critical example being the interactions of domperidone with receptor nano-polymers (Sliwoski, Kothiwale, Meiler & Lowe 2014).

## **6.2. Significance of the findings in the study**

The computational approaches and tools applied in this work and the combined experimentadata have successfully provided molecular insight into the design, structural, conformational and interaction features of the nano-drug delivery systems investigated in this thesis. Considering the aim, objectives and outcomes, the significance of the findings includes the following:

### *Recent pharmaceutical products:*

The novel DOMP-nanopolymeric particles successfully designed and characterized by molecular modelling tools in this study can stimulate local pharmaceutical industries to manufacture cost-effective superior medicines (Ullah, Khan, Ahmed, Govender, Faidah, de Matas, Shahid, Minhas, Sohail & Khurram 2018).

### *Invention of new knowledge to the scientific community*

The various studies and findings of the study have contributed to the pharmaceutical sciences knowledge database in several ways. These include the following:

- New knowledge was obtained through the in-silico studies that were performed to understand the possible interactions of DOMP and the different polymer molecules, investigate molecular mechanism behind the enhanced entrapment of domperidone, and determine the stability, structural and conformational features of these polymeric nanoparticles.
- In the case of the DOMP-nanopolymeric studies, new knowledge was obtained in that this is the first account of investigating the potential uses of DOMP-nanopolymers as potential oral antiParkinson's formulations using hybrid molecular modelling and experimental endorsements (Ullah 2018).

### **6.3. Recommendations for future studies**

Although a wide range of molecular modelling approaches were applied in this work and successfully demonstrated the applications of various tools to understand and characterize the

structural and dynamic aspects of different drug delivery systems including, DOMP-nanoparticles, further research is expedient to enhance and drive toward the design of future superior formulations. The following recommendations could be considered in future studies:

- In the case of DOMP, the use of wide range of drug nano-carriers various polymers, need to be explored for potential antibacterial activities. The applications of molecular modelling tools would serve as a powerful tool, as hundreds of drug-nanoparticles could be investigated using in silico

methods before performing experimental investigations. This could reduce the time and cost associated with experimental screening hundreds of molecules using wet lab

- More computational research could be done on the structure of domperidone, in relation with its biological interaction and consequent side-effects; and its physicochemical qualities and consequent low solubility and dissolution. This insight into quantitative structure activity relationship (QSAR) could open doors to more efficient therapy in PD and ND and conditions.

Finally, the general findings of this research therefore demonstrate the potential applications of the diverse molecular modelling approach in understanding, distinguishing and designing novel nano-based drug delivery systems in anti-Parkinson's therapy. This research has made consequential contributions to the field of Nano-based strategic mediations to deal with the challenges associated with BSC II and BSC IV drugs (Tsume, Mudie, Langguth & Amidon 2014). The realization of nanotechnology to address the present crisis in therapy of global neurodegenerative drug will be dependent on future exhaustive and multidisciplinary analysis.

## References

Dennison, T.J., 2016. Orally Disintegrating Tablets: Formulation Development, Novel Engineering Solutions and Fixed Dose Combinations.

Gigliobianco, M., Casadidio, C., Censi, R. and Di Martino, P., 2018. Nanocrystals of Poorly Soluble Drugs: Drug Bioavailability and Physicochemical stability. *Pharmaceutics*, 10(3), p.134.

Sliwoski, G., Kothiwale, S., Meiler, J. and Lowe, E.W., 2014. Computational methods in drug discovery. *Pharmacological reviews*, 66(1), pp.334-395.

Tsume, Y., Mudie, D.M., Langguth, P., Amidon, G.E. and Amidon, G.L., 2014. The Biopharmaceutics Classification System: subclasses for in vivo predictive dissolution (IPD) methodology and IVIVC. *European Journal of Pharmaceutical Sciences*, 57, pp.152-163.

Ullah, N., Khan, S., Ahmed, S., Govender, T., Faidah, H.S., de Matas, M., Shahid, M., Minhas, M.U., Sohail, M. and Khurram, M., 2018. Dexibuprofen nanocrystals with improved therapeutic performance:

fabrication, characterization, in silico modeling, and in vivo evaluation. *International journal of nanomedicine*, 13, p.1677.

## APPENDIX



# Domperidone nanocrystals with boosted oral bioavailability: fabrication, evaluation and molecular insight into the polymer-domperidone nanocrystal interaction

Stalielson Tatenda Ndlovu<sup>1</sup> & Naseem Ullah<sup>2</sup> & Shahzeb Khan<sup>1,3</sup> & Pritika Ramharack<sup>1</sup> & Mahmoud Soliman<sup>1</sup> & Marcel de Matas<sup>4</sup> & Muhammad Shahid<sup>5</sup> & Muhammad Sohail<sup>6</sup> & Muhammad Imran<sup>7</sup> & Syed Wadood Ali Shah<sup>3</sup> & Zahid Hussain<sup>8</sup> 

# Controlled Release Society 2018

## Abstract

The aim of this study was to employ experimental and molecular modelling approaches to use molecular level interactions to rationalise the selection of suitable polymers for use in the production of stable domperidone (DOMP) nanocrystals with enhanced bioavailability. A low-energy antisolvent precipitation method was used for the preparation and screening of polymers for stable nanocrystals of DOMP. Ethyl cellulose was found to be very efficient in producing stable DOMP nanocrystals with particle size of  $130 \pm 3$  nm. Moreover, the combination of hydroxypropyl methylcellulose and polyvinyl alcohol was also shown to be better in producing DOMP nanocrystals with smaller particle size ( $200 \pm 3.5$  nm). DOMP nanosuspension stored at 2–8 °C and at room temperature (25 °C) exhibited better stability compared to the samples stored at 40 °C. Crystallinity of the unprocessed and processed DOMP was monitored by differential scanning calorimetry and powder X-ray diffraction. DOMP nanocrystals gave enhanced dissolution rate compared to the unprocessed drug substance. DOMP nanocrystals at a dose of 10 mg/kg in rats showed enhanced bioavailability compared to the raw drug substance and marketed formulation. A significant increase in plasma concentration of 2.6 µg/mL with a significant decrease in time (1 h) to reach maximum plasma concentration was observed for DOMP nanocrystals compared to the raw DOMP. Molecular modelling studies provided underpinning knowledge at the molecular level of the DOMP-polymer nanocrystal interactions and substantiated the experimental studies. This included an understanding of the impact of polymers on the size of nanocrystals and their associated stability characteristics.

**Keywords** Domperidone . Nanocrystals . Molecular modelling . Polymers . Dissolution . Enhanced bioavailability

## Introduction

The oral route of administration is one of the most convenient, useful and frequently used means to administer drugs [1]. In

this regard, however, the poor aqueous solubility of drugs has been the leading factor, limiting the attractiveness of this route for some compounds and leading to low oral bioavailability and dissolution rate via this route. For drugs classified as class

\* Shahzeb Khan  
shahzeb\_333@hotmail.com; shahzebkhan@uom.edu.pk

\* Mahmoud Soliman  
Soliman@ukzn.ac.za

<sup>1</sup> Discipline of Pharmaceutical Sciences, College of Health Sciences, University of KwaZulu-Natal, Westville Campus, Durban, South Africa

<sup>2</sup> Department of Pharmacy, Abasyn University, Peshawar, KPK, Pakistan

<sup>3</sup> Department of Pharmacy, University of Malakand, Dir Lower Chakdara, KPK, Pakistan

<sup>4</sup> SEDA Pharmaceutical Development Services, The BioHub at Alderley Park, Cheshire, UK

<sup>5</sup> Department of Pharmacy, Sarhad University of Science and Information Technology, Peshawar, KPK, Pakistan

<sup>6</sup> Department of Pharmacy, COMSATS University Islamabad, Abbottabad 22060, Pakistan

<sup>7</sup> HEJ, Research Institute of Chemistry, International Centre for Chemical and Biological Sciences, University of Karachi, Karachi, Pakistan

<sup>8</sup> Department of Pharmaceutics, Faculty of Pharmacy, Universiti Teknologi MARA (UiTM) Selangor, Puncak Alam Campus 42300, Bandar Puncak Alam, Selangor, Malaysia

II according to the Biopharmaceutics Classification System (BCS), solubility and dissolution rate are of great importance and considered as the basic factors, which influence the rate and extent of drug absorption from the gastrointestinal tract (GIT) [2]. According to recent publications, approximately 40% of compounds in development are subject to poor water solubility [3]. To reach the therapeutic plasma concentrations, poorly water-soluble drugs are often given at high doses. With the variability in exposure, which is often observed for drugs of this nature, this provides risks of suboptimal efficacy and safety, particularly for drugs with low therapeutic index. In this regard, from a clinical perspective, it is more desirable to use low doses of drugs having greater dissolution rate, better absorption and enhanced bioavailability. A number of well-established strategies exist for enhancing the solubility and dissolution rates of drugs with low aqueous solubility [4, 5].

In the current pharmaceutical drug delivery research domain, nanotechnology is an emerging field, where drugs with sub-micron particle size are increasingly being considered as a means to address the problem of poor aqueous solubility. Owing to their significantly high surface area to volume ratio, the nanoparticles [6, 7] are believed to provide an excellent means to drive dissolution in the GI tract. The Noyes–Whitney equation gives a sound basis for this dissolution rate enhancement with reduction of the particle size to the nanosized range, enhancing the surface free energy and surface area leading to increases in water solubility and rate of dissolution [8].

In terms of methods of producing nanoparticulate drugs, two major techniques have been described, which include bottom-up and top-down methods. The typical top-down methods include wet milling and high pressure homogenisation [9], whereas the bottom-up methods are

mainly based on the principle of antisolvent crystallisation [10]. Nanosuspensions are the preparations composed of suspended particles in nanoform, stabilised by polymers and surfactants. The patented solvent displacement method was first used by Fessi et al. for the preparation of nanosuspensions [11].

Domperidone is a pharmacological antagonist of dopamine-2 receptor and belongs to class II of the BCS (Fig. 1). Domperidone (DOMP) is used as antiemetic as well

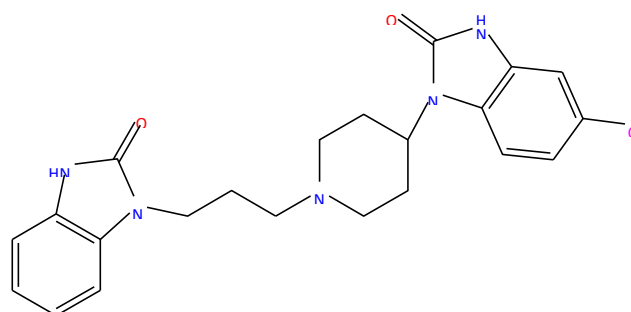


Fig. 1 Chemical structure of domperidone as prokinetic representative by producing its effect on the chemoreceptor trigger zone and also motor function of the small intestine and stomach. This drug has poor aqueous solubility (0.986 mg/L), while oral bio-availability is 12 to 18 % during fasting and 24% after food [12]. The poor water solubility seems to be one of the probable causes for its low bioavailability [13]. The conversion of DOMP into stable nanocrystals could potentially be one of the promising solutions to address this issue.

This study focussed on the production of stable nanocrystals of DOMP and investigated using molecular dynamics simulation studies the polymer-drug nanocrystal interactions underpinning the use of the low-energy antisolvent precipitation for nanocrystal manufacture. A number of studies have reported the impact of polymers on

particle sizes of drug nanoparticles. Despite these learnings, the molecular level interactions of polymers and drug nanocrystals are still an interesting issue yet to be fully resolved [14]. In this study, extensive molecular modelling was coupled with the experimental results to investigate and evaluate the correlation between molecular interactions and drug and stabilisers and nanoparticle properties. The traditional experiments cannot provide the molecular insight of the nanocrystal-polymer interactions in isolation [15, 16]. The comprehensive molecular level understanding gained from this study will be useful going forward for nanoformulation scientists to optimise polymer selection for stable nanocrystal production for a range of different APIs.

## Materials and methods

### Materials

DOMP was gifted by Stanley Pharma having batch no. BDOM/1302036 (Vasodha Pharma Chem Lab 78/A Vengal Rao Nagar Hyderabad-38 Andhra Pradesh, India), and ethanol, n-hexane, polyvinyl pyrrolidone (PVP) (CAS number: 9003-39-8) and hydroxypropyl methylcellulose (HPMC) (9004-65-3, USA) were also gifted by Stanley Pharma. Sprague-Dawley rats (150–200 g) were used for bioavailability studies.

### Preparation of DOMP nanosuspension

A low-energy antisolvent precipitation method was employed for the production of stable nanocrystals of DOMP [14]. The

DOMP solution (10 mg/mL) was prepared in dimethylformamide (DMF) and then filled into the syringe, and with the help of a syringe pump, the solution was quickly injected at a constant flow rate of 2–8 mL/min into the polymer solutions that served as antisolvent phase, with continuous stirring rate at 600–1000 rpm. Different polymers and subsequent combinations thereof were used to evaluate their impact on produced nanocrystals of DOMP. The polymer solutions were composed of 1% (w/v) of each of the polymers which included PVP, ethyl cellulose, HPMC, PVA, Pluronic F127 and Eudragit (EUD). Ethocel was dissolved in drug solutions in DMF and then injected into the water. The produced DOMP nanocrystals were filtered and vacuum dried.

## Physicochemical characterisation

### Particle size measurements

Particle size and associated polydispersity index (PI) measurements of the produced nanoparticles of DOMP were carried out in triplicate using dynamic light scattering (Zetasizer® NanoS, Malvern Instruments, UK), which measures the hydrodynamic diameter including the solvation layer around each particle.

### Morphological studies

**Scanning electron microscopy** The principle used in the operation of scanning electron microscopy (SEM) is light reflection microscopy. Reflection of electrons occurs as a result of incident light striking the surface of the powder sample and colliding with particle surfaces. The reflected electrons are picked up by the detector and are then transformed into an image by algorithm. Scanning electron microscopy is applied for the description of surface morphology of the powder sample and provides good resolution down to scale of several nanometers.

Surface morphology studies of the unprocessed DOMP were carried out by placing the sample on a grid covered with gold sputter coater (SPI, USA) using Jeol JSM5910 scanning electron microscope at an operating voltage of 30 mA for a duration of 2 min and an accelerating voltage of 20 kV.

**Transmission electron microscopy** The size and appearance of the produced DOMP nanoparticles were evaluated using transmission electron microscopy (TEM) (TEM-1200Ex; Japan Electron Optics Laboratory Corporation, Tokyo, Japan). The images of DOMP nanoparticles were taken at 120 kV. The drops of DOMP nanosuspensions were deposited on 200 mesh copper grid followed by coating with formvar/ carbon (code no: S162) and drying at room temperature. Owing to the low conductivity of the produced samples, they were negatively stained using 2% solution of magnesium uranyl acetate.

### Differential scanning calorimetry

To investigate and evaluate the impact of particle size on the thermal profile of the produced DOMP nanoparticles, the comparative differential scanning calorimetry (DSC)

studies were carried out. The samples were scanned using the Mettler Toledo Differential Scanning Calorimeter (MettlerToledo®, USA). Samples (2–3 mg) of unprocessed and processed DOMP were weighed into separate aluminium pans, which were sealed and then analysed by heating from 30 to 300 °C at a heating rate of 10 °C min<sup>-1</sup> and nitrogen flow of 40 mL/min. Indium was used as a standard for calibration of the instrument.

#### Powder X-ray diffraction studies

The prepared nanoparticles and unprocessed drug substance were subjected to testing for crystallinity using PXRD powder X-ray diffractometer (D8 ADVANCE, Bruker, Germany). The silicon-well sample holder was used for the analysis of nanoparticle samples, while the plastic sample holder was used for the raw drug substance. The nanoparticle sample and raw drug substance were scanned in triplicate in the range  $0^\circ \leq 2\theta \leq 70^\circ$  using copper K $\alpha$  as the radiation source with 1 mm slit at 1.542 Å wavelength. Step size was 0.05° and the time lapse between the steps was 2 s.

#### Stability studies

The stability of nanoparticles, particularly those produced by the bottom-up method, is very important, especially because agglomeration and particle growth can occur quickly, leading to the loss of rapid dissolution performance. In this study, the produced DOMP nanosuspensions were subjected to testing of physical stability over a duration of 90 days following storage at 2–8, 25 and 40 °C. This study was designed to monitor the rate and extent of particle growth with measurements of particle size being made using dynamic light scattering.

#### Computational methods

##### Molecular docking of polymers and DOMP

A short MD run was performed on the polymers to obtain relaxed energy conformers prior to docking. The Molecular docking software utilised included Raccoon [17], Autodock Graphical user interface supplied by MGL tools [18] and AutoDockVina [19] with default docking parameters. Prior to docking, Gasteiger charges [20] were added to polymers

as well as domperidone and the non-polar hydrogen atoms were merged to carbon atoms. The grid box was set to cover the entire polymer to allow for the best-docked pose. The optimal geometric conformation bearing the best binding energy was picked from the View Dock feature on Chimera [21] and the complex saved with the reference polymers. The polymer-domperidone for each system was prepared using Chimera and MMV molecular modelling suites [22] and later subjected to molecular dynamic simulations.

##### Molecular dynamic simulations

GPU version of the PMEMD engine in Amber14 software package was utilised to execute unrestrained all-atom MD simulations. The Restrained Electrostatic Potential (RESP) and the General AMBER Force Field (GAFF) [23] systems were used by ANTECHAMBER [24] to generate the atomic partial charges for the polymers and domperidone. The systems were solvated in a cubic box of TIP3P water, such that all atoms were within 10 Å of a box edge. Long-range electrostatic interactions were treated with the Ewald method and a van der Waals cut-off of 12 Å. Each of the systems was minimised for 1000 steps (500 steepest descent followed by 2500 steps of the conjugate gradient). The langevin thermostat, with a collision frequency of 1.0 ps<sup>-1</sup> with a harmonic restraint of 5 kcal/mol on the solutes, was applied during the gradual heating of the systems to a temperature of 300 K in the canonical ensemble for 50 ps. This was followed by 50 ps of density equilibration in the NPT ensemble and a final 500-ps equilibration at 300 K, 1 bar pressure and a coupling constant of 2 ps, and then by a MD production run of 50 ns. System coordinates were then saved every 1 ps and analysed using the PTRAJ module employed in AMBER14 [25]. The root mean square deviation (RMSD) was employed to establish the stability of the 12 systems over the 50-ns trajectory.

##### Binding free energy calculation

Calculations of free binding energies were engaged using the molecular mechanics/GB surface area method (MM/GBSA) [26]. This was carried out to evaluate the binding affinities of each system. Binding free energies were then averaged over 5000 snapshots extracted from the 50-ns trajectory. Figure 2 depicts free binding energy

( $\Delta G$ ), which was computed by the MM/GBSA method for each molecular species (complex, ligand and polymer).

### Bioavailability studies

The pharmacokinetics studies of unprocessed domperidone, its fabricated nanocrystals (DOMP-nano), prepared solid dosage form (DOMP-nano dosage form) and marketed formulations were carried out using rats as the animal model. SpragueDawley rats (150–200 g) were administered with an oral dose of 10 mg/kg of domperidone, its nanoparticles, its nanodosage form and marketed drug, and blood was collected after 0.25, 0.5, 1, 2, 3, 4, 6, 8, 10 and 12 h post-administration ( $n = 6$  rats each for different time periods). The collected blood samples were centrifuged and plasma was obtained. The blood plasma was quantified for DOMP using a reported HPLC method [27]. The pharmacokinetics parameters in the plasma were determined using the pharmacokinetic software WinNonLin (v 4.0; Pharsight Software, Mountain View, CA, USA). The pharmacokinetics parameters determined include maximal plasma concentration ( $C_{max}$ ), time to reach maximal plasma concentration ( $T_{max}$ ), half-life ( $t_{1/2}$ ) and the area under the concentration-time curve (AUC).

### Dissolution studies

Dissolution studies on pure DOMP as well as the nanoparticles prepared through EPN were performed using two separate dissolution tests, both using the U.S. Pharmacopoeia (USP) tablet dissolution test apparatus 2 (six stations) with the paddle rotating at 50 rpm in 900 mL of both pH 1.2 (0.1 N HCl) media and in a separate test 6.8 pH phosphate buffer at  $37 \pm 0.5$  °C. All drugs equivalent to 10 mg of DOMP were used as samples for the dissolution test. At 10, 30 and 60 min intervals, 5 mL samples were withdrawn, filtered through a syringe filter (0.02 $\mu$ m) and assayed for DOMP content by measuring the absorbance at 284 nm using a UVvisible spectrophotometer (Shimadzu UV-1700). Fresh medium (5 mL), pre-warmed at  $37 \pm 0.5$  °C, was added to the dissolution medium after each sampling to maintain a constant volume throughout the test. Dissolution studies were performed in triplicate ( $n = 3$ ) [15].

### Statistical analysis

All the tests were run in triplicate and the results were given as mean  $\pm$  standard mean error (SEM). Mean values were compared using ANOVA test and differences were considered statistically significant at the level of  $P < 0.05$  using Statistics 8.1 software.

## Results and discussion

### Preparation of DOMP nanosuspension using antisolvent precipitation method

Nanosuspensions of DOMP were produced by antisolvent precipitation. The particle sizes of nanosuspensions produced using this method are given in Table 1. Different polymer solutions were used as antisolvent phase with different combinations of polymers to investigate the impact of the polymers on particle sizes of the produced DOMP nanocrystals. It was observed that Ethocel was the most suitable single polymer to produce DOMP nanocrystals with small particle size  $130.0 \pm 3.0$  (Table 1 and Fig. 3). This shows that Ethocel strongly adsorbed onto the surface of DOMP nanocrystals to establish the steric

shows homogenous particle size distribution of the suspended particles [28, 29].

The highly concentrated drug solutions injected into the antisolvent phase can potentially produce high levels of supersaturation and, consequently, nanoparticles with small particle size. The SAS ratio is a very important process parameter, which should be optimised during APSP production of nanoparticles, whereby the barrier for the existing species to be grown during mixing of the solvent antisolvent phases is affected by this parameter. In this study, it has been observed that DOMP nanoparticles with

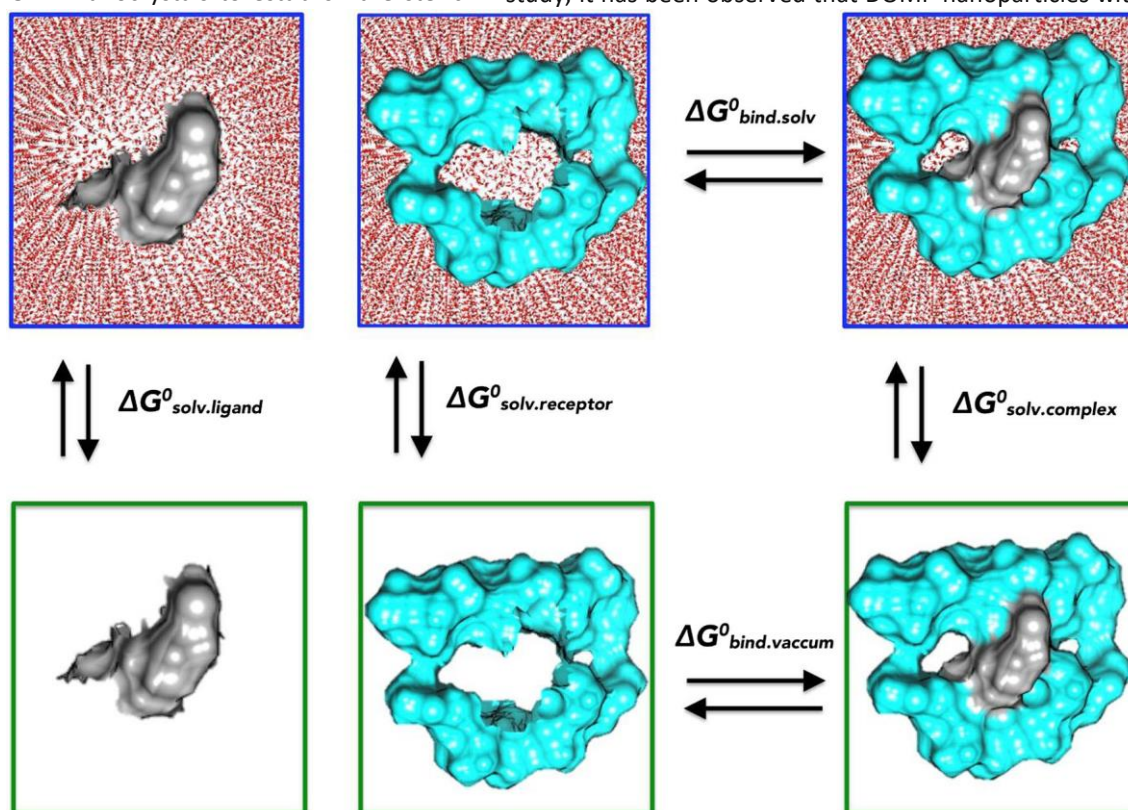


Fig. 2 Diagrammatic representation of thermodynamic calculation (MM/GBSA) used in the study (prepared by the authors)

stabilisation with subsequent small particle size and low PDI value. In addition, HPMC was also found comparatively effective as a single polymer to control the size of DOMP nanocrystals ( $300 \pm 4.0$ ) (Table 1). However, when HPMC was combined with PVA in the antisolvent phase, the impact became more predominant in terms of controlling the particle size. The combination of HPMC-PVA produced DOMP nanocrystals with particle size  $200 \pm 3.5$ . DOMP nanoparticles produced at optimised conditions were quickly recovered by vacuum evaporation of all solvent and antisolvent using a rotary evaporator and were then washed and dried. The resulted PDI was below 0.5, which

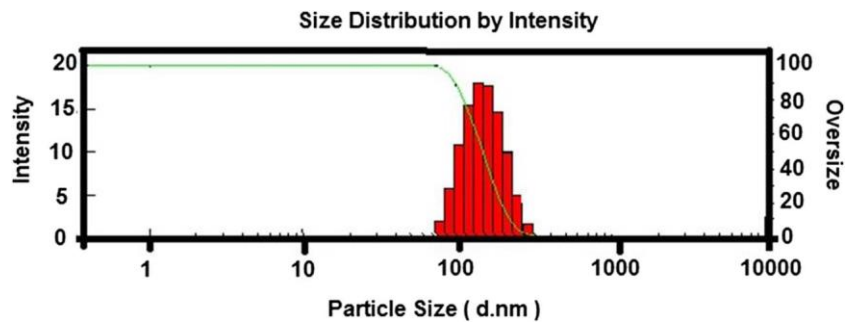
small particle size  $130.00 \pm 3.0$  nm were produced using a high SAS ratio (Fig. 3) while using the antisolvent phase with Ethocel. At low SAS ratio, the available diffusion distance for the growing species is low and can potentially lead to high nucleation with subsequent comparatively large particle sizes being produced [30, 31].

#### Morphological examination

The morphology studies of raw and processed DOMP were carried out by SEM and TEM, respectively. SEM observation showed some differences in size and shape of the unprocessed DOMP particles (Fig. 4a). The average particle size was found to be 10–15  $\mu\text{m}$  and most of the particles

were shown to be cuboidal and prism-like.  
Some traces of oval shape particles

Table 1 Impact of polymers on particle sizes and PDI values of DOMP nanosuspension



results exhibited that all the nanoparticles were homogeneously distributed with no clumps or aggregates. The particle size was shown to be approximately 100.0 nm in good agreement with DLS data. The minor difference in the particle size measured using DLS and TEM is related to the difference in the principles of the two techniques. In DLS, the electrical double layers surrounding the individual particle could be also measured, whereas TEM only measures the actual particles [29].

Fig. 3 Particle size distribution of DOMP nanoparticles

DOMP-polymer complexes	Particle size $\pm$ SD	PDI $\pm$ SD
Ethocel	130.0 $\pm$ 3.0	0.15 $\pm$ 0.01
Pluronic	1200 $\pm$ 7.5	0.85 $\pm$ 0.06
PVP	950.0 $\pm$ 5.0	0.77 $\pm$ 0.05
PVA	400.0 $\pm$ 4.5	0.50 $\pm$ 0.03
EUD	1175 $\pm$ 7.0	0.80 $\pm$ 0.06
HPMC	300 $\pm$ 4.0	0.40 $\pm$ 0.02
EUD-PVA	775 $\pm$ 6.0	0.65 $\pm$ 0.04
EUD-PVP	985 $\pm$ 5.7	0.80 $\pm$ 0.05
HPMC-PVA	200 $\pm$ 3.5	0.20 $\pm$ 0.02
HPMC-PVP	570.0 $\pm$ 5.0	0.52 $\pm$ 0.03
HPMC-EUD	550 $\pm$ 6.5	0.60 $\pm$ 0.04
PVA-PVP	650 $\pm$ 5.2	0.40 $\pm$ 0.02

were also observed, although all particles appeared to demonstrate regular crystalline morphologies (Fig. 4b). TEM images of the DOMP nanoparticles demonstrated that most of the particles were spherical in shape with some traces of the triangular shape particles. In addition, the TEM

#### PXRD analysis

PXRD analysis was carried out for raw and DOMP nanoparticles. PXRD diffractograms show that raw DOMP has sharp peaks of high intensity compared to DOMP nanoparticles (Fig. 5a). The nanoformulation gives lower intensity, broader peaks, which are typical of crystalline particles with low particle size peaks (Fig. 5b). X-ray diffractograms with lower peak intensities and the absence of some peaks have also been previously reported by other researchers for crystalline nanoparticles [32–34]. Furthermore, nanoparticles can result in broadening and disappearance of some peaks in X-ray diffractograms.

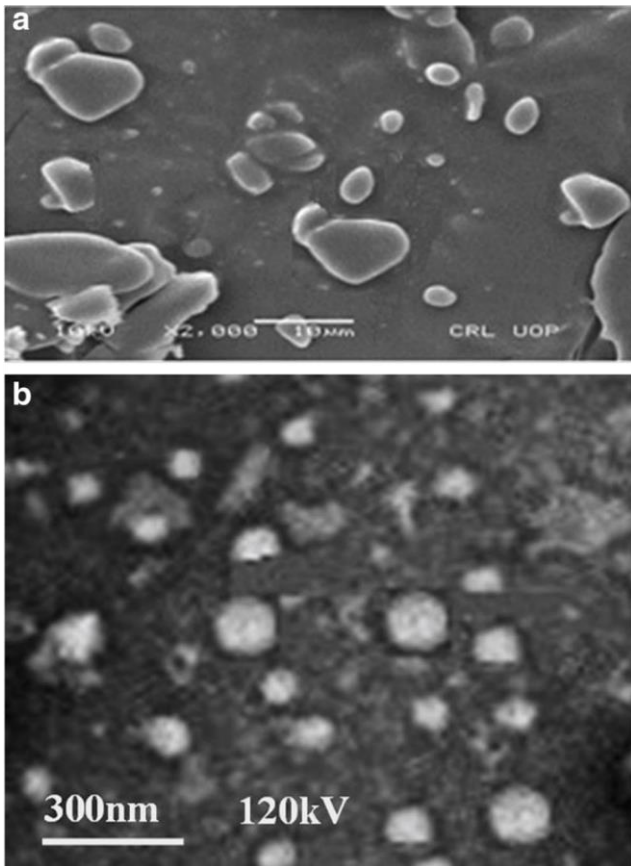


Fig. 4 SEM image of raw DOMP (a) and TEM micrographs of processed DOMP particles (b)

Owing to small angular reflection by the

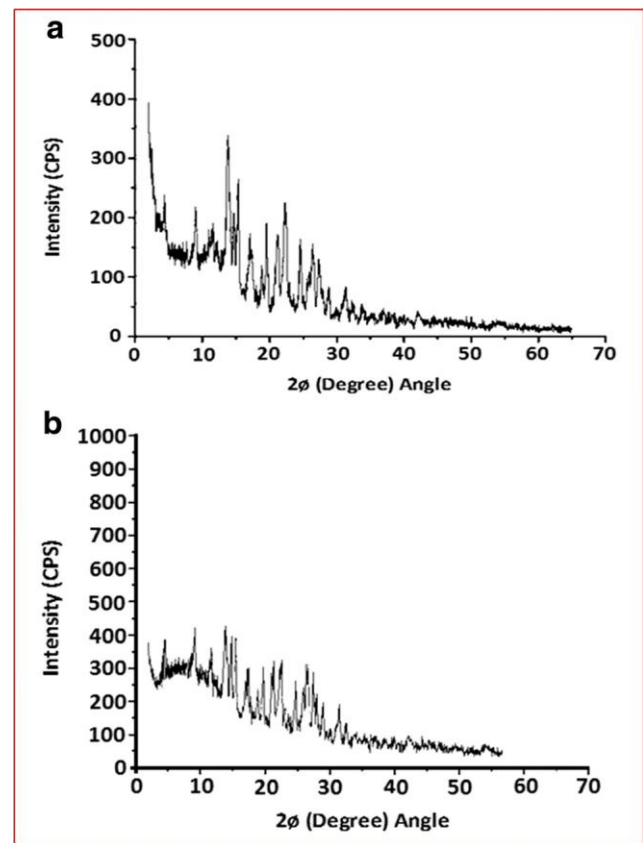


Fig. 5 PXRD patterns of the unprocessed (a) and DOMP nanoparticle (b)

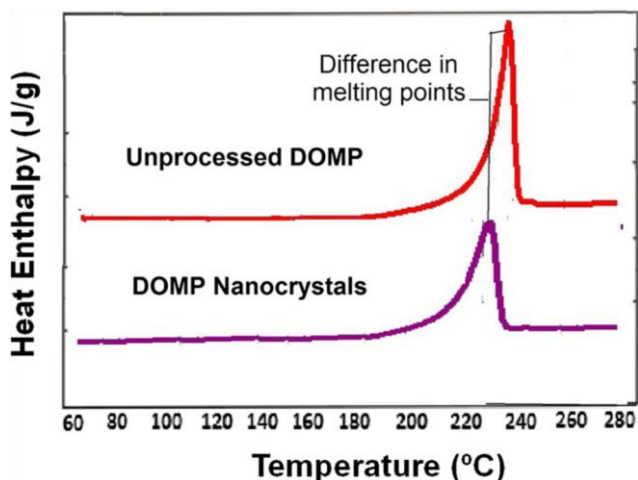


Fig. 6 DSC thermograms of the unprocessed DOMP and DOMP nanocrystals

smaller particles, the peak intensity of X-ray diffractograms is reduced. For domperidone nanoparticles, the small sample sizes with fewer particles can also result in lower intensity reflections.

#### DSC analysis

DSC thermograms of pure DOMP and the prepared nanocrystals are shown in Fig. 6. There appeared an intense endothermic peak

at approximately 238°C for the unprocessed DOMP. It is known that a crystalline structure will give a peak at the melting point temperature with high heat enthalpy ( $\Delta H$ ) values compared to that of amorphous structures of the same materials. The produced nanocrystals have low values of  $\Delta H$  representing reduction in crystallinity of the resulted nanocrystals. The produced nanocrystals have shown a melting point peak at lower temperature compared to the unprocessed DOMP, which is typical of nanocrystalline materials.

The endothermic peak of the processed DOMP was broadened, which is potentially caused by the packing density of the produced nanocrystals, incorporating traces of stabilising polymers [35].

#### Molecular docking and conformational analysis of polymer systems

Molecular docking is a conventional method in computational chemistry, which is utilised in the prediction of optimised geometric conformations of a ligand within an appropriate binding site [36]. Of the docked polymer-DOMP complexes (Figs. 7 and 8), the highest binding affinity was observed for the HPMC-EUD co-polymer ( $-6.0$  kcal/mol). Of the monopolymer complexes, PVP demonstrated the highest binding affinity ( $-5.2$  kcal/mol).

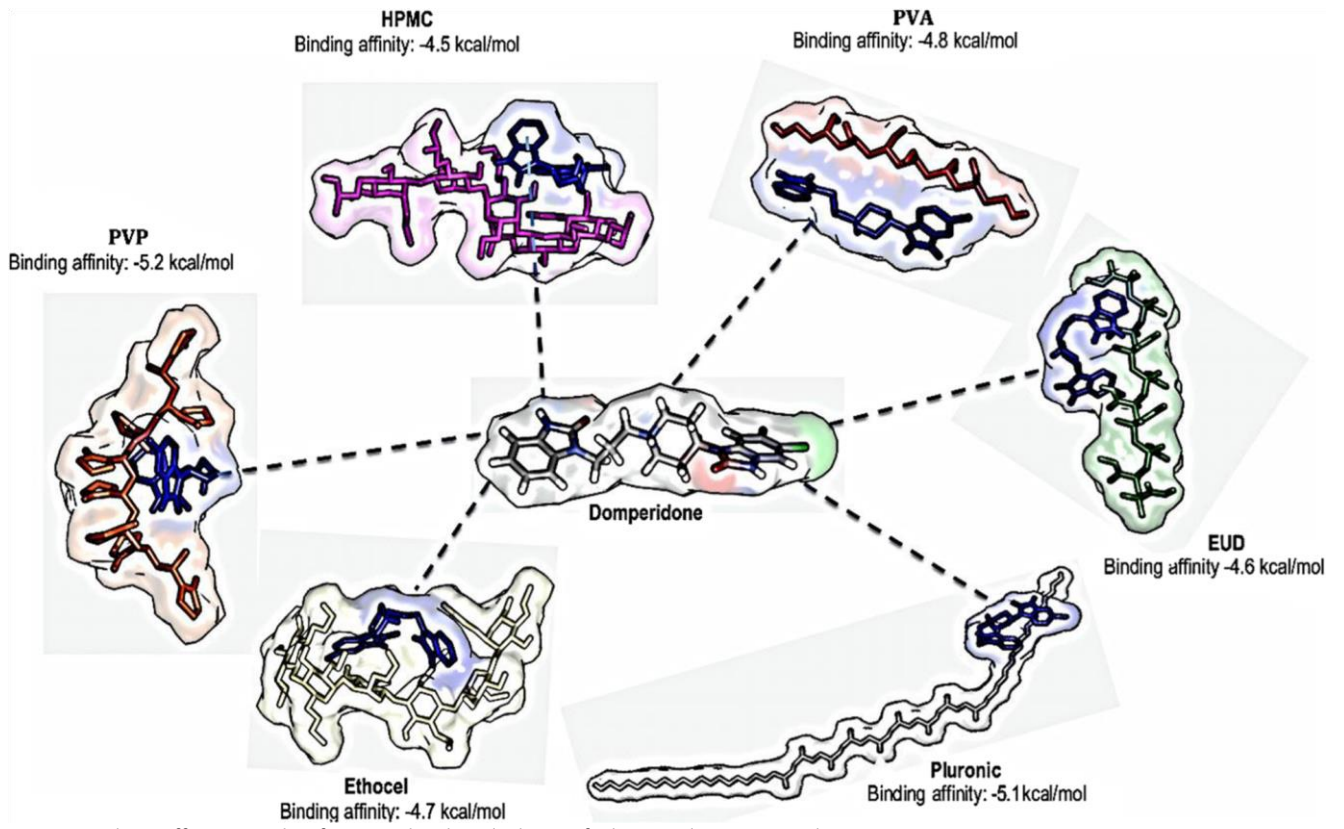
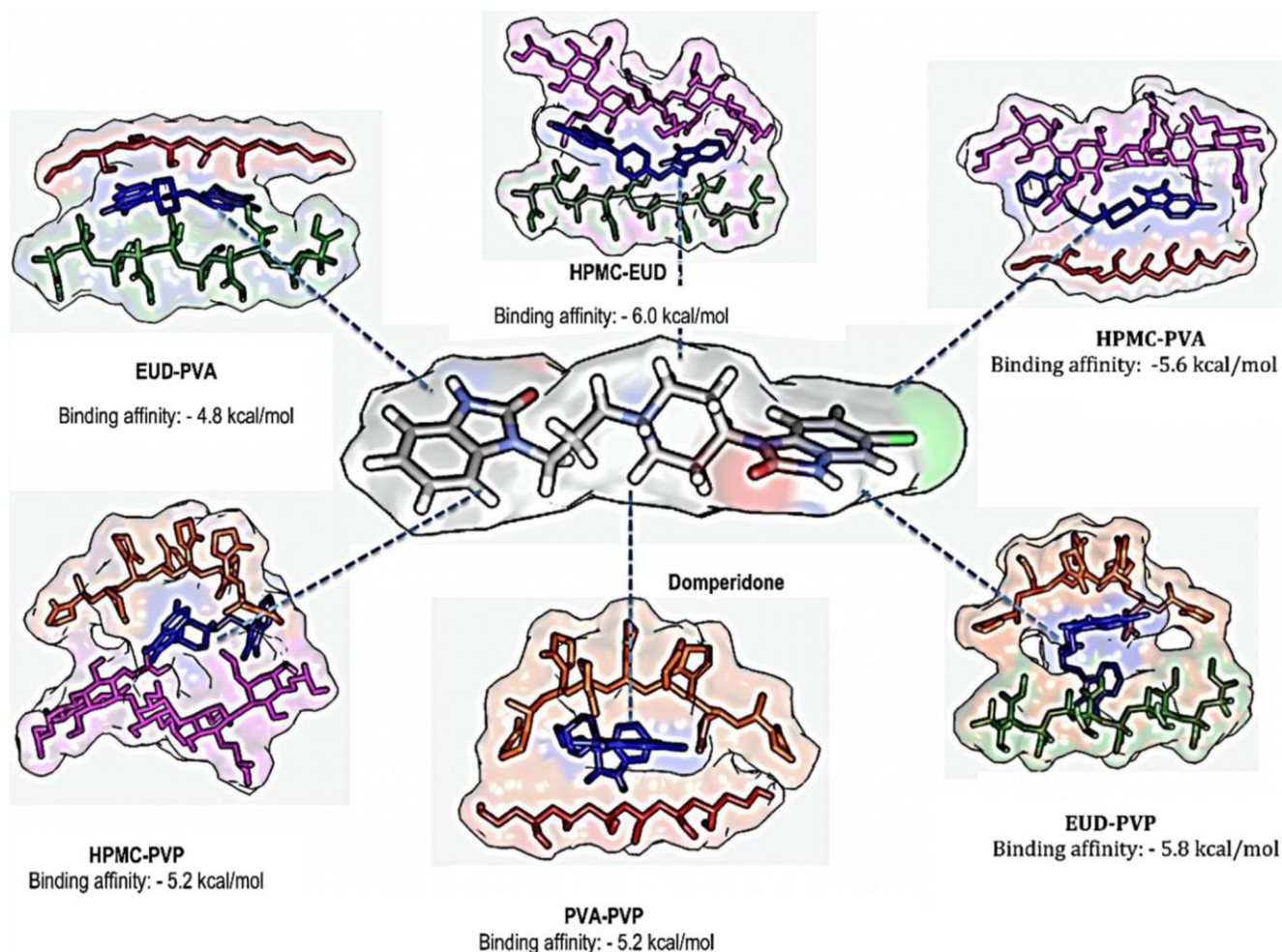


Fig. 7 Binding affinity results from molecular docking of domperidone-monopolymer



complexes Fig. 8 Binding affinity results from molecular docking of domperidone-copolymer complexes

The molecular docking results, however, only take into account the geometric orientation of domperidone when bound to suitable regions of the polymers and, thus, may be inconclusive when identifying the forces that stabilise domperidone to the polymers. To overcome any binding mode ubiquities, molecular dynamics were carried out to simulate the interaction of domperidone with the polymers over a 50-ns trajectory. After allowing domperidone to equilibrate with the polymers, the binding mechanism and stabilising intramolecular forces were investigated using binding free energy calculations.

#### Polymer system stability through molecular dynamic simulations

The stability of trajectories was identified using RMSD over the 50-ns simulation, the potential energy of the polymer-

domperidone remained stable during the MD trajectories and convergence was reached at approximately 20 ns.

#### Thermodynamic energy analysis

The total binding free energy for each of the 12 polymerdomperidone complexes was calculated using the MM/ GBSA approach to better understand the various energy contributions stabilising the polymer to domperidone and to assess which polymer-complex showed the most favourable intermolecular interactions. Based on Table 2, a conformational analysis was performed to distinguish between the most favourable polymer-domperidone complexes.

Calculating the thermodynamic energy between a polymer and a drug gives the approximate intensity and stability of interactions between the molecules; thus, a higher binding interaction will result in a more stable polymer-drug complex [37].

Upon analysis of Table 2, the most favourable interactions were observed in the Ethocel system ( $-27.26$  kcal/mol), while the Pluronic complex showed the least favourable binding free energy ( $-1.20$  kcal/mol). It was also interesting to note that the inclusion of EUD significantly lowered the thermodynamic energy of the co-polymer complexes, as the addition of EUD to PVA decreased the free binding energy by  $9.38$  kcal/mol. This

Table 2 Binding free energy analysis (kcal/mol) for polymer-domperidone complexes

Complex	Energy components ( kcal/mol )				
	$\Delta E_{vdW}$	$\Delta E_{elec}$	$\Delta G_{gas}$	$\Delta G_{solv}$	$\Delta G_{bind}$
Single-polymer systems					
Ethocel	$-30.37 \pm 0.24$	$-6.95 \pm 0.43$	$-37.32 \pm 0.43$	$10.06 \pm 0.33$	$-27.26 \pm 0.24$
Pluronic	$-3.69 \pm 0.05$	$0.29 \pm 0.079$	$-3.40 \pm 0.96$	$2.19 \pm 0.09$	$-1.20 \pm 0.54$
PVP	$-5.52 \pm 2.68$	$-20.94 \pm 1.12$	$-26.46 \pm 1.87$	$18.75 \pm 0.52$	$-7.72 \pm 1.95$
PVA	$-31.77 \pm 5.23$	$-25.19 \pm 11.32$	$-56.96 \pm 12.24$	$38.08 \pm 8.33$	$-18.88 \pm 6.39$
EUD	$-4.10 \pm 2.09$	$-5.55 \pm 0.60$	$-9.64 \pm 1.84$	$7.73 \pm 0.31$	$-1.91 \pm 1.97$
HPMC	$-20.35 \pm 0.92$	$-22.42 \pm 0.79$	$-42.77 \pm 1.04$	$20.04 \pm 0.43$	$-22.73 \pm 0.82$
Dimer systems					
EUD-PVA	$-13.83 \pm 0.34$	$0.00 \pm 0.00$	$-13.83 \pm 0.34$	$4.33 \pm 0.10$	$-9.50 \pm 0.36$
EUD-PVP	$-10.78 \pm 0.73$	$-5.08 \pm 0.43$	$-15.87 \pm 0.56$	$9.19 \pm 0.33$	$-6.67 \pm 0.64$
HPMC-PVA	$-39.84 \pm 0.74$	$-12.88 \pm 0.85$	$-42.72 \pm 1.00$	$17.50 \pm 0.62$	$-25.22 \pm 0.79$
HPMC-PVP	$-15.15 \pm 1.37$	$-24.91 \pm 0.71$	$-40.06 \pm 1.19$	$24.46 \pm 0.44$	$-15.60 \pm 1.13$
HPMC-EUD	$-13.17 \pm 0.81$	$-27.93 \pm 0.78$	$-41.10 \pm 0.85$	$27.00 \pm 0.40$	$-14.10 \pm 0.84$
PVA-PVP	$-26.09 \pm 1.23$	$-12.77 \pm 1.11$	$-28.86 \pm 1.53$	$16.09 \pm 0.56$	$-12.77 \pm 0.60$

trend was also observed in both the HPMC and PVP complexes. This confirms that molecular docking demonstrates only the geometric fit<sup>^</sup> of two molecules and free energy binding calculations are still required when estimating molecular interactions [38]. As observed in the HPMC-PVA complex, significant improvements were noted in the thermodynamic energy upon inclusion of HPMC compared to the monopolymer PVA complex (Figs. 9 and 10). This may have been a result of increased intermolecular surface area based on the interaction size of HPMC. The above characteristic features may also be used to explain the high binding energy of the Ethocel complex (Fig. 11). Increased molecular surface area due to the conformational flexibility of Ethocel may have allowed for greater hydrophobic interactions with domperidone. As a general trend, greater stability was seen in the polymer that showed enhanced interactive binding surfaces such as HPMC and Ethocel.

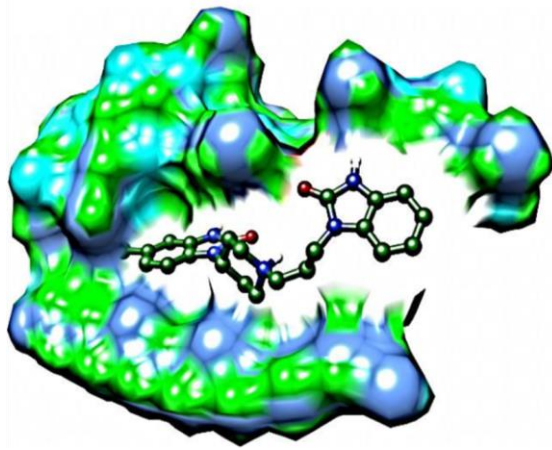
The pharmacokinetic profile of domperidone in plasma after oral administration of 10 mg/kg dose of DOMP, its nanocrystals, tablets having DOMP in nanoform and marketed product (Motilium<sup>®</sup>) via oral administration is shown in Fig. 12.

## Bioavailability studies

Numerous pharmacokinetic parameters, including area under the concentration-time curve, maximal plasma concentration, time to reach maximal plasma concentration and biological half-life, are shown in Table 3.

Administration of domperidone at a dose of 10mg/kg

**a**



**b**

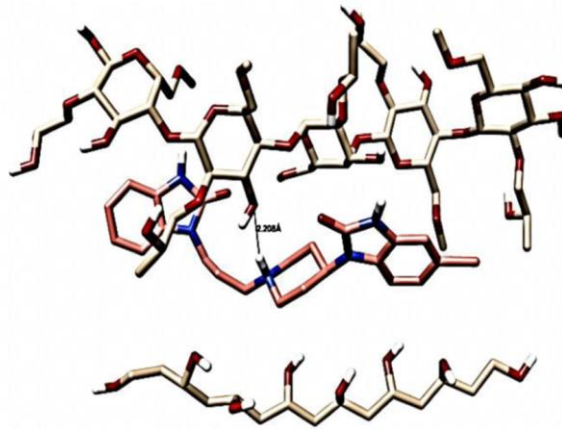


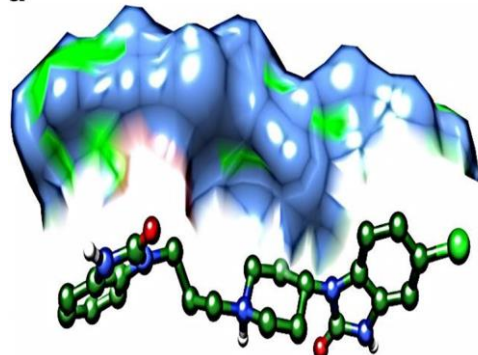
Fig. 9 The lowest energy conformation of the HPMC-PVA-DOMP complex ( $-25.25$  kcal/mol): a the molecular surface of HPMC-PVA encapsulating DOMP and b the hydrogen bond interaction between DOMP and HPMC

showed an elimination phase from 10 to 12 h with an elimination half-life of 4.18 h with a clearance of 4051.3

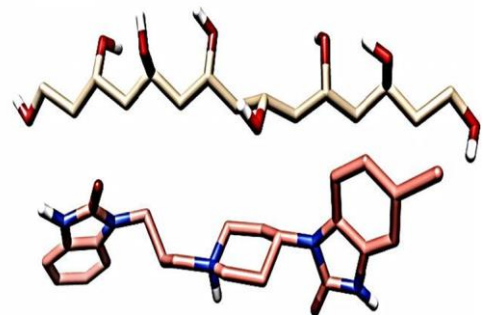
observed ( $13.3 \mu\text{g}/\text{mL}$ ,  $P < 0.001$ ). Similarly, the nanodosage form also showed an

Fig. 10 The PVA-DOMP complex ( $-18.88$  kcal/mol): a molecular surface interaction between PVA and DOMP and b graphical representation of the lack of hydrogen bonds between PVA and DOMP

**a**



**b**



mL/h. The distribution phase was observed from 6 to 8 h with an observed volume of distribution of 24,470.8 mL. The absorption phase was noted from 0.3 to 4 h. The maximum plasma concentration was observed as  $1.3 \mu\text{g}/\text{mL}$  at 2 h;  $4.9 \mu\text{g h}/\text{mL}$  was the area under the concentration-time curve from time 0 to 12 h. Marked changes in the pharmacokinetics of nanocrystals were observed. Administration as nanocrystals increased the plasma concentration of domperidone throughout the study; however, a noteworthy escalation has been noted at 0.5 h ( $P < 0.01$ ), 1–2 h ( $P < 0.001$ ) and 4 h ( $P < 0.05$ ). The nanocrystal formulations resulted in a decreased elimination rate of domperidone as reflected from a significant increase in half-life of 13.34 h ( $P < 0.001$ ). A significant increase in plasma concentration of  $2.6 \mu\text{g}/\text{mL}$  ( $P$

enhancement in the pharmacokinetic parameters, i.e. half-life (8.3 h,  $P < 0.001$ ), maximal plasma concentration ( $2.4 \mu\text{g}/\text{mL}$ ,  $P < 0.01$ ), time to reach maximal plasma concentration (1.0 h,  $P < 0.01$ ) and AUC ( $11.3 \mu\text{g h}/\text{mL}$ ,  $P < 0.001$ ), as compared to domperidone treatment. For the marketed drug, a significant increase in the apparent half-life (6.45 h,  $P < 0.05$ ) and AUC ( $7.73 \mu\text{g h}/\text{mL}$ ,  $P < 0.05$ ) was observed compared to the domperidone-alone-treated animals.

#### Stability studies

The physical stability studies of DOMP nanosuspensions stored at 2–8, 25 and 40 °C for 90 days showed that nanosuspensions stored at 2–8 and 25 °C (Fig. 13a, b) were

stable compared to the samples stored at 40 °C (Fig. 13c). The nanosuspension stored at 2–8 °C exhibited adequate stability (Fig. 13a) with no marked changes in key nanosuspension characteristics. The nanosuspensions stored at 2–8 and 25 °C maintained their PDI values, and there was no significant difference ( $P > 0.05$ , paired t test,

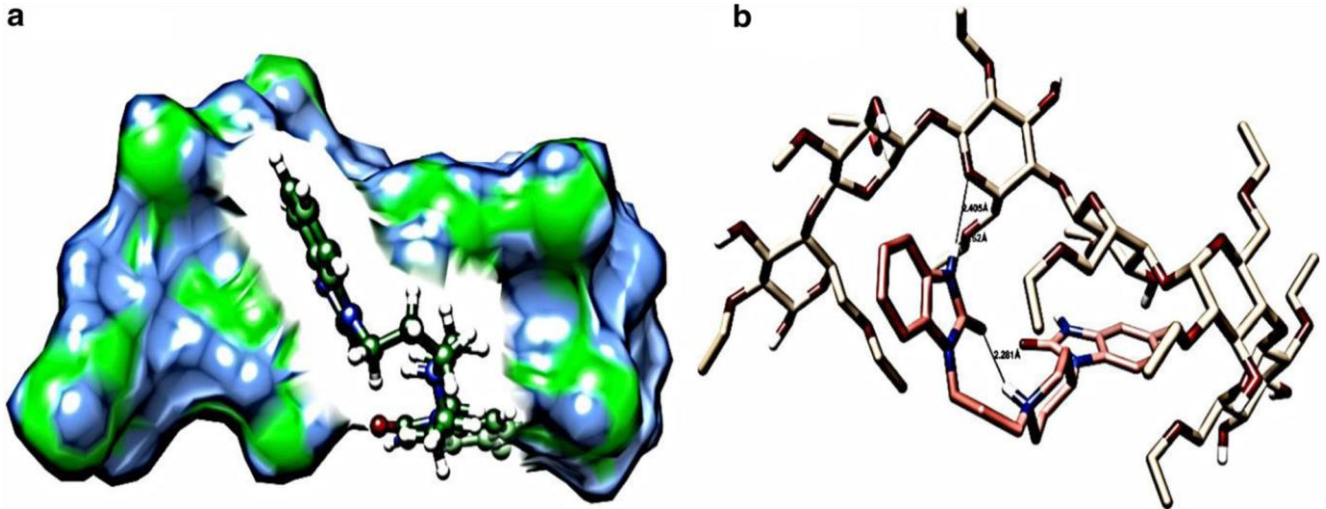
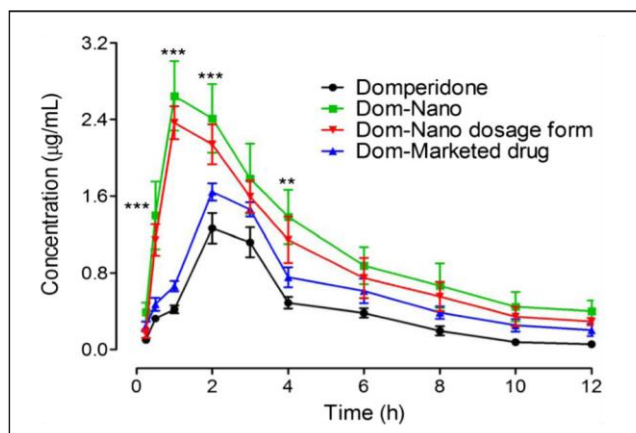


Fig. 11 The lowest energy conformation of the Ethocel-DOMP complex ( $-27.26$  kcal/mol) after molecular dynamic simulations: a molecular surface interaction between Ethocel and DOMP and b three stabilising hydrogen bonds of the Ethocel-DOMP complex

one-way ANOVA) in and shape of crystallised materials [40, 41]. Moreover, the polymeric media and associated stabilising agent are also considered very important and are known to facilitate surface stabilisation and consequent control of particle size during the nucleation process [42]; 0.5% Ethocel was found the most suitable single polymer to effectively control the growth of the DOMP nanocrystals, which remained stable for 90 days

25 °C (b) and 40 °C (c)

(Table 4). This study demonstrated that sufficient adsorption of the polymers occurred onto the surfaces of the produced DOMP nanocrystals which resulted into strong repulsion of the particles and subsequent colloidal stabilisation. The molecular modelling studies also substantiated the experimental



**Fig. 12** Comparative in vivo pharmacokinetic profile of domperidone ( $n = 6$ ,  $\pm$ SD). \*\* $P < 0.01$ ; \*\*\* $P < 0.001$

the mean values of particle size after 90 days of storage, which confirms that a homogeneous particle size distribution of DOMP nanocrystals has been achieved, and consequently, the Ostwald ripening process which is very common in the nanosuspensions could be hindered.

Among the different factors influencing physical stability of nanosuspensions, temperature has been reported the major factor to be controlled for the production of stable nanoparticles [14, 39]. At high temperature, kinetic energy of the suspended particles increases which results in strong van der Waals forces and increased attraction among the particles followed by agglomeration and destabilisation of the suspensions. For maximum stabilisation of nanoparticles, a temperature range of 2–8 °C has been recommended by Friez and Muller. In addition, increases in temperature and high intensity of light radiation can cause rapid particle growth. Nucleation is the key step in antisolvent crystallisation methods which can be manipulated for tailoring particle size

Table 3 Summary of

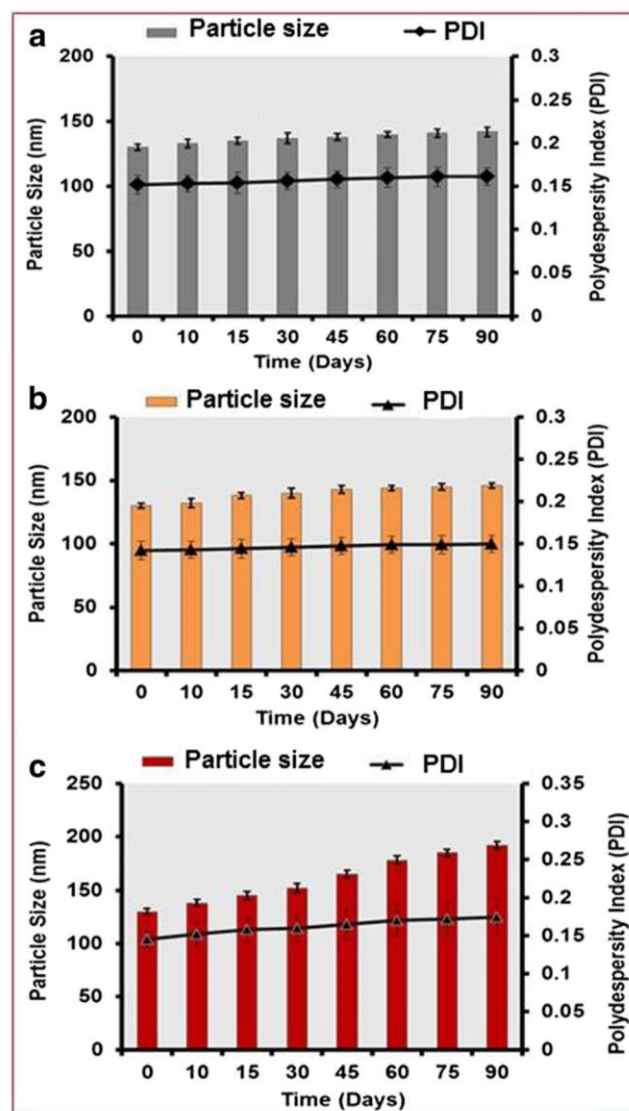


**Fig. 13** Stability studies of DOMP nanoparticles stored at 2–8 °C (a),

Sample	Pharmacokinetic parameters			
	$t_{1/2}$ (h)	$T_{max}$ (h)	$C_{max}$ (µg/mL)	$AUC_{0-t}$ (µg h/mL)
Raw DOMP	$4.182 \pm 0.43$	$2.0 \pm 0.11$	$1.3 \pm 0.26$	$4.91 \pm 0.31$
DOMP nanocrystals	$13.34 \pm 0.32^{***}$	$1.0 \pm 0.07^{**}$	$2.6 \pm 0.18^{**}$	$13.3 \pm 0.44^{***}$
Tablets (DOMP nanocrystals)	$8.334 \pm 0.71^{***}$	$1.0 \pm 0.09^{**}$	$2.4 \pm 0.21^{**}$	$11.3 \pm 0.39^{***}$
DOMP marketed formulation	$6.451 \pm 0.52^*$	$2.0 \pm 0.16$	$1.6 \pm 0.31$	$7.73 \pm 0.37^*$

pharmacokinetic parameters for domperidone

n = 6,  $\pm$  SD

\*P &lt; 0.05; \*\*P &lt; 0.01; \*\*\*P &lt; 0.001

Table 4 Stability study of DOMP optimised nanocrystals as a function of time

DOMP-polymer complexes	Average particle sizes of DOMP nanocrystals with $\pm$ SD						
	Day 0	Day 15	Day 30	Day 45	Day 60	Day 75	Day 90
Ethocel-DOMP	130.0 $\pm$ 2.5	135 $\pm$ 3.0	140 $\pm$ 4.0	143 $\pm$ 3.5	144 $\pm$ 4.5	145 $\pm$ 3.8	147 $\pm$ 3.5
Pluronic-DOMP	1200 $\pm$ 4.5	1280 $\pm$ 5.0	1385 $\pm$ 3.5	1450 $\pm$ 4.5	1600 $\pm$ 5.5	1730 $\pm$ 6.5	1850 $\pm$ 6.0
PVP-DOMP	950.0 $\pm$ 5.0	980 $\pm$ 5.5	1070 $\pm$ 6.0	1200 $\pm$ 4.5	1280 $\pm$ 4.0	1390 $\pm$ 7.0	1470 $\pm$ 7.5
PVA-DOMP	400.0 $\pm$ 4.5	440 $\pm$ 3.0	455 $\pm$ 2.7	470 $\pm$ 3.2	490 $\pm$ 2.4	520 $\pm$ 3.5	545 $\pm$ 2.8
EUD-DOMP	1175 $\pm$ 7.0	1220 $\pm$ 3.7	1260 $\pm$ 3.5	1325 $\pm$ 3.7	1410 $\pm$ 2.5	1500 $\pm$ 2.0	1610 $\pm$ 3.0
HPMC-DOMP	300 $\pm$ 4.0	325.0 $\pm$ 2.0	338 $\pm$ 2.7	350 $\pm$ 2.0	370 $\pm$ 3.0	385 $\pm$ 3.5	392 $\pm$ 2.5
EUD-PVA-DOMP	775 $\pm$ 6.0	800 $\pm$ 5.4	860 $\pm$ 5.5	930 $\pm$ 4.0	1020 $\pm$ 6.4	1100 $\pm$ 5.6	1170 $\pm$ 6.0
EUD-PVP-DOMP	985 $\pm$ 5.7	1015 $\pm$ 6.5	1090 $\pm$ 5.5	1210 $\pm$ 7.0	1300 $\pm$ 6.5	1410 $\pm$ 7.5	1515 $\pm$ 5.8
HPMC-PVA-DOMP	200 $\pm$ 3.5	210 $\pm$ 2.5	217 $\pm$ 2.0	230 $\pm$ 2.4	240 $\pm$ 3.0	245 $\pm$ 2.7	250 $\pm$ 2.5
HPMC-PVP-DOMP	570.0 $\pm$ 5.0	600 $\pm$ 2.8	645 $\pm$ 3.5	680 $\pm$ 3.0	730 $\pm$ 3.7	790 $\pm$ 3.0	830 $\pm$ 3.2
HPMC-EUD-DOMP	550 $\pm$ 5.5	575 $\pm$ 4.5	615 $\pm$ 5.0	650 $\pm$ 4.0	690 $\pm$ 4.5	710 $\pm$ 5.5	750 $\pm$ 6.0
PVA-PVP-DOMP	650 $\pm$ 5.2	695 $\pm$ 5.5	730 $\pm$ 6.0	780 $\pm$ 6.5	830 $\pm$ 5.0	900 $\pm$ 4.5	945 $\pm$ 6.5

results and suggested that Ethocel gave higher binding free energy ( $-27.26 \pm 0.24$  kcal/mol) compared to other complexes which in turn provided higher level of surface polymer adsorption and more effective stabilisation. In addition, DOMP nanocrystals produced by 1% HPMC were also shown to be stable compared to other single polymers. These binding free energies resulted for DOMP nanocrystals and HPMC ( $-22.73 \pm 0.82$  kcal/mol) also suggest that HPMC could be effectively adsorbed onto the surface of DOMP nanocrystals with subsequent controlled particle growth. In the case of polymer combinations, the combination of HPMC-PVA was found the most suitable combination to retard the particle growth, because of its higher binding free energy ( $-25.22 \pm 0.79$  kcal/mol) compared to other counterparts.

### Dissolution studies

Figure 14 clearly shows that dissolution of DOMP has been increased enormously with the conversion of pure/raw DOMP to nanocrystals prepared by the antisolvent precipitation method. The difference in dissolution profiles of the produced DOMP nanocrystals formed in acidic and basic media is attributed to its physicochemical attributes. DOMP is basic in nature; therefore, it dissolves efficiently in

acidic media [23]. The dissolution study of DOMP conducted in a buffer (pH 6.8) medium resulted in approximately 80 and 20% release of the drug within the first 10 min, from nanocrystals and raw DOMP formulations, respectively. In addition, the dissolution studies conducted at acidic pH (0.1 M HCl) also resulted in enhanced dissolution rate for DOMP nanocrystals (38%) compared to the raw DOMP. Dissolution has been reported as being the rate-limiting step for BCS II class drug compounds, because they have high permeability but low dissolution rate [43]. Owing to increased dissolution rate of DOMP nanocrystals, the bioavailability could also potentially be enhanced, which is substantiated by the oral bioavailability

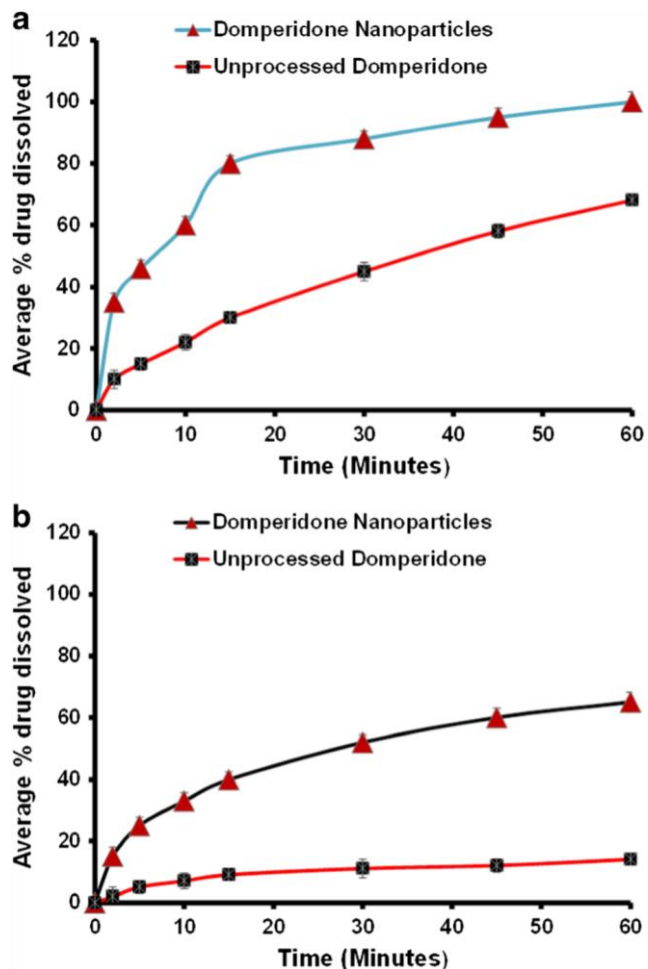


Fig. 14 Comparative dissolution profile of unprocessed and DOMP nanoparticles at acidic pH: 0.1 M HCl (a) and phosphate buffer pH: 6.8 (b)

studies in rats. Furthermore, nanocrystals have increased surface area and improved adhesiveness to the cell membrane which subsequently leads to high bioavailability [44]. The dissolution studies confirmed that the produced DOMP nanocrystals maintained their surface area and particle size.

## Conclusion

This study concluded that polymers play an important role in the production of stable nanocrystals using the antisolvent precipitation method. This study provided molecular insight into the interactions between polymers and drugs at nanocrystal surfaces, the knowledge of which is not easily accessible through experiments. Ethocel was found the most effective polymer to control the particle size of DOMP nanocrystals ( $130.0 \pm 2.5$ ). Furthermore, the 1% (w/v) HPMC-PVA combination also showed strong

binding potential with DOMP nanocrystals demonstrating particle size  $200.0 \pm 3.5$ . The molecular modelling studies provided molecular level insight into polymer-drug interactions underpinning the mode of binding of polymers with DOMP at the surfaces of nanocrystals. This has provided an opportunity for the formulation scientist to rationally select the suitable polymers, most likely to achieve desirable particle size control for nanocrystals and deliver stable formulations which deliver optimal in vivo performance.

DOMP nanocrystals showed enhanced dissolution rate at both acidic and basic pH conditions compared to the unprocessed form of DOMP. The dissolution enhancement for this BCS II class drug compound can potentially provide the opportunities to develop a more cost-effective dosage form having the same therapeutic performance but at much lower dose compared to the existing marketed drug product.

Pharmacokinetic studies in rats have shown that the improved dissolution performance leads to markedly improved rate and extent of drug absorption in vivo. Future studies will be focussed on transforming the prototype formulations tested in this project into drug products suitable for clinical testing and commercialisation.

**Acknowledgments** The authors acknowledge Abdullah Jan at Central Research Laboratory, University of Peshawar for the scanning electron microscope, differential scanning calorimetry, and Fourier transform infrared spectroscopy instrumentation time and assistance by Mr. Sadiq Afridi at Pakistan Council of Scientific and Industrial Research Laboratory Peshawar KP. The authors also extend their thanks to Mr. Iqbal Central Research Laboratory Peshawar University for his contribution in carrying out the X-ray diffraction analysis.

## Compliance with ethical standards

**Conflict of interest** The authors declare that they have no conflicts of interest.

## References

1. Sastry SV, Nyshadham JR, Fix JA. Recent technological advances in oral drug delivery—a review. *Pharm Sci Technol Today*. 2000;3(4):138–45.
2. Kawabata Y, Wada K, Nakatani M, Yamada S, Onoue S. Formulation design for poorly water-soluble drugs based on biopharmaceutics classification system: basic approaches and practical applications. *Int J Pharm*. 2011;420(1):1–10.
3. O'Driscoll C, Griffin B. Biopharmaceutical challenges associated with drugs with low aqueous solubility—the potential impact of lipid-based formulations. *Adv Drug Deliv Rev*. 2008;60(6):617–24.
4. Sarkar N. Mifepristone: bioavailability, pharmacokinetics and useeffectiveness. *Eur J Obstet Gynecol Reprod Biol*. 2002;101(2): 113–20.

5. Dressman JB, Reppas C. In vitro–in vivo correlations for lipophilic, poorly water-soluble drugs. *Eur J Pharm Sci.* 2000;11:73–80.
6. Salah N, Habib SS, Khan ZH, Memic A, Azam A, Alarfaj E, et al. High-energy ball milling technique for ZnO nanoparticles as antibacterial material. *Int J Nanomedicine.* 2011;6:863–9.
7. Seo WS, Lee JH, Sun X, Suzuki Y, Mann D, Liu Z, et al. FeCo/graphitic-shell nanocrystals as advanced magnetic-resonance imaging and near-infrared agents. *Nat Mater.* 2006;5(12):971–6.
8. Kesisoglou F, Panmai S, Wu Y. Nanosizing—oral formulation development and biopharmaceutical evaluation. *Adv Drug Deliv Rev.* 2007;59(7):631–44.
9. Verma S, Gokhale R, Burgess DJ. A comparative study of topdown and bottom-up approaches for the preparation of micro/nanosuspensions. *Int J Pharm.* 2009;380(1–2):216–22.
10. Chan H-K, Kwok PCL. Production methods for nanodrug particles using the bottom-up approach. *Adv Drug Deliv Rev.* 2011;63(6):406–16.
11. Jacobs C, Müller RH. Production and characterization of a budesonide nanosuspension for pulmonary administration. *Pharm Res.* 2002;19(2):189–94.
12. Saritha D, Sathish D, Rao YM. Formulation and evaluation of gastroretentive floating tablets of domperidone maleate. *J Appl Pharm Sci.* 2012;2(3):68–73.
13. Reddymasu SC, Soykan I, McCallum RW. Domperidone: review of pharmacology and clinical applications in gastroenterology. *Am J Gastroenterol.* 2007;102(9):2036–45.
14. Ullah N, Khan S, Ahmed S, Govender T, Faidah HS, de Matas M, et al. Dexibuprofen nanocrystals with improved therapeutic performance: fabrication, characterization, in silico modeling, and in vivo evaluation. *Int J Nanomedicine.* 2018;13:1677–92.
15. Anwar J. From virtual molecule to formulate medicine; a review of the potential of molecular simulation in drug delivery and formulation. *LPT.* 2007;10(7):66–72.
16. Seedat N, Kalhapure RS, Mocktar C, Vepuri S, Jadhav M, Soliman M, et al. Co-encapsulation of multi-lipids and polymers enhances the performance of vancomycin in lipid–polymer hybrid nanoparticles: in vitro and in silico studies. *Mater Sci Eng C.* 2016;61:616–30.
17. Cosconati S, Forli S, Perryman AL, Harris R, Goodsell DS, Olson AJ. Virtual screening with AutoDock: theory and practice. *Expert Opin Drug Discovery.* 2010;5(6):597–607.
18. Morris GM, Huey R, Lindstrom W, Sanner MF, Belew RK, Goodsell DS, et al. AutoDock4 and AutoDockTools4: automated docking with selective receptor flexibility. *J Comput Chem.* 2009;30(16):2785–91.
19. Seeliger D, de Groot BL. Ligand docking and binding site analysis with PyMOL and Autodock/Vina. *J Comput Aided Mol Des.* 2010;24(5):417–22.
20. Selvi BR, Batta K, Kishore AH, Mantelingu K, Varier RA, Balasubramanyam K, et al. Identification of a novel inhibitor of CARM1-mediated methylation of histone H3R17. *J Biol Chem.* 2010;285(10):7143–52.
21. Yang Z, Lasker K, Schneidman-Duhovny D, Webb B, Huang CC, Pettersen EF, et al. UCSF Chimera, MODELLER, and IMP: an integrated modeling system. *J Struct Biol.* 2012;179(3):269–78.
22. Kusumaningrum S, Budiarto E, Kosela S, Sumaryono W, Juniarti F. The molecular docking of 1, 4-naphthoquinone derivatives as inhibitors of polo-like kinase 1 using Molegro Virtual Docker. *J Appl Sci.* 2014;4:47–53.
23. Özpınar GA, Peukert W, Clark T. An improved generalized AMBER force field (GAFF) for urea. *J Mol Model.* 2010;16(9):1427–40.
24. Wang J, Wang W, Kollman PA, Case DA. Antechamber: an accessory software package for molecular mechanical calculations. *J Am Chem Soc.* 2001;222:403–10.
25. Galindo-Murillo R, Robertson JC, Zgarbová M, Sponer J, Otyepka M, Jurečka P, et al. Assessing the current state of AMBER force field modifications for DNA. *J Chem Theory Comput.* 2016;12(8):4114–27.
26. Godschalk F, Genheden S, Söderhjelm P, Ryde U. Comparison of MM/GBSA calculations based on explicit and implicit solvent simulations. *Phys Chem Chem Phys.* 2013;15(20):7731–9.
27. Alhumayyd M, Bukhari I, Almotrefi A. Effect of piperine, a major component of black pepper, on the pharmacokinetics of domperidone in rats. *J Physiol Pharmacol.* 2014;65:785–9.
28. Shah SMH, Ullah F, Khan S, Shah SMM, de Matas M, Hussain Z, et al. Smart nanocrystals of artemether: fabrication, characterization, and comparative in vitro and in vivo antimalarial evaluation. *Drug Des Dev Ther.* 2016;10:3837–45.
29. Ali HS, York P, Blagden N. Preparation of hydrocortisone nanosuspension through a bottom-up nanoprecipitation technique using microfluidic reactors. *Int J Pharm.* 2009;375(1–2):107–13.
30. Kakran M, Sahoo N, Li L, Judeh Z, Wang Y, Chong K, et al. Fabrication of drug nanoparticles by evaporative precipitation of nanosuspension. *Int J Pharm.* 2010;383(1–2):285–92.
31. Cao G. *Nanostructures & nanomaterials: synthesis, properties & applications.* 2nd ed. London: Imperial College Press; 2004.
32. O'Mahony M, Leung AK, Ferguson S, Trout BL, Myerson AS. A process for the formation of nanocrystals of active pharmaceutical ingredients with poor aqueous solubility in a nanoporous substrate. *Org Process Res Dev.* 2015;19(9):1109–18.
33. Ali HS, York P, Ali AM, Blagden N. Hydrocortisone nanosuspensions for ophthalmic delivery: a comparative study between microfluidic nanoprecipitation and wet milling. *J Control Release.* 2011;149(2):175–81.
34. Khan S, Matas M, Zhang J, Anwar J. Nanocrystal preparation: lowenergy precipitation method revisited. *Cryst Growth Des.* 2013;13(7):2766–77.
35. Rahim H, Sadiq A, Khan S, Khan MA, Shah SMH, Hussain Z, et al. Aceclofenac nanocrystals with enhanced in vitro, in vivo performance: formulation optimization, characterization, analgesic and acute toxicity studies. *Drug Des Dev Ther.* 2017;11:2443–52.
36. Mura C, McAnany CE. An introduction to biomolecular simulations and docking. *Mol Simul.* 2014;40(10–11):732–64.
37. Clark AJ, Gindin T, Zhang B, Wang L, Abel R, Murrett CS, et al. Free energy perturbation calculation of relative binding free energy between broadly neutralizing antibodies and the gp120 glycoprotein of HIV-1. *J Mol Biol.* 2017;429(7):930–47.
38. Ślędz P, Cafilisch A. Protein structure-based drug design: from docking to molecular dynamics. *Curr Opin Struct Biol.* 2018;48:93–102.
39. Plakkot S, De Matas M, York P, Saunders M, Sulaiman B. Comminution of ibuprofen to produce nano-particles for rapid dissolution. *Int J Pharm.* 2011;415(1–2):307–14.
40. Dalvi SV, Dave RN. Analysis of nucleation kinetics of poorly water-soluble drugs in presence of ultrasound and

- hydroxypropyl methyl cellulose during antisolvent precipitation. *Int J Pharm.* 2010;387(1):172–9.
41. Voorhees PW. The theory of Ostwald ripening. *J Stat Phys.* 1985;38(1–2):231–52.
  42. Anwar J, Khan S, Lindfors L. Secondary crystal nucleation: nuclei breeding factory uncovered. *Angew Chem.* 2015;54(49):14681–4.
  43. Chavda H, Patel C, Anand I. Biopharmaceutics classification system. *Sys Rev Pharm.* 2010;1(1):62–9.
  44. Möschwitzer JP. Drug nanocrystals in the commercial pharmaceutical development process. *Int J Pharm.* 2013;453(1):142–56.